



A re-evaluation of the notosuchian crocodyliform *Eremosuchus elkoholicus* from the lower Eocene of Algeria and the evolutionary and biogeographic history of sebecids

Cecily S. C. Nicholl, Paul M. J. Burke, Ella M. Marwood, Jeremy E. Martin, Mohammed Mahboubi, Rodolphe Tabuce & Philip D. Mannion

To cite this article: Cecily S. C. Nicholl, Paul M. J. Burke, Ella M. Marwood, Jeremy E. Martin, Mohammed Mahboubi, Rodolphe Tabuce & Philip D. Mannion (21 Nov 2025): A re-evaluation of the notosuchian crocodyliform *Eremosuchus elkoholicus* from the lower Eocene of Algeria and the evolutionary and biogeographic history of sebecids, *Journal of Vertebrate Paleontology*, DOI: [10.1080/02724634.2025.2572964](https://doi.org/10.1080/02724634.2025.2572964)

To link to this article: <https://doi.org/10.1080/02724634.2025.2572964>



© 2025 Cecily S. C. Nicholl, Paul M. J. Burke, Ella M. Marwood, Jeremy E. Martin, Mohammed Mahboubi, Rodolphe Tabuce, Philip D. Mannion. Published with license by the Society of Vertebrate Paleontology



[View supplementary material](#)



Published online: 21 Nov 2025.



[Submit your article to this journal](#)



Article views: 775



[View related articles](#)



[View Crossmark data](#)



ARTICLE

A RE-EVALUATION OF THE NOTOSUCHIAN CROCODYLIFORM *EREMOSUCHUS ELKOHOLICUS* FROM THE LOWER EOCENE OF ALGERIA AND THE EVOLUTIONARY AND BIOGEOGRAPHIC HISTORY OF SEBECIDS

CECILY S. C. NICHOLL,^{1*} PAUL M. J. BURKE,¹ ELLA M. MARWOOD,² JEREMY E. MARTIN,³ MAHAMMED MAHBOUBI,⁴ RODOLPHE TABUCE,⁵ and PHILIP D. MANNION¹

¹Department of Earth Sciences, University College London, Gower Street, London WC1E 6BT, U.K., cecily.nicholl@ucl.ac.uk;

²Division of Biosciences, University College London, Gower Street, London WC1E 6BT, U.K.;

³Université de Lyon, Université de Lyon 1, ENSL, CNRS, LGL-TPE, Villeurbanne, France;

⁴Laboratoire de Paléontologie Stratigraphique et Paléoenvironnement, Université d'Oran 2, El M'naouer, 31000, Oran, Algeria;

⁵Institut des Sciences de l'Évolution (UM, CNRS, IRD, EPHE), Université Montpellier, Montpellier, France

ABSTRACT—Notosuchian systematics have been highly debated in recent decades, particularly the placement of sebecids and closely related species. As the only notosuchian lineage to have survived the Cretaceous–Paleogene mass extinction, reconciliation of conflicting views on the group's relationships is required to better understand extinction selectivity. Here, we redescribe and newly diagnose *Eremosuchus elkoholicus* from the Lower Eocene El Kohol Formation of Algeria, known from the holotypic dentary and several referred remains. A new, smaller dentary is also considered to represent an immature individual of this species, providing a rare notosuchian ontogenetic series. *Eremosuchus* is incorporated into one of the largest notosuchian-focused character-taxon matrices yet to be compiled, comprising 450 characters and 130 taxa. Focus is placed on improved sampling of mandibular characters and putative sebecids, especially frequently neglected taxa from Europe and Africa. Phylogenetic analyses, incorporating continuous characters, consistently recover *Eremosuchus elkoholicus* as a sebecid, though its precise position within this clade is uncertain. Under equal weighting, Sebecidae is recovered as the sister taxon to all other notosuchians, whereas a monophyletic Sebecosuchia is retrieved using extended implied weighting. The latter weighting approach finds the early Paleogene South American species, *Lorosuchus nodosus* and *Sahitisuchus fluminensis*, within Peirosauria, which would indicate the survival of a second notosuchian lineage across the Cretaceous/Paleogene boundary. The taxonomic and spatiotemporal expansion of Sebecidae via the inclusion of fragmentary material from Africa and Europe hints at a more complicated biogeographic and evolutionary history of the clade, and it remains unclear whether sebecids originated in Gondwana or Europe.

SUPPLEMENTARY FILE(S)—Supplementary file(s) are available for this article for free at www.tandfonline.com/UJVP.

Citation for this article: Nicholl, C. S. C., Burke, P. M. J., Marwood, E. M., Martin, J. E., Mahboubi, M., Tabuce, R., & Mannion, P. D. (2025) A re-evaluation of the notosuchian crocodyliform *Eremosuchus elkoholicus* from the lower Eocene of Algeria and the evolutionary and biogeographic history of sebecids. *Journal of Vertebrate Paleontology*. <https://doi.org/10.1080/02724634.2025.2572964>

Submitted: November 19, 2024

Revisions received: August 9, 2025

Accepted: August 12, 2025

INTRODUCTION

Notosuchians are an extinct, speciose clade of crocodyliforms noted for their unusual, morphologically disparate bauplans and broad ecological diversity, as well as their general preference for hot, semi-arid terrestrial environments (Carvalho et al., 2010;

Klock et al., 2022; Leardi et al., 2015; Pochat-Cottilloux et al., 2023; Pol et al., 2014). Their fossil record extends from the Middle Jurassic to the Middle Miocene (Dal Sasso et al., 2017; Langston, 1965; Paolillo & Linares, 2007), with a primarily Gondwanan distribution (Carvalho et al., 2010; Nicholl et al., 2021; Pol & Leardi, 2015), although notosuchians are also known from Eurasia (Company et al., 2005; Sellés et al., 2020; Wu & Sues, 1996). The systematics of the group have been increasingly studied and revised in recent decades (e.g., Darlim et al., 2021; Geroto & Bertini, 2019; Martins dos Santos et al., 2024; Pol et al., 2014; Ruiz et al., 2021; Sereno & Larsson, 2009); however, a major dispute persists, concerning the phylogenetic placement of the notosuchian lineage, Sebecidae (Buckley & Brochu, 1999; Larsson & Sues, 2007; Ortega et al., 2000; Pol, 2003; Pol et al., 2014; Riff & Kellner, 2011). In some studies, Sebecidae and close relatives are united with Baurusuchia *sensu* Leardi et al. (2024), forming Sebecosuchia, which in recent years has consistently been recovered as deeply nested within Notosuchia (Buffetaut, 1980; Colbert et al., 1946; Fiorelli et al., 2016; Gasparini, 1972,

*Corresponding author.

© 2025 Cecily S. C. Nicholl, Paul M. J. Burke, Ella M. Marwood, Jeremy E. Martin, Mahammed Mahboubi, Rodolphe Tabuce, Philip D. Mannion. This is an Open Access article distributed under the terms of the Creative Commons Attribution License (<http://creativecommons.org/licenses/by/4.0/>), which permits unrestricted use, distribution, and reproduction in any medium, provided the original work is properly cited. The terms on which this article has been published allow the posting of the Accepted Manuscript in a repository by the author(s) or with their consent.

Color versions of one or more of the figures in the article can be found online at www.tandfonline.com/UJVP.

1984; Gasparini et al., 2006; Geroto & Bertini, 2019; Leardi et al., 2015; Nicholl et al., 2021; Ortega et al., 1996, 2000; Pol et al., 2004, 2014, 2009; Pol & Apósteguía, 2005; Sereno et al., 2001, 2003; Turner & Calvo, 2005). By contrast, sebecids have also been recovered as the sister group to Peirosauria (Leardi et al., 2024) with these clades (Sebecidae + Peirosauridae) forming Sebecia (e.g., Geroto & Bertini, 2019; Larsson & Sues, 2007; Meunier & Larsson, 2017; Pinheiro et al., 2018, 2021, 2023; Riff & Kellner, 2011; Ruiz et al., 2021; Sereno et al., 2003). Sebecia is positioned either at the ‘base’ of Notosuchia or even outside of this clade (Larsson & Sues, 2007; Ruiz et al., 2021; Sereno & Larsson, 2009). Part of the problem stems from the fact that members of Sebecidae share several derived traits with both baurusuchians and peirosaurians, including large caniniform teeth, a relatively altirostral skull, a notch on the premaxilla–maxilla boundary for the reception of enlarged dentary teeth, a sigmoidal dentary tooth row, a large choanal opening, a reduced antorbital fenestra, and posteriorly orientated retroarticular process (e.g., Pol et al., 2014). Moreover, the repeated use of largely unchanged iterations of the two main morphological data matrices used to recover Sebecia and Sebecidae, typically with the addition of only a single new species, precludes any real consensus on this matter. As the only group of notosuchians to survive the Cretaceous–Paleogene (K–Pg) mass extinction, 66 Ma (Kellner et al., 2014), resolving the phylogenetic placement of sebecids and closely related species is crucial to understanding selectivity across this event (e.g., Aubier et al., 2023), as well as the biogeographic history of the clade.

Sebecids and closely related taxa that are neither baurusuchians nor peirosaurians have a predominantly South American distribution that spans the Paleocene to the Middle Miocene, including the multispecific *Sebecus* and the large-bodied species *Barinasuchus arveloi* (Bravo et al., 2021; Busbey, 1986; Gasparini, 1984; Kellner et al., 2014; Paolillo & Linares, 2007; Pol & Leardi, 2015; Pol et al., 2012). *Pehuenchesuchus enderi*, from the Santonian (Upper Cretaceous) Bajo de la Carpa Formation of Argentina, might represent a Mesozoic South American member of the clade, although this species is only known from a mandible and its affinities remain uncertain (Pol et al., 2014; Turner & Calvo, 2005). Several potential members of the sebecid lineage are known from elsewhere (Table 1). Primarily, these non-South American species are represented by fragmentary remains; accordingly, only a small number of morphological characters can be scored from such sparse material and many of these species are often excluded from phylogenetic analyses, despite their potential biogeographic importance. The stratigraphically earliest known putative member is *Razanandrongobe sakalavae* from the Middle Jurassic Sakahara (=Isalo IIIb) Formation of Madagascar (Dal Sasso et al., 2017; Maganuco & Dal Sasso, 2006). The holotype specimen comprises a fragmentary right maxilla and several isolated teeth, with further remains, including cranial fragments, referred to the species (Dal Sasso et al., 2017). Whereas some analyses have supported close affinities with Sebecidae (Sellés et al., 2020), Martins et al. (2024) recovered *Razanandrongobe* within Baurusuchia. Given that *Razanandrongobe* is also the stratigraphically earliest known putative notosuchian, its recovered position as a phylogenetically well-nested species should be treated with caution. Otherwise, the fossil record of putative non-South American members of the sebecid lineage extends from the latest Cretaceous to the late Eocene (Table 1). This might include *Pabwehshi pakistanensis* from the upper Maastrichtian Vitakri Formation in Pakistan (e.g., Pol et al., 2014), which is known only from an anterior snout fragment (Wilson et al., 2001), though some studies suggest baurusuchian affinities instead (e.g., Darlim et al., 2021; Turner & Calvo, 2005; Wilson et al., 2001). Six species from Europe are currently regarded as possible members of the sebecid lineage (Fig. 1): (1) *Doratodon*

carcharidens from the lower Campanian Grünbach Formation of Austria, with the holotype material comprising a mandible and maxillary fragment (Bunzel, 1871; Company et al., 2005); (2) *Doratodon ibericus* from the upper Campanian–lower Maastrichtian Sierra Perenchiza Formation of Spain, known only from an incomplete mandible (Company et al., 2005); (3) *Ogresuchus furatus* from the lower Maastrichtian Tremp Formation of Spain, known from the anterior region of the rostrum and several axial and appendicular elements (Sellés et al., 2020); (4) *Iberosuchus macrodon* from the lower–middle Eocene Felgueira Grande Formation of Portugal, with the holotype consisting of the anterior portion of the snout (Antunes, 1975); (5) *Bergisuchus dietrichbergi* from the Lutetian (middle Eocene) Messel Formation of Germany, with the holotype comprising an anterior snout fragment (Kuhn, 1968; Rossmann et al., 2000); and (6) *Dentaneosuchus crassiproratus* from the Bartonian (middle Eocene) Sables du Castrais Formation of France, known from skull fragments and postcranial elements (Martin et al., 2023), though some of these placements are disputed (e.g., Martin et al., 2023). *Eremosuchus elkoholicus*, represented by a mandible and several referred postcranial elements from the Ypresian (lower Eocene) El Kohol Formation of Algeria (Buffetaut, 1982, 1989), is the only named species with possible sebecid affinities from the African mainland. Despite its near-unique spatial distribution, this species has been largely neglected since its description (see below). A generically indeterminate skull fragment and partial dentary from the Priabonian (upper Eocene) Birket Qarun Formation of Egypt potentially represents an additional occurrence of this group (Stefanic et al., 2019).

History of *Eremosuchus elkoholicus* Collection and Study

The holotype (UO-KB-301) and previously referred materials of *Eremosuchus elkoholicus* were collected in 1982, as part of several expeditions to the El Kohol site in northern Algeria that were jointly conducted by the Université d’Oran, Sorbonne Universités (at the time, Université de Paris VI), and Université de Montpellier (at the time, Montpellier Université des Sciences et Techniques du Languedoc). They were recovered from the El Kohol Formation, which is represented at the locality by 350 m of folded continental deposits unconformably overlying Turonian (lower Upper Cretaceous) marine sedimentary rocks (Mahboubi et al., 1986), and which is constrained, at the top, to the upper Ypresian (Lower Eocene, Chron C22r) (Coster et al., 2012). The fossil-bearing level of the El Kohol Formation, dated to the middle Ypresian (Chron C23n.1n), comprises lacustrine limestones with oncolites, interbedded with clays and marls (Coster et al., 2012; Mahboubi et al., 1986). In addition to *Eremosuchus*, the marly layers have yielded abundant fossils of other vertebrate groups, namely mammals, squamates, amphibians, birds, teleosts, and lungfish (Benoit et al., 2016; Buffetaut, 1989; Court, 1994; Kowalski & Rzebik-Kowalska, 1991; Mahboubi et al., 1984a, b, 1986; Ravel et al., 2011).

Three sub-localities (KA, KB, and KC), positioned just a few meters apart, but belonging to the same stratigraphic level within the El Kohol Formation, were excavated during the 1982 expedition (Fig. 2). A fourth spatially proximal sub-locality (KD), interpreted to be from the same unit as that bearing the type material (Coster et al., 2012; Ravel et al., 2011), was discovered during a more recent expedition in 2007, conducted by the Université d’Oran, Université de Tlemcen, and Université de Montpellier. This sub-locality is stratigraphically lower than KA–KC but co-eval in age (Coster et al., 2012; Ravel et al., 2011). A partial dentary of a smaller individual was collected from the same El Kohol locality during an expedition in 1990, but the precise site and stratigraphic position are unknown.

Initially reported by Buffetaut (1982), specimen UO-KB-301 was subsequently described as the holotype of *Eremosuchus*

TABLE 1. Spatiotemporal distribution of remains previously referred to Sebecidae and closely related taxa from outside of South America. An ** indicates that this is the holotype specimen.

Taxon	Material	Country	Formation/ locality	Age	Reference
<i>Doratodon carcharidens</i>	Mandible with teeth, maxilla fragment	Hungary	Csehbánya	Late Cretaceous	Rabi & Sebők 2015
<i>Doratodon carcharidens*</i>	Mandible	Austria	Grünbach	Late Cretaceous	Bunzel 1871
<i>Doratodon ibericus*</i>	Mandible with teeth	Spain	Sierra Perenchiza	Late Cretaceous	Company et al. 2005
<i>Pabwehshi pakistanensis*</i>	Partial rostrum and mandible	Pakistan	Pab	Late Cretaceous	Wilson et al. 2001
<i>Ogresuchus furatus*</i>	Cranial fragments, vertebrae, appendicular elements	Spain	Tremp	Late Cretaceous	Sellés et al. 2020
<i>Iberosuchus</i> sp.	Osteoderms	Spain	Duero Basin	Eocene	Martín de Jesús et al. 1987
<i>Eremosuchus elkoholicus</i> *	Dentary with teeth, fragmentary articular region, vertebrae, fibula, osteoderms	Algeria	El Kohol	early Eocene	Buffetaut 1982, 1989
<i>Iberosuchus macrodon</i> *	Anterior snout fragments, teeth	Portugal	Feligueira	middle Eocene	Antunes 1975
<i>Bergisuchus dietrichbergi</i> *	Partial skull	Germany	Messel	middle Eocene	Rossman et al. 2000
<i>Bergisuchus dietrichbergi</i>	Anterior dentaries	Germany	Geiseltal	middle Eocene	Rossman et al. 2000
<i>Dentaneosuchus crassiproratus</i>	Partial skull including mandible, humerus, ischium, osteoderms	France	Réalmont	middle Eocene	Martin et al. 2023
<i>Dentaneosuchus crassiproratus*</i>	Partial mandible	France	Issel	middle Eocene	Ortega et al. 1996
cf. <i>Iberosuchus</i>	Two dentaries from different individuals and an articular	Spain	Caenes	middle Eocene	Ortega et al. 1996
cf. <i>Iberosuchus macrodon</i>	Skull material	Spain	Tosalet del Morral	middle Eocene	Berg & Crusafont 1970; Buffetaut 1982
"cocodrilos Iberoccitanos"	Skull and mandible fragments	Spain	El Cerro de El Viso	middle Eocene	Ortega et al. 1993
<i>Iberosuchus</i> sp.	Skull fragments	France	Aumelas	middle Eocene	Martin 2016
<i>Iberosuchus</i> sp.	Skull fragments	France	Saint-Martin-de-Londres	middle Eocene	Martin 2016
<i>Iberosuchus</i> sp.	Osteoderms	France	Robiac	middle Eocene	Martin 2016
cf. <i>Iberosuchus</i> sp.	Nearly complete tooth crown	France	Chéry-Chartreuve	middle Eocene	Prasad & Lapparent de Broin, 2002
cf. <i>Iberosuchus</i> sp.	Multiple teeth	France	Robiac-Nord	middle Eocene	Prasad & Lapparent de Broin, 2002
cf. <i>Iberosuchus</i> sp.	Teeth and osteoderms	France	Lissieu	middle Eocene	Martin, 2014
? <i>Iberosuchus</i> Fayum sebecid	Jugal, vertebrae, and isolated teeth	France	La Livinière	late Eocene	Buffetaut 1986
	Dentary fragment	Egypt	Birket Qarun	late Eocene	Stefanic et al. 2019

elkoholicus by Buffetaut (1989). The holotype is an almost complete right dentary, and several additional remains were referred to the species, comprising: the posterior part of a left mandibular ramus (UO-KA-401), five isolated teeth (UO-KA-117, 118, 402–404), several thoracic and caudal vertebrae (UO-KA-405, 406 and UO-KA-407, 408, respectively), and a fibula (UO-KA-114). Osteoderms were also mentioned from the type locality, although were not explicitly referred to *Eremosuchus*. With the exception of the holotype and a single caudal vertebral centrum, the current location of these remains is unknown.

Despite the incompleteness of *Eremosuchus*, comparisons with other taxa available at the time enabled Buffetaut (1982, 1989) to make a proposal regarding its phylogenetic affinity. The tooth morphology was described as being representative of a “ziphodont mesosuchian” (Buffetaut, 1982, p. 176; 1989, p. 2). “Globular” posterior dentary teeth led Buffetaut (1989) to refer *Eremosuchus* specifically to Trematochampsidae, although the validity of this group (including the type genus *Trematochamps*) has since been questioned, and it is now largely considered synonymous with Peirosauridae (Buckley & Brochu, 1999; Filippi et al., 2018; Larsson & Sues, 2007; Meunier & Larsson, 2017; Nicholl et al., 2021; Rasmussen Simons & Buckley, 2009; Turner & Sertich, 2010). Buffetaut’s (1982) comparisons also suggested a close relationship with the latest Cretaceous Brazilian taxon *Baurusuchus* based on the depth of the dentary. He also remarked on similarities of the referred articular

region (UO-KA-401) with *Sebecus* and *Trematochamps*, as well as suggesting the resemblance of the vertebrae to some “undescribed ziphodont mesosuchian” vertebrae from the late Eocene of France (Buffetaut, 1982:p. 177; Buffetaut, 1986; Martin, 2016). However, affinities with *Baurusuchus* and *Sebecus* were later rejected, with Buffetaut (1989) instead favoring a closer relationship with the Late Cretaceous Gondwanan taxa, *Itasuchus jesuinoi*, *Peirosaurus tormini*, and *Trematochamps*. Having been shown to be distinct in its morphology, *Eremosuchus elkoholicus* was diagnosed as a new species, with the following combination of characters:

a very deep and narrow lower jaw. Twelve close-set teeth in the dentary, the first and fourth teeth being the largest in the tooth row. Teeth slightly compressed with serrated carinae. Posterior teeth not reduced, with a blunt apex and ornamented enamel. Surangular bearing a glenoid cavity and taking part in the craniomandibular articulation. Vertebrae amphicoelous. Caudal vertebrae with deep, laterally compressed centra. (Buffetaut, 1989:p. 3)

Very few studies have tested the phylogenetic position of *Eremosuchus*. Ortega et al. (1996) were the first to include it in an analysis, in which they supported sebecosuchian affinities, recovering *Eremosuchus* as the sister taxon of *Baurusuchus* based on the presence of a sigmoidal tooth row. Turner and Calvo

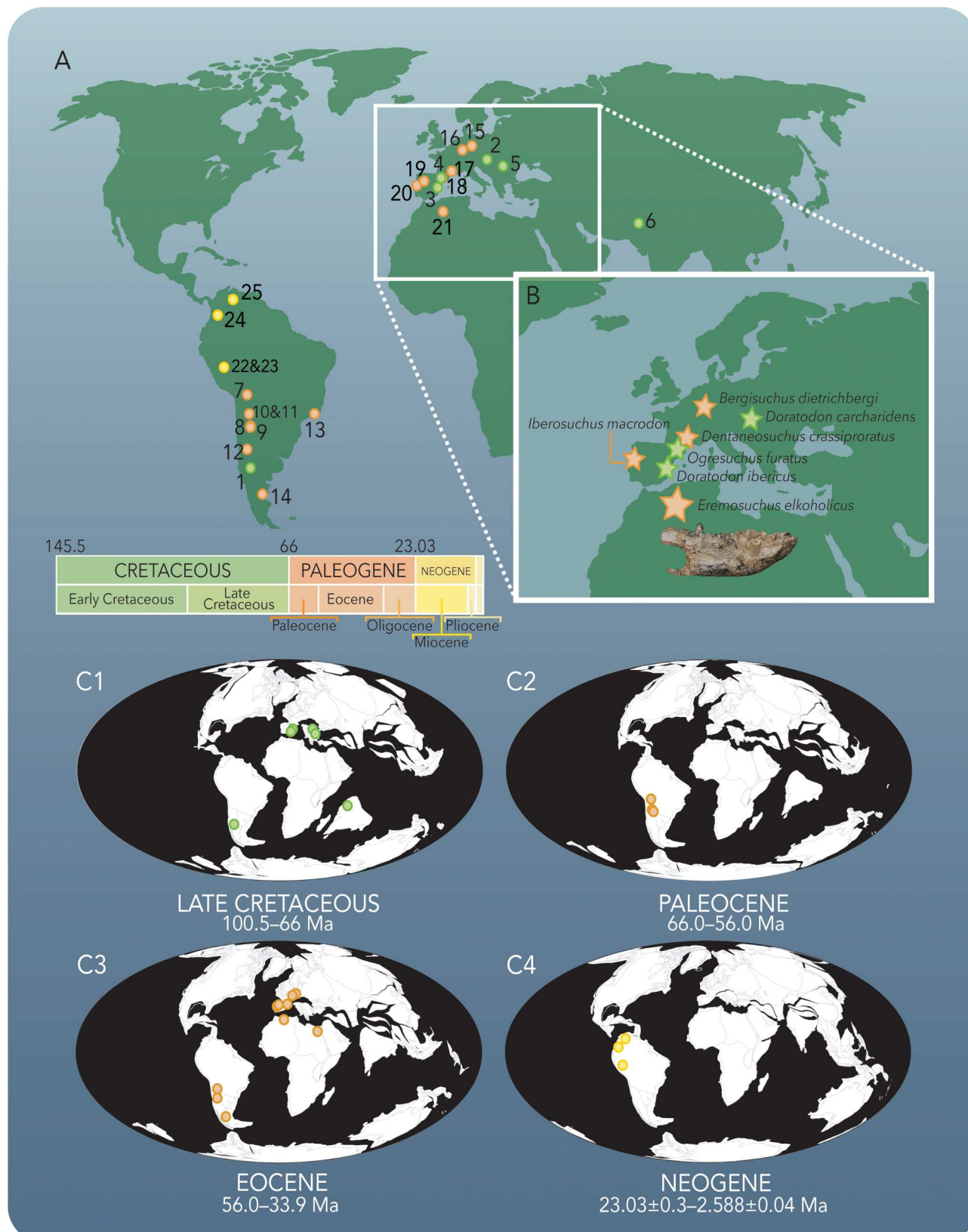


FIGURE 1. **A**, map showing occurrences typically assigned to Sebecidae and closely related taxa, identified to species level: **1**, *Pehuenchesuchus enderi*; **2**, *Doratodon carcharidens*; **3**, *Doratodon ibericus*; **4**, *Ogresuchus furatus*; **5**, *Doratodon carcharidens*; **6**, *Pabwehshi pakistanensis*; **7**, *Zulmasuchus querejazus*; **8**, *Bretesuchus bonapartei*; **9**, *Lorosuchus nodosus*; **10**, *Ayllusuchus fernandezii*; **11**, *Sebecus ayrampu*; **12**, *Ilchunaia parva*; **13**, *Sahittosuchus fluminensis*; **14**, *Sebecus icaeorhinus*; **15**, *Bergisuchus dietrichbergi*; **16**, *Bergisuchus dietrichbergi*; **17**, *Dentaneosuchus crassiproratus*; **18**, *Iberosuchus macrodon*; **19**, *Iberosuchus macrodon*; **20**, *Iberosuchus macrodon*; **21**, *Eremosuchus elkoensis*; **22**, *Barinasuchus arveloi*; **23**, *Sebecus huilensis*; **24**, *Sebecus huilensis*; **25**, *Barinasuchus arveloi*. **B**, location of European and North African holotype occurrences. **C**, paleogeographic reconstructions showing the distribution of species-level occurrences for the Late Cretaceous (C1), Paleocene (C2), Eocene (C3), Neogene (C4). Paleogeographic reconstructions produced using the Paleobiology Database Navigator (<https://paleobiodb.org/navigator/>).

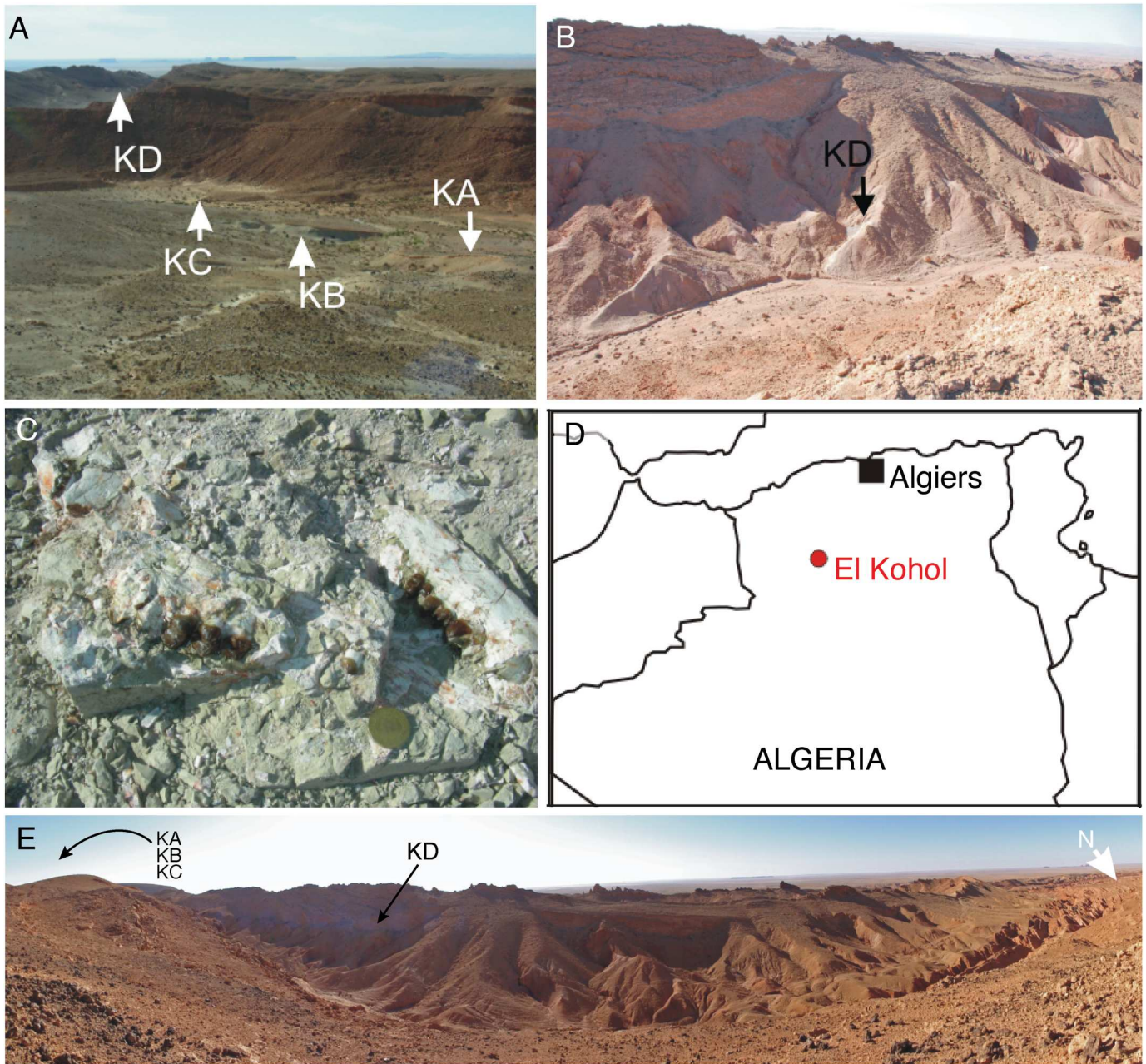


FIGURE 2. A, general view of sites KA, KB, and KC excavated at the lower Eocene El Kohol locality in northern Algeria. The holotype specimen of *Eremosuchus elkoholicus* was recovered from site KB. B, view of site KD, from which several osteoderm fragments were recovered. C, richness of vertebrate remains from the locality (here the proboscidean *Numidotherium koholense*). D, location of the El Kohol locality. E, panoramic view of the El Kohol anticline.

(2005) also recovered *Eremosuchus* within Sebecosuchia, as a relatively early diverging member of the clade. Following their phylogenetic analysis, Montefeltro (2013) suggested that the taxon belongs to Baurusuchidae instead. Most recently, Bravo et al. (2025) suggest a close relationship of the El Kohol taxon to Sebecosuchia, finding alternative positions within either Baurusuchia or Sebecoidea in their most parsimonious trees (MPTs).

Here, we re-describe the holotype and referred remains of *Eremosuchus elkoholicus*, as well as previously undescribed specimens from the type locality. Via detailed comparisons with other notosuchian taxa, including sebecids, a new diagnosis is formed for *Eremosuchus elkoholicus*. Several newly documented anatomical features are identified amongst sebecids, forming

the basis of novel morphological phylogenetic characters. We test the phylogenetic position of *Eremosuchus* in a revised and expanded data matrix, incorporating several other putative sebecids that are frequently excluded from such analyses. Finally, we consider the biogeographic implications of our revised view of the phylogenetic affinities of *Eremosuchus*.

MATERIALS AND METHODS

Anatomical Data Collection

The holotype dentary, and one caudal vertebral centrum were studied first-hand. All other specimens previously referred to

Eremosuchus were re-evaluated from the description and photographs presented in Buffetaut (1989). This was supplemented by first-hand study of previously unpublished materials from the type locality, comprising the aforementioned small dentary, teeth from sub-localities KA and KB, and osteoderms from sub-locality KD. Specimens used for comparative purposes were studied either first-hand or from photographs. In-person measurements were collected using digital calipers, whilst measurements from photographs were obtained using the image processing software ImageJ (Schneider et al., 2012).

Computed Tomography Scanning and Segmentation

The two dentaries from El Kohol were characterized at the NHMUK with X-ray micro-computed tomography (CT) using a Nikon Metrology XTH 225 ST system (Nikon Metrology, Leuven, Belgium). Due to the size of the holotype specimen, the acquisition was implemented in three parts, with a voltage of 160 kV and a current of 181 μ A, resulting in a reconstructed isotropic voxel size of 33.602 μm^3 and 3849 projections with an average of two frames, with an exposure time of 0.708 seconds per frame. The data from each of the three parts were made into three TIFF stacks. For the smaller dentary, acquisition was implemented in one part, with a voltage of 150 kV and a current of 127 μ A, resulting in a reconstructed isotropic voxel size of 15.638 μm^3 and 6663 projections with an average of four frames, with an exposure time of 0.354 seconds per frame. The data were merged into a single TIFF stack. Both specimens were subsequently segmented in Avizo v. 9.7 (FEI Visualization Science Group; <https://www.thermofisher.com>), smoothed in Blender (Stichting Blender Foundation, Amsterdam), and rendered in Inkscape (Inkscape Project, 2020).

Phylogenetic Dataset and Analytical Approach

To evaluate the phylogenetic affinities of *Eremosuchus*, we utilized an adapted version of the character-taxon matrix (CTM) of Nicholl et al. (2021), which samples a large number of crocodyliiforms, particularly notosuchians, and is itself built upon the matrix of Pol et al. (2014), with subsequent iterations by Leardi et al. (2015, 2018), Fiorelli et al. (2016), and Martínez et al. (2018) (Supplementary File 1). Both the holotype specimen (UO-KB-301) and the small dentary (UOK 347) were initially scored separately, with only one character (87) scorables in the latter that was not preserved in the holotype specimen. As both specimens received identical scores and were found to be morphologically similar in our personal observations, they were combined as a single operational taxonomic unit (OTU) (Analyses 1–3). The matrix was expanded to provide increased sampling of putative sebecids from North Africa and Europe, with the addition of: (1) *Doratodon carcharidens*, based on scorings presented in Rabi and Sebők (2015); (2) *Doratodon ibericus*, based on information provided in Company et al. (2005); (3) DPC 20814, the indeterminate specimen (the ‘Fayum form’) from the late Eocene of Egypt, based on the descriptions and figures of Stefanic et al. (2019); and (4) *Dentaneosuchus crassiproratus*, based on the scores of Martin et al. (2023). In addition, we added the sebecid *Sahitisuchus fluminensis* from the lower Eocene Itaboraí Formation of Brazil, based on the scorings of Kellner et al. (2014) and personal observations (CSCN). Three baurusuchians were also added from the uppermost Cretaceous Adamantina Formation of Brazil: (1) *Apestosuchus sordidus*, (2) *Aphaurosuchus escharafacies*, and (3) *Gondwanasuchus scabrosus*. These scorings were based on information presented in Marinho et al. (2013), Godoy et al. (2014), Darlim et al. (2021), and Martins dos Santos et al. (2024), as well as personal observations in the case of the latter taxon (CSCN).

Ninety existing character scores for taxa already in the matrix were modified based on personal observations, photographs, and the published literature (see Supplementary Files 2–3). All previous analyses focusing on notosuchian systematics have discretized quantitative characters, rather than using continuous data. Seven new continuous characters relating to the mandible were added to the character list of Nicholl et al. (2021) as C1–7 (Supplementary Files 1 and 4). Measurements for continuous characters were obtained first-hand where possible, or using the image processing program ImageJ. Measurements were incorporated into MESQUITE v.3.70 (Maddison & Maddison, 2023), where they were converted into a tnt file and combined manually in a text editor with the discrete character scores. Continuous characters were processed using the protocol described in Groh et al. (2020), in which the reciprocal of the total range of the continuous character is taken to obtain a weighting factor, and then multiplied by 100 to be proportional to initial character weight of 100. The resultant data matrix comprises 130 OTUs scored for 450 characters and is presented as a nexus and TNT file, along with the character list, in Supplementary Files 1–4.

Analyses were run using equal weighting schemes (Analysis 1) and, following several recent phylogenetic analyses of crocodyliiforms (Bravo et al., 2021; Nicholl et al., 2021; Rio & Mannion, 2021; Ristevski et al., 2021), using extended implied weighting (EIW) with k -values of 3 (Analysis 2) and 8 (Analysis 3). Extended implied weighting is shown to downweight homoplastic characters in relation to their average homoplasy, with low concavity constants (k -values) downweighting homoplastic characters more than higher values. Fifty characters were ordered (1, 2, 3, 4, 5, 6, 7, 8, 10, 13, 17, 30, 44, 50, 51, 52, 56, 72, 74, 76, 78, 80, 84, 86, 93, 97, 98, 103, 104, 112, 123, 133, 147, 149, 150, 156, 174, 189, 194, 200, 204, 233, 235, 286, 346, 363, 364, 371, 375, and 408). As implemented by Pol et al. (2014: supplementary information, p. 3), Character 12 (previously Character 5 in Pol et al. [2014]) was made inactive due to ‘dependence with the modified definition of character 6’. Character 84 (previously character 77) was removed as it was found to assess similar morphological variation as Character 5. Characters 120 and 162 (previous characters 113 and 155) were also made inactive due to problems with character construction and resultant inconsistencies in scoring (Supplementary File 1). These four characters are coded as being inactive in the Combined character-taxon matrix but should be activated following the protocol in the Supplementary File 5 (i.e., Data > Character Settings > active > CHARACTERS > Ok > APPLY > Ok). Character 167 (previously character 160) was modified following discrepancies in scoring. Pol et al. (2014) identified three problematic/unstable taxa within the CTM, which were also established in our preliminary searches via the Pruned Trees function. These three taxa (*Coringasuchus anisodontis*, *Pabwehshi pakistanensis*, and *Pehuanchesuchus enderi*) were therefore excluded a priori from all of our final analyses. Following additional searches, *Sebecus huilensis*, *Neuquen-suchus universitas*, the ‘Lumbra form,’ and the ‘Fayum form’ were consistently identified as problematic taxa responsible for poor resolution under all weighting schemes (via Pruned Trees), and they were also excluded from our final analyses. These seven taxa are excluded from the analysis via the protocol provided in Supplementary File 5 (i.e., Data > Active taxa > Select taxa > select taxa to be inactive > Ok > Ok). The analyses were conducted under maximum parsimony using a ‘New Technology Search’ in TNT v. 1.5 (Goloboff & Catalano, 2016; Goloboff et al., 2008). *Gracilisuchus stipanicicorum* was set as the operational outgroup. The search applied sectorial searches (using 10 drifting cycles), drift (10 cycles), ratchet (10 iterations) and tree fusing (10 rounds), and the minimum tree length was found 100 times. Five initially added sequences were used for the Driven Search, and the random seed was set to 1. The resultant trees were used as the starting trees for a ‘Traditional

Search' using Tree Bisection-Reconstruction. For analyses conducted under extended implied weighting schemes (Analyses 2 and 3), EIW was turned on before loading the file, as follows: Settings > Implied weights > Basic settings > using implied weights > k -value = x > Ok. After opening the data file, the following steps were undertaken: Settings > Implied weights > Extended weighting > Check "downweight characters with missing entries" keeping the pre-set values > Ok. Following these analyses, the strict consensus tree was calculated using the default settings in TNT.

Institutional Abbreviations—**DPC**, Duke University Primate Center, Durham, NC, U.S.A.; **GM**, Geiseltalmuseum, Halle an der Saale, Germany; **IPUW**, Institut für Paläontologie Universität Wien, Vienna, Austria; **MGUV**, Museo del Departamento de Geología, Universidad de Valencia, Valencia, Spain; **NHMUK**, Natural History Museum, London, U.K.; **UO**, Département de Géologie de l'Université d'Oran, Oran, Algeria; **UT**, Université de Tlemcen, Tlemcen, Algeria.

SYSTEMATIC PALEONTOLOGY

CROCODYLOMORPHA Walker, 1970

CROCODYLIFORMES Hay, 1930 (*sensu* Clark in Benton and Clark, 1988)

MESOEUCROCODYLIA Whetstone and Whybrow, 1983
NOTOSUCHIA Gasparini, 1971
SEBECIDAE Simpson, 1937
EREMOSUCHUS Buffetaut, 1989
EREMOSUCHUS ELKOHOLICUS Buffetaut, 1989

Holotype—UO-KB-301, an isolated right dentary with one complete tooth.

Referred Material—UOK 347, left dentary of a juvenile individual with multiple teeth preserved.

Tentatively Referred Material—UO-KA-401, articular region of left mandible; UO-KA-117–118, UO-KA 402–404, UOK 344–345 (KB locality), isolated teeth; UOK 346 (KA locality), UO-KA 405–406, isolated dorsal vertebrae; UO-KA 407–408, isolated caudal vertebrae; UO-KA 114, right fibula; UT-KD-04 a nearly complete osteoderm; UT-KD-05, several fragmentary osteoderms.

Locality and Stratigraphic Horizon—El Kohol locality, near to Brezina in south-western Algeria; middle Ypresian, lower Eocene, 52–51 Ma (Coster et al., 2012), El Kohol Formation.

Revised diagnosis—A sebecid notosuchian with the following unique combination of characters: (1) pronounced anteroposterior ridge on the ventrolateral surface of the dentary; (2) enlarged first dentary alveolus (and by assumption, tooth); (3) mildly labiolingually compressed tooth crowns in the middle to posterior dentary tooth row; (4) short distance between the fourth and fifth mandibular teeth; (5) mediolaterally compressed dentary; (6) majority of the dentary teeth separated by thin, bony laminae; (7) tooth row extends posteriorly along the dentary; (8) 12 dentary teeth; and (9) dentary maintains most of its dorsoventral height posterior to the fourth dentary tooth.

DESCRIPTIONS

Description of *Eremosuchus elkoensis* Holotype

Dentary—The holotype right dentary (UO-KB-301) is largely undistorted, although the surface preservation is generally poor, and the specimen is cracked in many places, most notably towards its posterior region (Fig. 3). Both the anterior and posterior tips of the dentary are heavily abraded, as well as its dorsal edge.

The total preserved anteroposterior length of the dentary is 156 mm. It is mediolaterally slender, and, though somewhat

damaged, the dorsoventral height to mediolateral width ratio at the level of the fourth tooth is estimated to be between 0.5–0.6. The mandibular ramus is essentially straight along most of its length, although it curves very slightly medially in its posterior-most region (Fig. 4). In life, it would have diverged from the sagittal midline at an estimated angle of 10–15°.

From its anteriormost tip, the lateral margin of the dentary is mildly convex, before becoming essentially straight in its posterior half along the mandibular ramus (Fig. 4). This anterior curvature suggests that the mandibular symphyseal region was approximately 'U'-shaped, albeit relatively mediolaterally narrow. Despite not being fully preserved, it can be inferred that the mandibular symphysis was anteroposteriorly elongate, though due to the absence of the splenial, it is not possible to estimate the ratio of the symphysis length to width. The dorsal surface of the mandibular symphysis is reasonably smooth, sloping strongly ventromedially. On the dorsal surface of the mandibular symphysis, the dentary-dentary suture reaches posteriorly to the level of the 5th alveolus (Fig. 4). The medial margin of the dentary, along its contact surface with the (absent) splenial on the dorsal mandible surface, is approximately straight. This margin is directed anteromedially from the posterior level of the 5th alveolus; it can therefore be inferred that the dentary-splenial suture on the ventral surface was 'V'-shaped.

The dentary increases in dorsoventral height from its anterior tip to the level of the 4th alveolus, at which point it reaches its maximum height of 50 mm (though note that this region is slightly damaged, and so it may have been dorsoventrally taller). Posterior to this, the dorsal margin of the dentary is very slightly concave for the remainder of its length. In its middle to posterior region, the lateral and ventral surfaces of the dentary are sculpted by short and narrow (maximum ~5 mm in length), anteroposteriorly orientated, shallow grooves (Fig. 3). Towards the anterior end of the dentary, these surfaces are instead adorned with shallow pits that reach up to 5 mm in diameter. The lateral surface immediately ventral to the tooth row is also sculpted with pits, though these are smaller and less developed.

From the 6th alveolus posteriorly, the dorsal two-thirds of the lateral surface of the dentary are essentially vertical. The ventral third of the surface expands laterally and is ventrolaterally convex. This expansion forms a distinct, dorsoventrally broad ridge that extends posteriorly along the remaining anteroposterior length of the dentary (Figs. 3, 4). The prominence of this ridge means that, in dorsal view, the lateral margin of the dentary does not appear to curve medially posterior to the level of the enlarged 4th alveolus. Dorsal to this ridge, the space laterally adjacent to the vertical dentary wall likely formed an area for the reception of maxillary teeth, although it is possible that, due to the ridge, its size appears superficially expanded (Fig. 3). The posterior region of the dentary is too poorly preserved to ascertain whether a mandibular fenestra is present, and no sutural contacts with the angular or surangular are preserved.

Due to the absence of the splenial, the medial surface of the dentary is exposed, and is essentially vertical. The Meckelian groove extends anteriorly to a level adjacent with the posterior boundary of the 5th alveolus (Fig. 5). This groove is dorsoventrally narrowest at its anterior end, increasing in dorsoventral height and mediolateral depth posteriorly, reaching a maximum height and depth of ~20 mm and ~5 mm, respectively, at its most posterior region. Though the splenial is absent, it can be inferred that it participated in the mandibular symphysis given that the internal surface of the dentary is exposed just posterior to the vertical surface of the dentary symphysis (Figs. 4–7).

Dentition—Twelve alveoli are preserved, which are considered to represent the full tooth row. Teeth are only preserved in the 4th and 10th dentary alveoli (Figs. 3, 8A). Most

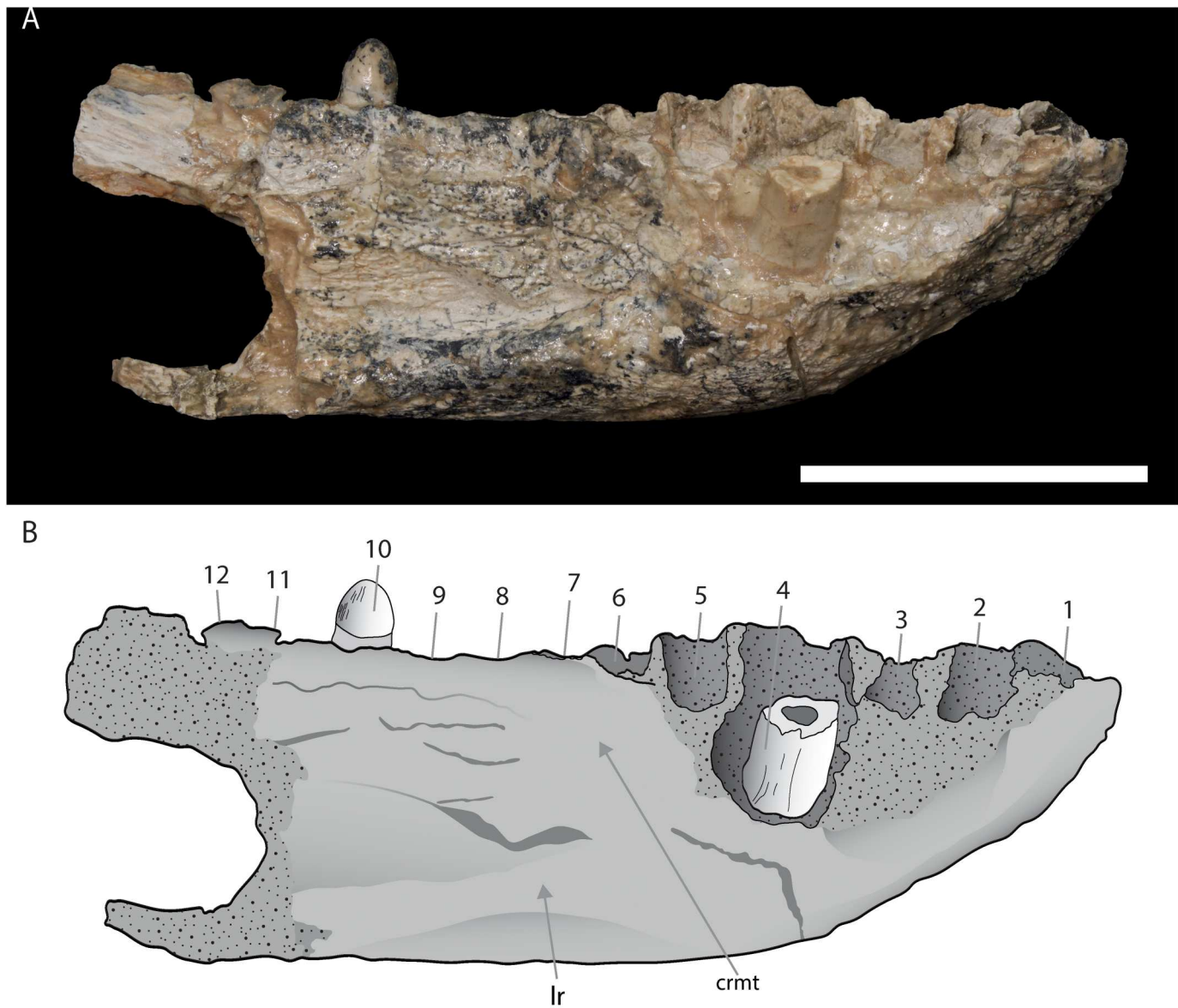


FIGURE 3. A, photograph and B, line drawing of the holotype right dentary of *Eremosuchus elkholicus* (UO-KB-301) in lateral view. **Abbreviations:** crmt, concavity for the reception of maxillary teeth; lr, longitudinal ridge. Numbers adjacent to alveoli refer to tooth position. Scale bar equals 50 mm.

of the crown of the 4th dentary tooth is missing, whereas the 10th dentary tooth is essentially complete, though poorly preserved. The dentary tooth row is distinctly sigmoidal, curving laterally in its anterior half and medially in its posterior region (Fig. 4). The 4th dentary alveolus is the largest, followed very closely by the 1st (Table 2). Posterior to the 4th alveolus, the alveoli are relatively consistent in size to one another,

ranging in diameter between 8–11 mm. The 1st–4th alveoli project anterodorsally, with the greatest anterior deflection present in the first two alveoli, such that the apicobasal axes of both teeth were likely deflected at ~50° from the horizontal. The alveoli become increasingly mediolaterally compressed towards the posterior end of the dentary (Table 2). All well-preserved alveoli are separated by bony septa which extend

TABLE 2. Alveolus measurements of the holotypic (KB-301) and referred dentary (UOK 347) of *Eremosuchus elkholicus*.

Specimen	Measurement (mm)	Alveolus number											
		1	2	3	4	5	6	7	8	9	10	11	12
UO-KB-301	length	16.0	10.0	7.6	16.7	10.0	8.6	8.7	9.0	9.8	8.7	8.1	7.5
	width	12.7	?	?	?	7.3	7.4	7.7	7.9	8.0	7.0	?	?
Referred	length	6.0	3.5	3.6	8.4	4.1	2.7	2.1	2.3	5.0	5.8	?	-
	width	5.4	3.2	3.0	6.4	3.5	2.3	2.1	2.2	3.8	4.2	?	-

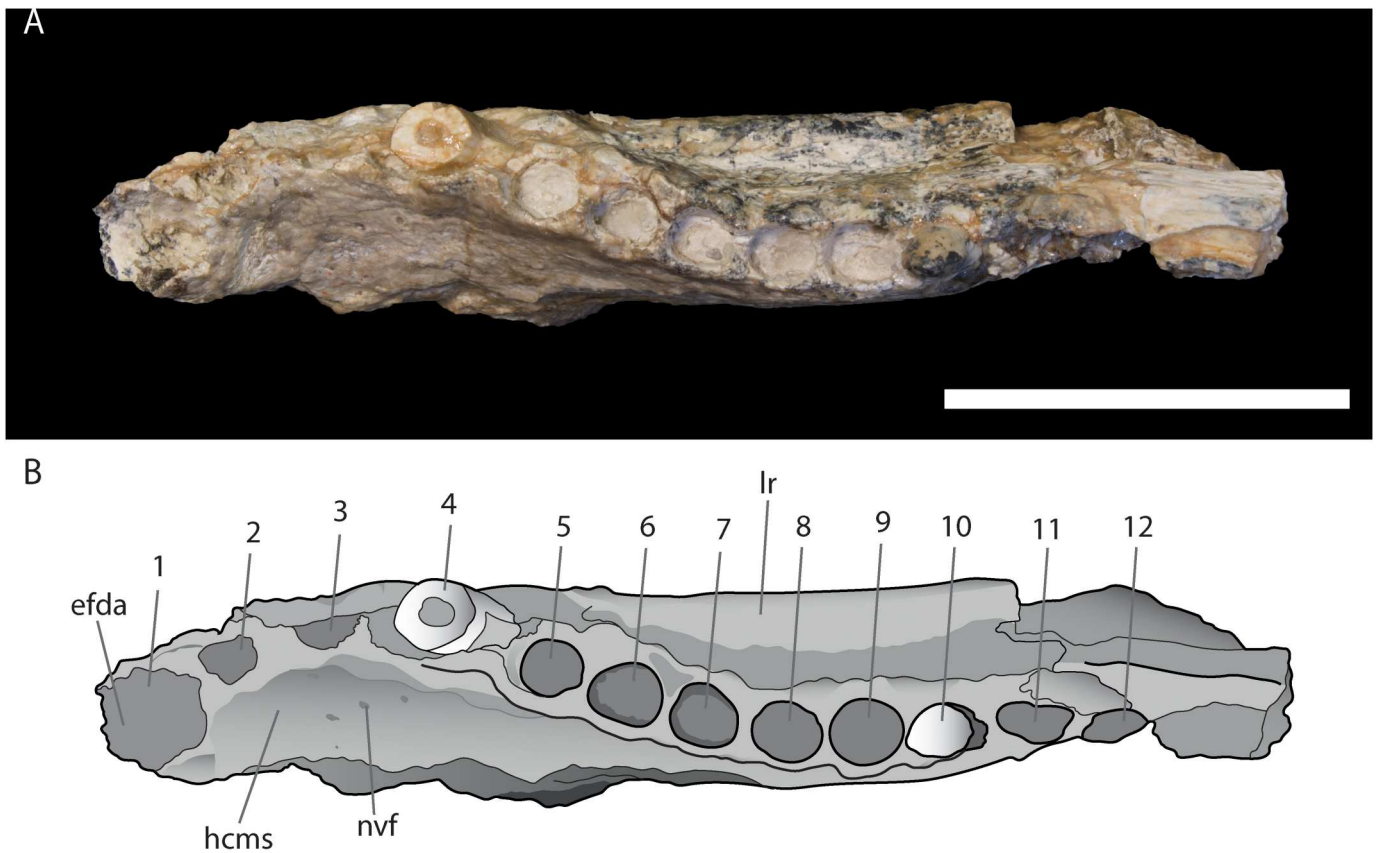


FIGURE 4. A, photograph and B, line drawing of the holotype right dentary of *Eremosuchus elkoholicus* (UO-KB-301) in dorsal view. **Abbreviations:** **efda**, enlarged first dentary alveolus; **hcms**, highly concave mandibular symphysis; **nvf**, neurovascular foramen. Numbers adjacent to alveoli refer to tooth position. Scale bar equals 50 mm.

to the dentary's dorsal surface. These septa are particularly thin towards the posterior region of the tooth row, their mesiodistal length never exceeding a quarter of the diameter of the adjacent alveoli.

The 10th dentary tooth is labiolingually compressed such that the crown has a maximum mesiodistal width to apicobasal length ratio of 0.71, and its alveolus of 0.81. The tooth is lanceolate in labial and lingual views, with a mildly rounded apex (Fig. 8A). Carinae are present on the mesial and distal margins of the tooth; they possess symmetrical denticles along their preserved length, resulting in a serrated appearance. There are approximately 4–5 denticles per mm. Where preserved, the denticles do not substantially vary in size along the apicobasal length of the tooth. They are separated from each other, representing the 'true' ziphodont condition *sensu* Prasad and Lapparent de Broin (2002). Though not well preserved, the enamel is relatively smooth towards the base of the crown, but slightly more wrinkled towards the apex. There are no apicobasal ridges present, and no evidence of wear facets on either the lingual or labial surfaces of the tooth. Much of the crown of the 4th tooth has broken off and therefore its full shape cannot be determined (Figs. 3, 8A); however, its overall morphology appears to be less labiolingually compressed than the preserved posterior tooth and is typically caniniform.

Description of the Immature Specimen Referred to *Eremosuchus elkoholicus*

Dentary—The left dentary of UOK 347 is missing its posterior-most portion. A posteroventral fragment, detached from the

main body, is also preserved (Fig. 9). In general, the specimen is in good condition, with surface patterns and small-scale morphological features more clearly visible than in the holotype specimen. Several large cracks run throughout the dentary, although they do not distort its overall morphology. The majority of the damage is restricted to the teeth, most of which are either missing or incomplete. Despite this, we find evidence of tooth replacement in alveoli 4, 6, 9, and 10.

The main dentary fragment is 60 mm in anteroposterior length, and, when combined with the smaller posterior fragment, this extends to 85 mm. In its anterior region, the dentary is dorsoventrally expanded, with a mediolateral width to dorsoventral height ratio of 0.66 at the level of the fourth tooth. Although the splenial is absent, it can be estimated that each mandibular ramus diverged at an angle of between 15–20° from the sagittal midline, potentially at a slightly higher angle than in the holotype. In dorsal view, the lateral margin curves anteromedially to form a mandibular symphysis that is 'U'-shaped, similar to the morphology in UO-KB-301 (Fig. 10). However, the enlarged 4th dentary tooth of the immature specimen results in a substantial lateral expansion of the mandibular symphysis at the equivalent level, such that the dentary reaches a maximum mediolateral width of 12 mm at the level of the posterior margin of the 4th alveolus. It therefore appears that the mandibular symphyseal surface is relatively broader than that of the holotype specimen. The dorsal surface of the dentary symphysis is smooth, as in UO-KB-301. Other than a singular linear row of seven equidistantly spaced neurovascular foramina positioned 3 mm ventromedial to the tooth row, the dorsal surface lacks a

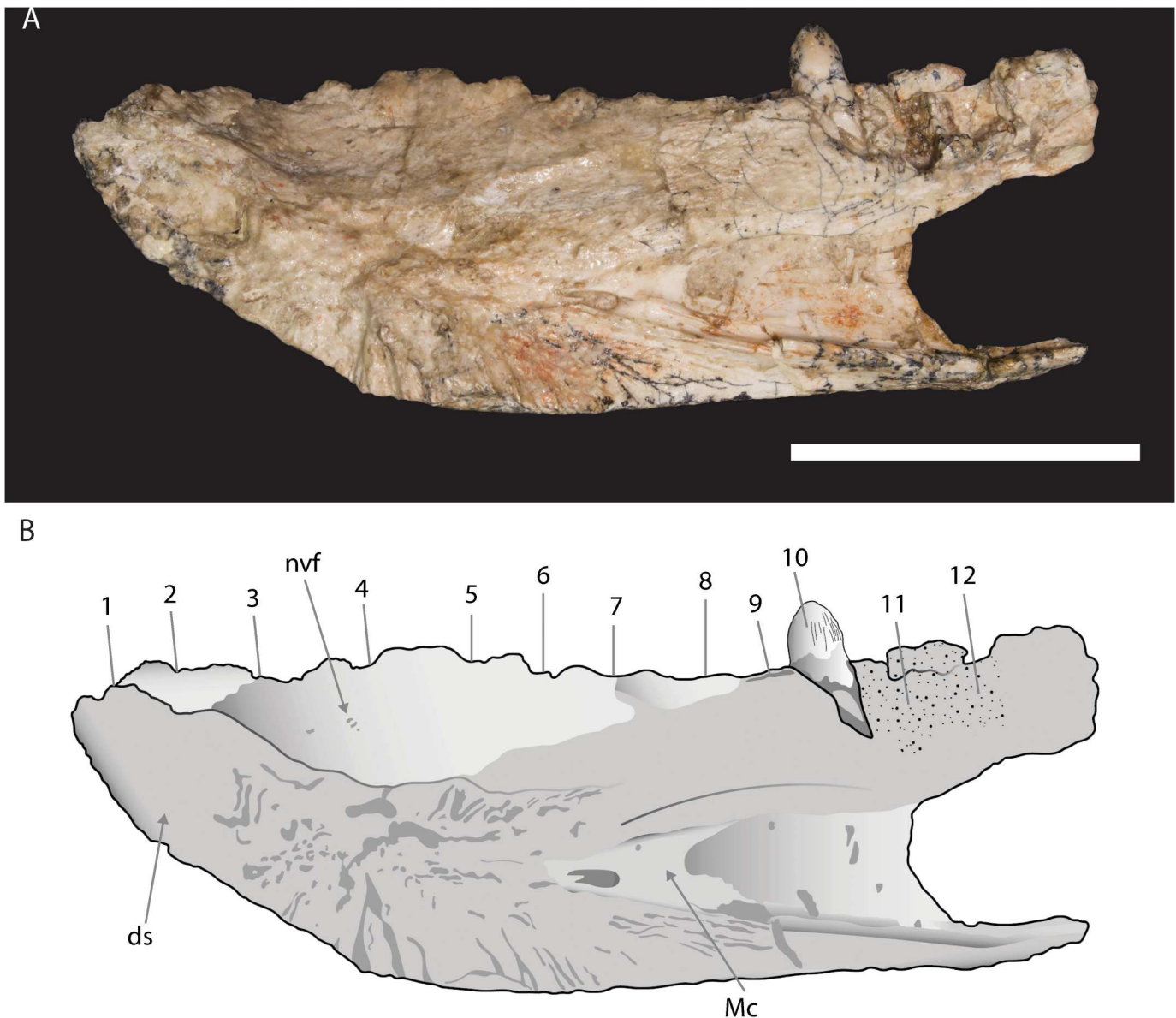


FIGURE 5. **A**, photograph and **B**, line drawing of the holotype right dentary of *Eremosuchus elkoensis* (UO-KB-301) in medial view. Abbreviations: **ds**, dentary symphysis; **Mc**, Meckelian canal; **nvf**, neurovascular foramen. Numbers adjacent to alveoli refer to tooth position. Scale bar equals 50 mm.

similar degree of ornamentation as the lateral and ventral surfaces. The dorsal surface slopes ventromedially at an angle of around 45° from the horizontal, contrasting with the slightly steeper surface in the holotype of *Eremosuchus*. On the dorsal surface of the dentary symphysis, the dentary-dentary suture is estimated to extend posteriorly to the level of the 6th alveolus and is therefore slightly anteroposteriorly longer than in UO-KB-301, in which it extends to the 5th alveolus. The medial margin of the dentary, along its contact surface with the splenial, is approximately straight and is directed anteromedially, likely forming a 'V'-shaped suture, as in the holotype specimen.

In lateral view, the anterior convexity of the dorsal margin expands to a maximum dorsoventral height of ~20 mm at the level of the 4th alveolus. Posterior to this, the dorsal margin is concave, reducing to a dorsoventral height of 17 mm at the level of the 7th alveolus, before expanding dorsally towards the posterior end. The overall curvature of the dorsal margin into

two distinct 'waves' is similar to that of the holotype of *Eremosuchus*. Anteroposteriorly orientated, evenly spaced, shallow grooves sculpt the lateral and ventral surfaces of the dentary, rarely exceeding 5 mm in length. Larger, more circular pits are only present on the ventral and anterior surfaces of the dentary, as in the holotype.

From the 7th alveolus posteriorly, the dorsal two-thirds of the dentary are mediolaterally compressed and are essentially vertical. The lateral surface is confluent with the dorsolateral margin of the tooth row, as in the holotype. The ventral third of the dentary is laterally expanded, such that a ridge runs posteriorly from the level of the 8th alveolus (Figs. 9–12). Though prominent, this ridge is not as conspicuous as in the holotype *Eremosuchus* specimen. Dorsal to this ridge, the space laterally adjacent to the vertical dentary wall likely formed an area for the reception of several maxillary teeth. As in UO-KB-301, the dentary is broken towards its posterior end, and therefore

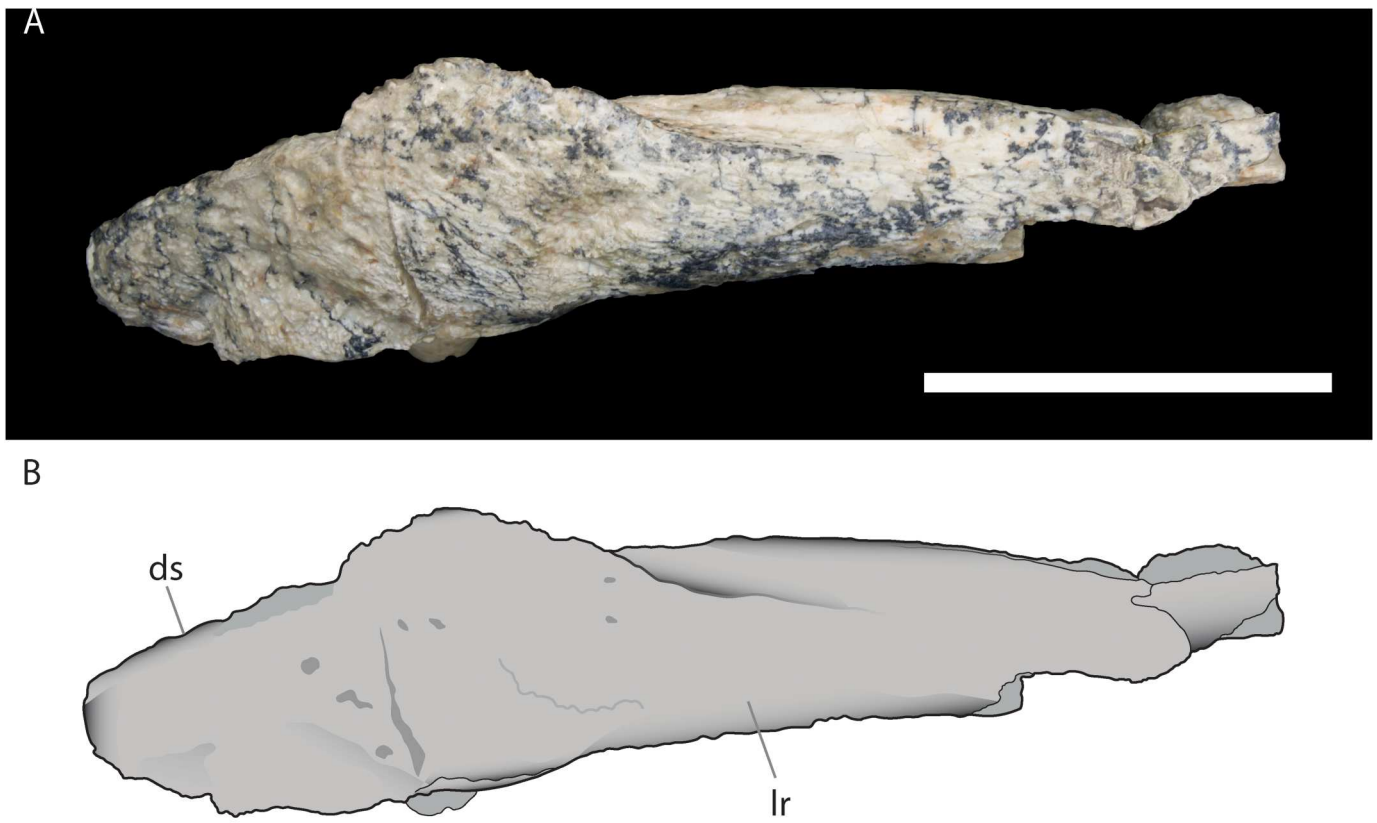


FIGURE 6. **A**, photograph and **B**, line drawing of the holotype right dentary of *Eremosuchus elkoholicus* (UO-KB-301) in ventral view. **Abbreviations:** **ds**, dentary symphysis; **lr**, longitudinal ridge. Scale bar equals 50 mm.

it is not possible to evaluate whether a mandibular fenestra is present.

The medial dentary surface is essentially vertical. On the exposed medial surface of the mandibular symphysis, the Meckel's groove extends to a level adjacent with the posterior boundary of the 4th alveolus, reaching further anteriorly than that in the holotype of *Eremosuchus* (Fig. 11). This groove is dorsoventrally narrowest at its anterior end, increasing in dorsoventral height and mediolateral depth posteriorly.

Dentition—Twelve dentary alveoli are present, though the total number is unclear given the preservation of this specimen. The 2nd, 3rd, 5th, 8th, and 11th dentary teeth are missing, and the 1st tooth is present but unerupted. The 4th, 6th, 7th, 9th, and 10th teeth are erupted, but only the 4th and 9th are essentially complete (Figs. 8, 13). In dorsal view, the dentary tooth row is mildly sinusoidal, with the anterior half being substantially more curved laterally than the posterior region is curved medially (Fig. 10). It seems likely that the mesial edge of the 1st alveolus is broken and missing, but it is possible that it was genuinely absent, such that the paired jaws lacked a complete septum between the two anteriormost teeth. Septa separate all adjacent alveoli, except those of the 6th and 7th teeth, which are set in a continuous groove. As in the holotype, the septa of UOK 347 are narrow, particularly in the posterior region of the tooth row. A small diastema is present between the 7th and 8th alveoli. Similarly to UO-KB-301, the 4th alveolus is the largest, followed by the 1st (Table 2), though the latter is much smaller than the former, unlike the holotype. Posterior to the 4th alveolus, the alveoli reduce in size up to the 7th alveolus, before increasing in size again posteriorly, seemingly differing from the condition in UO-

KB-301, wherein the alveoli remain approximately the same size. The 1st tooth is conical, and is closest to circular at its base, narrowing to an acute point at its apex. It is strongly recurved. The 4th tooth is slightly more labiolingually compressed, though is still classically caniniform in its shape. This tooth thins labiolingually towards its mesial and distal ends, creating flange-like crests (*sensu* Prasad and Lapparent de Broin, 2002). The 1st tooth is procumbent, and the 4th leans mildly anteriorly. From the positioning of the 2nd alveolus, it can be inferred that this tooth was procumbent too, almost as strongly as the 1st.

The 6th tooth is greatly reduced in size compared with those preserved anteriorly to it. Though the apex is missing, it is lanceolate in lingual and labial views, and is mildly labiolingually compressed. The 9th tooth is also lanceolate in shape, but is more triangular than the 6th, having straighter mesiodistal margins. It is more labiolingually compressed than the teeth situated anteriorly to it. Both the 6th and 9th teeth thin labiolingually towards their mesiodistal margins, creating a flange that encircles the crown of the tooth. From the 5th tooth posteriorly, all crowns are essentially orientated dorsoventrally along their major axis. The enamel of the lingual and buccal surfaces of all the teeth is smooth. Serrated carinae are present on the mesial and distal tooth margins of all teeth, and are adorned with regularly spaced denticles (3–4 denticles within 1 mm). The teeth lack evidence of wear facets, or of apicobasal ridges.

Tooth Replacement—The 4th, 6th, 9th, and 10th alveoli are characterised by 'replacement' teeth, with evidence of new teeth growing under those that are protruding, as seen from the CT scan data (Fig. 14). The replacement of the 10th tooth appears to be the most advanced, in Stage V of the proposed

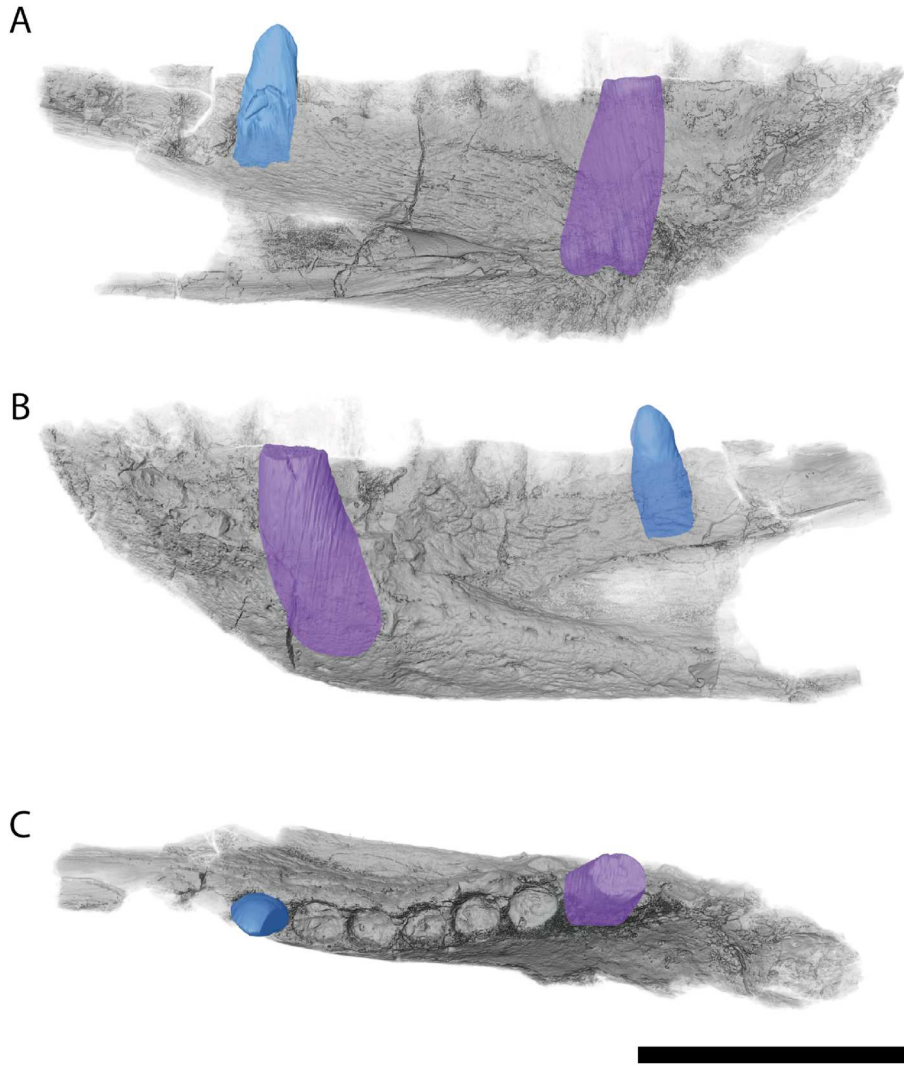


FIGURE 7. Computed tomography scans of the *Eremosuchus elkoensis* holotype right dentary (UO-KB-301) in **A**, medial; **B**, lateral; and **C**, dorsal view. Scale bar equals 10 mm.

seven growth stages in living crocodylians, whereby the replacement tooth starts to erode the labial side of its predecessor (Hanai & Tsuihiji, 2019; Fig. 14D). The replacement of the 4th and 9th teeth appear to be in Stage IV of tooth growth in crocodylians (Fig. 14A, C), whereby the replacement tooth moves into the pulp cavity of its predecessor (Hanai & Tsuihiji, 2019). The replacement of the 6th tooth is the least advanced, appearing to also be in Stage IV, but earlier than teeth 4 and 9 (Fig. 14B).

Description of Material Tentatively Referred to *Eremosuchus*

Mandible—The mandibular fragment (UO-KA-401) consists of the poorly preserved posterior region of the surangular and angular, as well as the complete articular (Fig. 15C, D). Though the specimen is missing, descriptions and photographs of the lateral and dorsal surfaces (Fig. 15C, D) are included in Buffetaut (1989:pl. 2c). Buffetaut (1989) suggested that a continuous sheet of bone in the anterior region of the specimen indicates the absence of a mandibular fenestra; however, the damage to this region means that this cannot be ascertained with any certainty. Precise sutures between the mandibular elements are difficult to determine from the photographs in Buffetaut (1989), making identification of individual bones difficult; however, the

surangular is described as being mediolaterally expanded in its dorsal region, becoming thinner ventrally. The surangular participates in both the glenoid fossa and the retroarticular process, forming approximately one third of the latter's mediolateral width. The dorsal surface of the surangular exposed on the retroarticular process is heavily excavated. Its medial-most surface is steeply inclined (though the extent is unclear from the photographs) and faces posterolaterally (Fig. 15C). The lateral half of the surangular exposed on the retroarticular process is shallower, forming a shelf.

The glenoid facet for the reception of the quadrate condyle is mediolaterally wider than anteroposteriorly long, though the exact dimensions cannot be determined. It is separated from the retroarticular surface by a prominent, dorsally protruding ridge that extends mediolaterally across the mandibular ramus (Fig. 15C). The boundary between the surangular and the articular on the dorsal surface of the retroarticular surface occurs along an approximately anteroposteriorly orientated ridge, with only very mild posterolateral deflection (Fig. 15D). In lateral view, this ridge is concave and asymmetric, such that its anterior margin is positioned dorsally to the posterior margin. At its posterior-most end, the lateral flange of the retroarticular process is mildly upturned. The medial flange of the retroarticular process

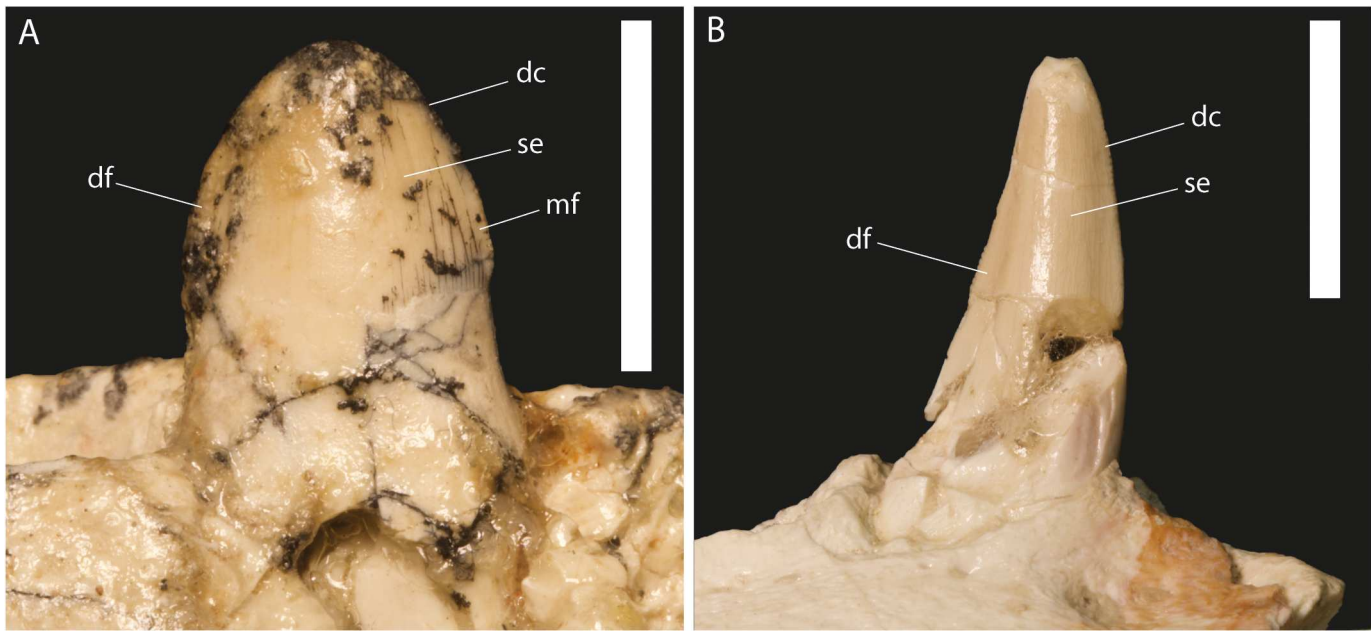


FIGURE 8. **A**, photograph of the 10th tooth of the holotype right dentary of *Eremosuchus elkholicus* (UO-KB-301) in labial view; **B**, photograph of the 4th tooth of the referred *Eremosuchus* left dentary (UOK 347) in lingual view. **Abbreviations:** **dc**, denticulated carina; **df**, distal flange; **mf**, medial flange; **se**, smooth enamel. Scale bars equal 10 mm.

has a strong ventromedial deflection from the horizontal, such that its dorsal surface is almost perpendicular to that of the lateral flange. Its medial margin is gently convex in dorsal view. On the proximal region of the dorsal surface of the medial flange, it appears as though there is a small, approximately circular prominence, likely no more than one third of the mediolateral width of the medial flange in its circumference (Fig. 15D). It is possible that this bulge is associated with the foramen aerum, though this cannot be confirmed from the photographs. The dorsal surface of the lateral retroarticular flange is strongly inclined such that it almost faces completely laterally, except for the ventral-most section, which forms a small, laterally protruding shelf. In dorsal view, the lateral margin is only very mildly convex. The preserved section of the angular is exposed on the lateral surface of the mandible; however, the location of its boundaries with adjoining elements are unclear.

Dentition—Of the five isolated teeth mentioned, three (UO-KA-118, UO-KA-117, UO-KA-402) are figured in Buffetaut (1989:pl. 2a, b, e, f, g).

Specimen UO-KA-118 (Fig. 15G) is conical, with a well-worn but pointed apex; it is closest to the typical caniniform morphology. Thus, it is likely that the tooth was positioned within the first four teeth of the dentary tooth row. The tooth is mildly lingually curved, such that its buccal surface is convex, and, although only figured in distal view, it is assumed to be recurved. Though not clearly visible in the photographs, it

appears that fine-scale apicobasal ridges are present on the enamel towards the apex of the tooth. It is not possible to determine the presence or absence of denticles on the mesiodistal cutting edges due to a large amount of wear in the relevant regions.

Specimen UO-KA-117 is also close to a typical caniniform morphology (Fig. 15A, B), being slightly more labiolingually compressed than UO-KA-118, suggesting an anterior to middle position in the tooth row. The tooth is subtriangular in labial and lingual views, forming an acute point at its apex, and is slightly recurved. Its crown is relatively labiolingually compressed, having a basal labiolingual width to mesiodistal length ratio of 0.75. Again, it is difficult to determine the nature of the enamel pattern; however, it appears that fine-scale, bifurcating apicobasal ridges are present, particularly towards the apex of the tooth. The tooth thins in labiolingual width towards its mesiodistal margins, creating a flange-like structure along each cutting edge. These carinae possess denticles along their length, though it is unclear whether their size is consistent.

Apicobasally shorter than UO-KA-117 and 118, UO-KA-402 (Fig. 15E, F) is interpreted as being from the posterior region of the tooth row, due to its more globular, lanceolate shape. It is labiolingually compressed, such that the crown has a maximum labiolingual width to mesiodistal length ratio of ~0.7. The quality of the photographs means that it is difficult to determine finer scale details; however, the enamel at the apex of the tooth appears to be adorned with narrow anastomizing apicobasally

TABLE 3. Results of phylogenetic analyses including the number of most parsimonious trees (MPTs), tree length of the MPTs, and consistency (CI) and retention (RI) indices obtained from the MPTs.

Analysis	Included material	Weighting	MPTs	Tree length	CI	RI
1	holotype and referred dentary	equal	12	18,4690.5	0.286	0.737
2	holotype and referred dentary	$k = 3$	42	15,742.7	0.276	0.725
3	holotype and referred dentary	$k = 8$	15	9371.1	0.283	0.733

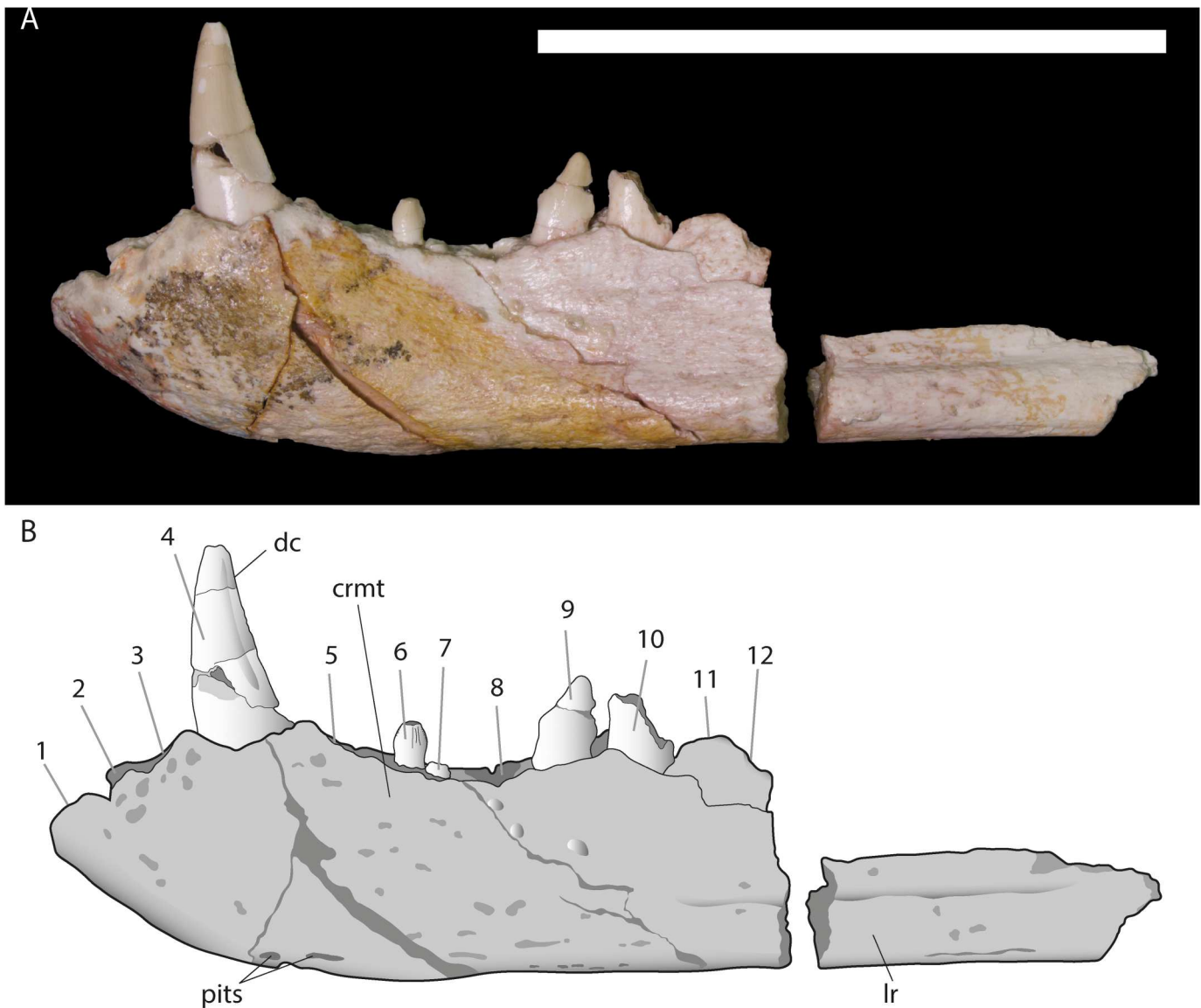


FIGURE 9. A, photograph and B, line drawing of the referred *Eremosuchus* dentary (UOK 347) in lateral view. Abbreviations: crmt, concavity for the reception of maxillary teeth; dc, denticulated carina; lr, longitudinal ridge. Numbers adjacent to alveoli refer to tooth position. Scale bar equals 50 mm.

directed ridges. It is unclear whether this ornamentation continues towards the base of the crown. Denticulated carinae adorn the mesial and distal margins; however, it cannot be determined if there is variation in the size of individual denticles along the cutting edge. The tooth has its maximum constriction at the boundary between the crown and the root.

In addition to these previously described specimens, three unpublished teeth collected during the 1982 expedition are known from the type locality: two from the KB site (UOK 344–345), and one from KA (UOK 346). Specimen UOK 345 (Fig. 16E–H) is conical in shape, recurved, and curved slightly medially. The caniform appearance suggests an anterior position in the tooth row. Fine striations run from the apex towards the base of the preserved enamel, diminishing in their prominence towards the base, such that the enamel surface becomes smooth in this region. Denticulated carinae adorn the distal and mesial margins, with approximately four denticles per mm. The size of the denticles does not vary along the apicobasal length.

The entirety of the UOK 344 (Fig. 16A–D) crown is complete, as well as a substantial part of its root. The crown is bulbous and cordate in buccal and lingual views, suggesting a posterior position in the dentary tooth row. It is labiolingually compressed, with a maximum labiolingual width to mesiodistal length ratio of approximately 0.6. The enamel is patterned with fine, anastomizing ridges towards the crown apex, but is ornamented with more globular protrusions towards the base. Denticulate carinae are present on the mesiodistal margins of the tooth (approximately four denticles per mm). There is minimal variation in the size of denticles along the carinae. The tooth thins labiolingually towards its mesiodistal margins, creating a small flange on each.

Specimen UOK 346 (Fig. 16I–L) is small and globular, being cordate in buccal and lingual views, suggesting a more posterior position in the tooth row. It is highly labiolingually compressed, having a maximum labiolingual width to mesiodistal length ratio of approximately 0.55. Undulating apicobasal ridges are present on the enamel of the dorsal-most three quarters of the crown,

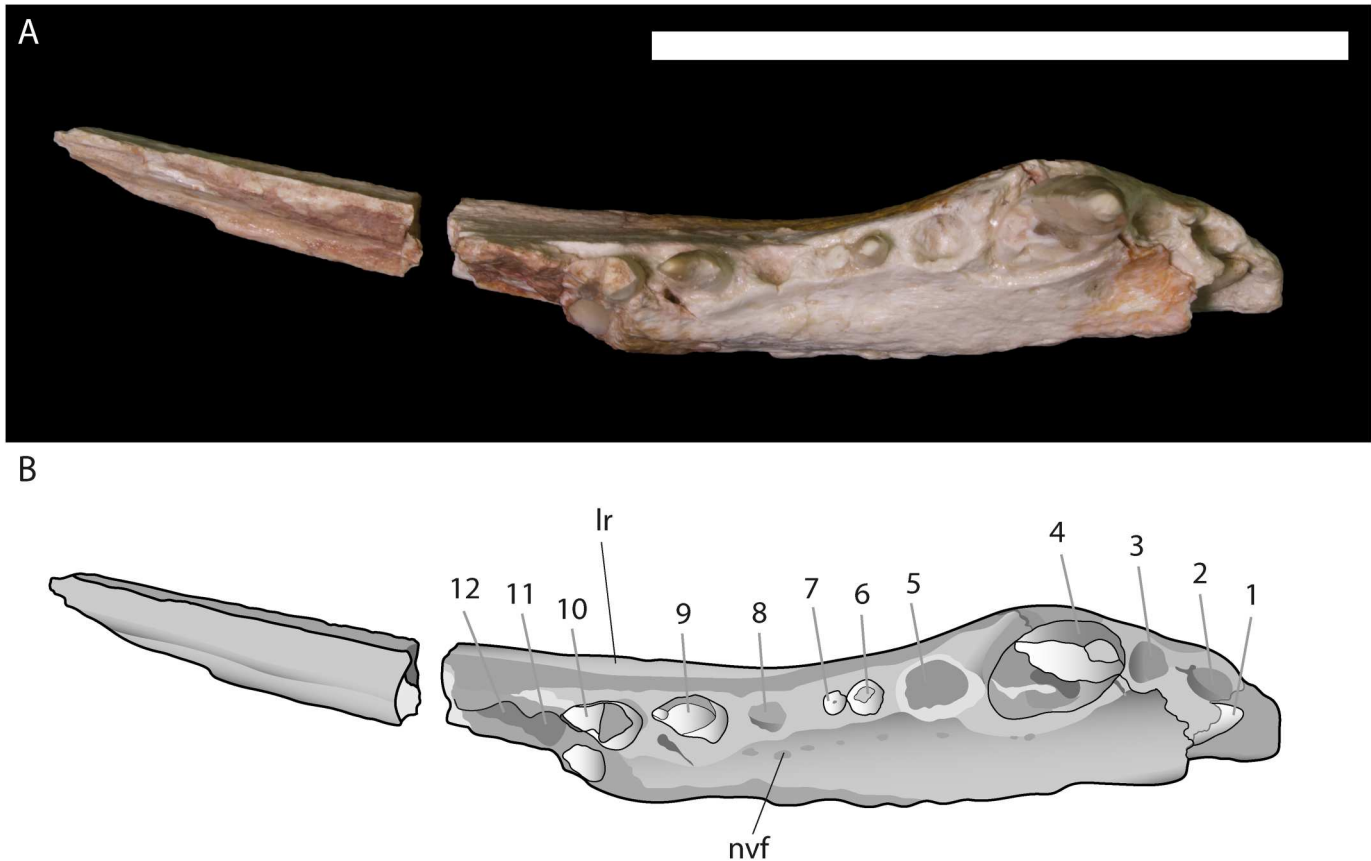


FIGURE 10. **A**, photograph and **B**, line drawing of the referred *Eremosuchus* dentary (UOK 347) in dorsal view. **Abbreviations:** **lr**, longitudinal ridge; **nvf**, neurovascular foramen. Numbers adjacent to alveoli refer to tooth position. Scale bar equals 50 mm.

though these ridges become less continuous towards the base of the crown, creating a more globular appearance. Prominent carinae form the mesiodistal margins, with approximately five denticles per mm.

Vertebrae—Buffetaut (1989) assigned two dorsal vertebrae (UO-KB-405 and UO-KB-406) and two caudal vertebrae (UO-KB-407 and UO-KB-408) to *Eremosuchus elkoensis*. Of these, only the caudal vertebrae were figured by Buffetaut (1989:pl. 2h–j), and only a single caudal centrum (UO-KA-408) can be located out of any of the vertebral remains (Fig. 15H, L–P). It is unclear from the description in Buffetaut (1989:p. 5) as to the completeness of KB-405 and KB-406, as the only information provided is that they are amphicoelous, “with a rounded ventral edge and a pronounced constriction in the middle,” suggesting that the remains may just be represented by centra. It is also unclear how Buffetaut (1989) determined the position of these two elements in the vertebral column.

Vertebra UO-KA-408 is amphicoelous, with relatively shallow convexities on the anterior and posterior articular surfaces of the centrum (Fig. 15O, P). The anterior articular surface is very slightly elliptical and is dorsoventrally taller than it is mediolaterally wide. Though not fully preserved, the posterior articular surface is likely closer to circular; however, its dorsoventral height is slightly greater than its width. Both articular surfaces are delineated by a relatively broad ridge around their entire circumference. The centrum has a maximum mediolateral width (taken at its posterior articular surface) to maximum anteroposterior length of 0.6, which is indicative of an anterior position in the caudal vertebral series (Darlim et al., 2021; Georgi & Krause, 2010; Iori et al., 2013; Nascimento & Zaher, 2010). The centrum of UO-KA-408 is mediolaterally constricted at its

center, such that the ratio of the narrowest mediolateral width of the centrum to its maximum mediolateral width is 0.42 (Fig. 15N). The ventral surface of the centrum is anteroposteriorly concave, and is close to symmetric; with the neural canal held horizontally, the anteroventral and posteroventral margins are positioned at the same dorsoventral level. This ventral surface is adorned with two longitudinal, parallel ridges running either side of the vertebral midline. The ridges are low, and are located at the centrum anteroposterior mid-point, their total length forming approximately one third of the maximum vertebral length (Fig. 15N). Despite the presence of these ridges, the centrum lacks hemapophyses, suggesting that the centrum could represent the first or second caudal vertebra.

UO-KA-407 is also amphicoelous (Fig. 15I, J). The posterior articular surface of the centrum is close to circular, with a mediolateral width to dorsoventral height of 0.95. This surface is marked by a small central concavity, bounded around its circumference by an especially broad, flat rim (Fig. 15J). It is unclear whether the neurocentral suture is visible in lateral view due to the poor quality of the photographs. The centrum is mediolaterally constricted at the anteroposterior midpoint, though likely not as strongly as in UO-KA-408. In lateral view, the ventral surface of the centrum is asymmetric, such that the posteroventral margin is more ventrally positioned than the anteroventral margin. Two parallel ridges on the ventral surface of the centrum extend from the anteroposterior mid-length to the hemapophyses. The latter are eroded, though still prominent. The presence of hemapophyses generally occurs from caudal vertebra 2 or 3 posteriorly (Georgi & Krause, 2010) and is consistent with UO-KA-408 being an anterior caudal vertebra. The pedicle of the neural arch is preserved on the left side of the vertebra,

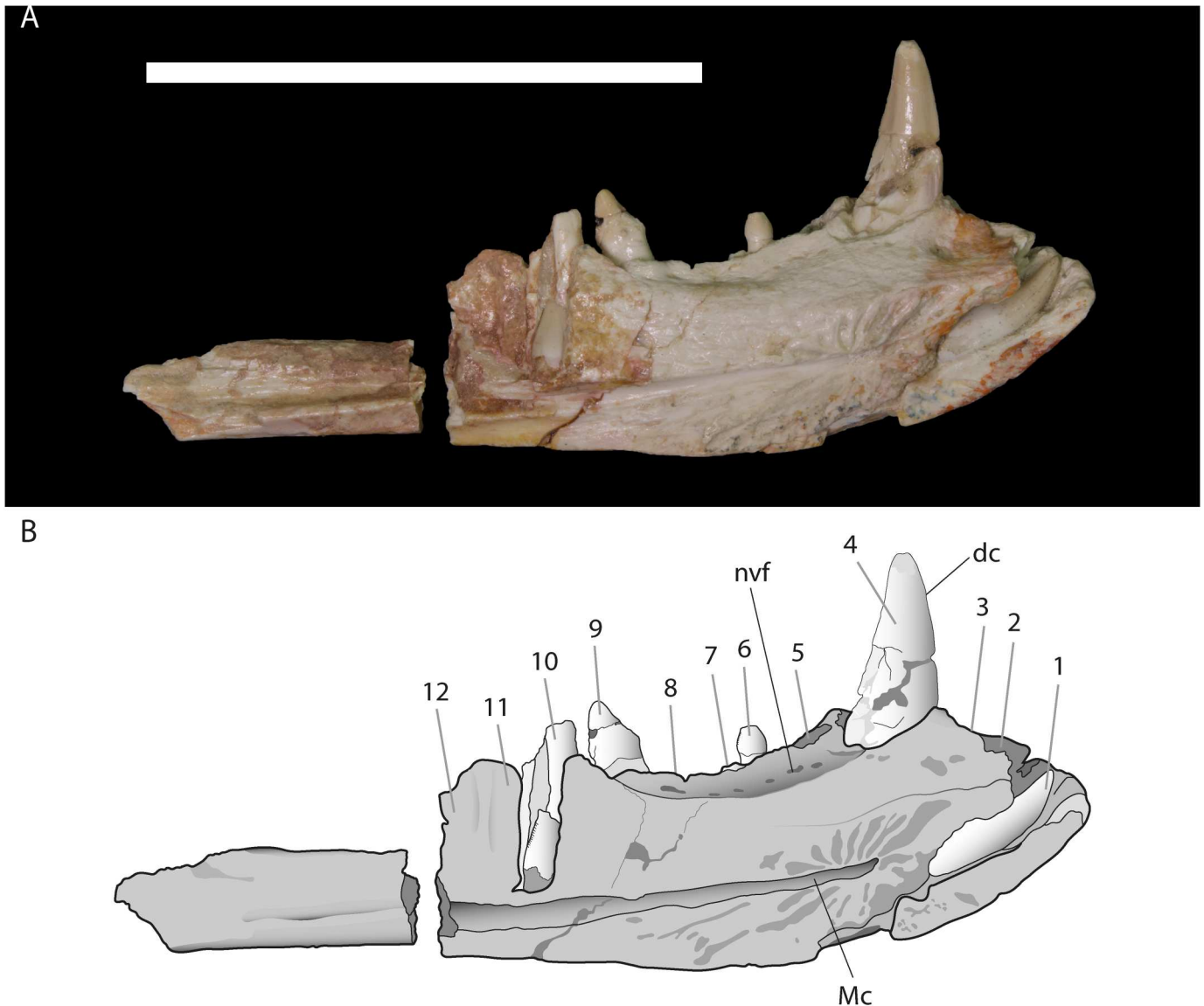


FIGURE 11. **A**, photograph and **B**, line drawing of the referred *Eremosuchus* dentary (UOK 347) in medial view. **Abbreviations:** **dc**, denticulated carina; **Mc**, Meckelian canal; **nvf**, neurovascular foramen. Numbers adjacent to alveoli refer to tooth position. Scale bar equals 50 mm.

and is approximately three quarters of the anteroposterior length of the centrum, with a slight anterior bias.

Fibula—The right fibula (UO-KA-114) is figured in Buffetaut (1989:pl. 2k) in medial view (Fig. 15K). Although the photograph is of low quality, several morphological features can be distinguished. The fibula is proximodistally elongate and slender, particularly mediolaterally. From its proximal end to approximately three quarters of the way along the length of the bone, the shaft gradually decreases in anteroposterior width. It is anteroposteriorly expanded along the distal quarter, albeit to a lesser extent than the proximal end. Both the proximal and distal ends are mediolaterally compressed, whereas the central shaft is more elliptical in its transverse cross section. The proximal fibular head is strongly domed, with at least one well-exposed face exposed proximomedially, and it has a weak, well-rounded posterior projection. A shallow and relatively broad crest runs from the proximal region of the fibula, running proximodistally along the center of the shaft's lateral surface, extending to

between one quarter and one third of the fibula's proximodistal length (though its full proximal and distal extent cannot be ascertained due to damage on the surface of the bone) (Fig. 15K). This crest is probably for the insertion of the *M. iliofibularis*. The distal half of the fibular shaft is strongly bowed posteriorly.

Osteoderms—Buffetaut (1989) listed two osteoderms from the El Kohol locality, though he did not specifically refer them to *Eremosuchus*. They were not figured, with only a brief description that stated that they are rectangular and thin, with “a reduced ornamentation of small pits and irregular grooves” (Buffetaut, 1989:p. 5). Several osteoderm fragments from the KD sub-locality have been identified in the collections of the Université de Montpellier as part of the historical collecting efforts and match the morphology described by Buffetaut (1989); however, we cannot be certain that these are the same elements. One specimen is nearly complete, missing only the dorsal tip of the midline process (Fig. 17A, B, C, D). This osteoderm is approximately 20 mm in anteroposterior

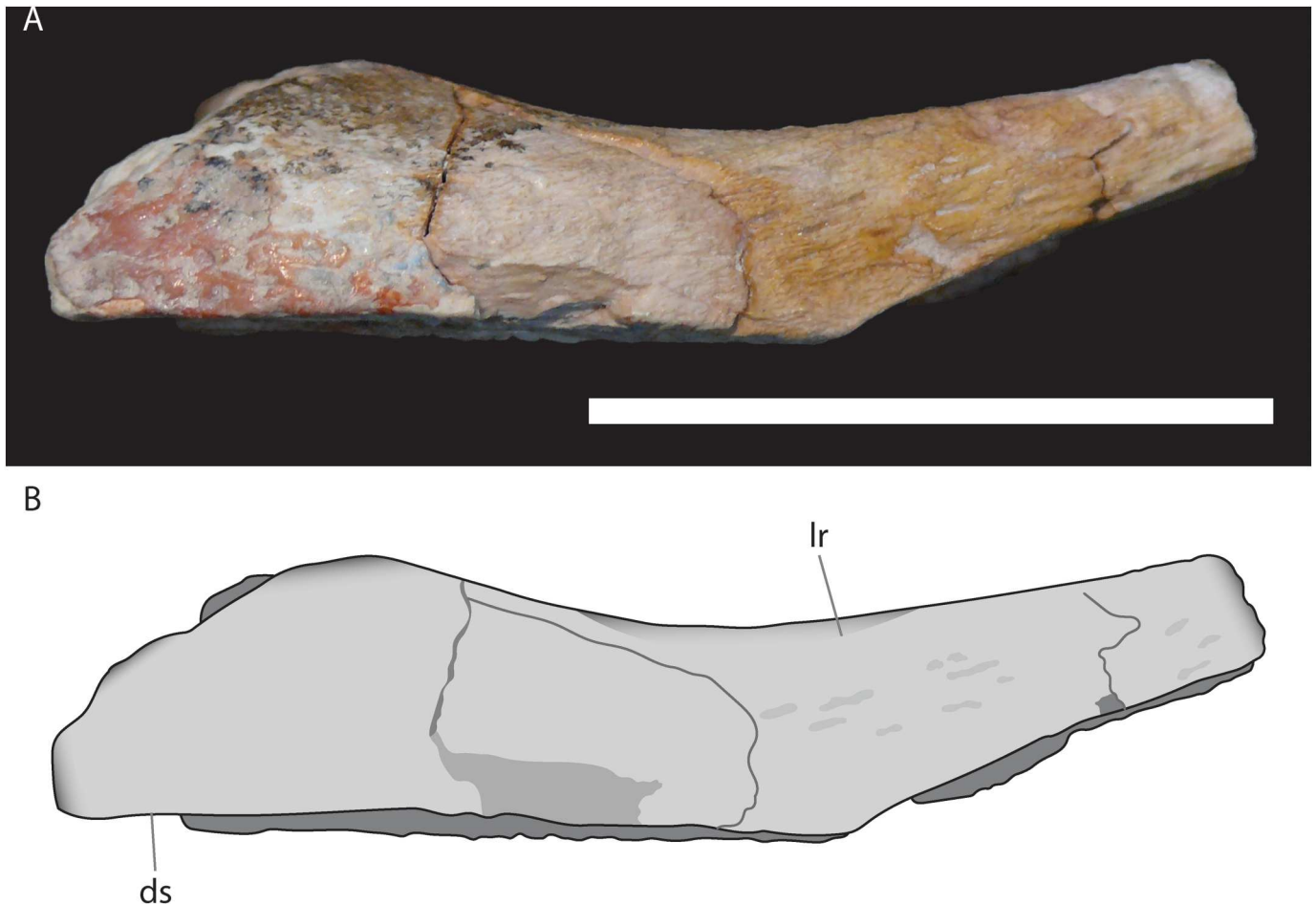


FIGURE 12. A, photograph and B, line drawing of the referred *Eremosuchus* dentary (UOK 347) in ventral view. Abbreviations: ds, dentary symphysis; lr, longitudinal ridge. Scale bar equals 50 mm.

length and 15 mm in mediolateral width. A broad, prominent crest extends for essentially the entire length of the osteoderm. In lateral view, the profile of this crest is convex, and it is taller at one extremity, which is suggested to correspond to the posterior margin (Fig. 17C). In this region, the apex of the crest is broken; however, its dimensions indicate that it may have terminated dorsally as a spine. The lateral margins of the osteoderm are bevelled. In lateral view, these areas show strong indentations that resemble sutures for adjoining osteoderms. As in other osteoderm fragments, the dorsal surface of the bone bears a rugose ornamentation, with narrow, elongated furrows running perpendicular or sub-perpendicular to the midline crest. These fragments are concave on their ventral surface, preserving an interwoven layer for muscular attachment (Fig. 17E). A differing ornamentation is present on the dorsal surface of three osteoderm fragments, in which small, deep, approximately circular pits are interconnected by shallow grooves (Fig. 17F). The overall shape of these osteoderms cannot be interpreted, and the absence or presence of a medial ridge is unknown.

PHYLOGENETIC RESULTS

Analysis 1 – Equal Weights Topology

The equal weights analysis produced 12 most parsimonious trees (MPTs) of length 184690.5 steps (Supplementary File 6)

(Figs. 18, S1) (Table 3). In the strict consensus tree, a monophyletic Sebecosuchia is not recovered; instead Sebecidae and closely related taxa form one of two basal bifurcations of Notosuchia. Sebecidae is moderately well resolved. *Ogresuchus* and *Barinasuchus* form the most deeply nested clade, with *Razanandrongobe* and the European taxa *Iberosuchus* + *Bergisuchus*, and *Dentaneosuchus* forming successive sister species to this pair (Fig. 18). This group forms one branch of a polytomy that also comprises *Ayllusuchus*, *Eremosuchus*, and *Bretesuchus* as separate branches. *Sebecus icaeorhinus* is the sister taxon to this 4-tomy, as one lineage of a more “basal” polytomy from which *Sahitisuchus* and *Zulmasuchus* also diverge. *Loirosuchus* is the sister taxon to Sebecidae under the latter’s minimum clade definition provided by Leardi et al. (2024). *Loirosuchus* + Sebecidae forms one branch of a 3-tomy with *Doratodon carcharidens* and *Doratodon ibericus* comprising the other two lineages (Fig. 18). Amongst the 12 MPTs, *Eremosuchus* is relatively labile, though is most commonly (8 out of 12 trees) allied closely with *Ayllusuchus* and *Bretesuchus*.

In the second branch of Notosuchia, *Stolokrosuchus* forms the sister taxon to all other members of the clade, which are split into two lineages: one comprising Peirosauria, and another formed of Uruguaysuchidae as the sister taxon to Ziphosuchia (Fig. 18). Within Ziphosuchia, *Candidodon*, *Libicosuchus*, *Simosuchus*, and *Pakasuchus* + *Malawisuchus mwakasyungutiensis* split off as early diverging

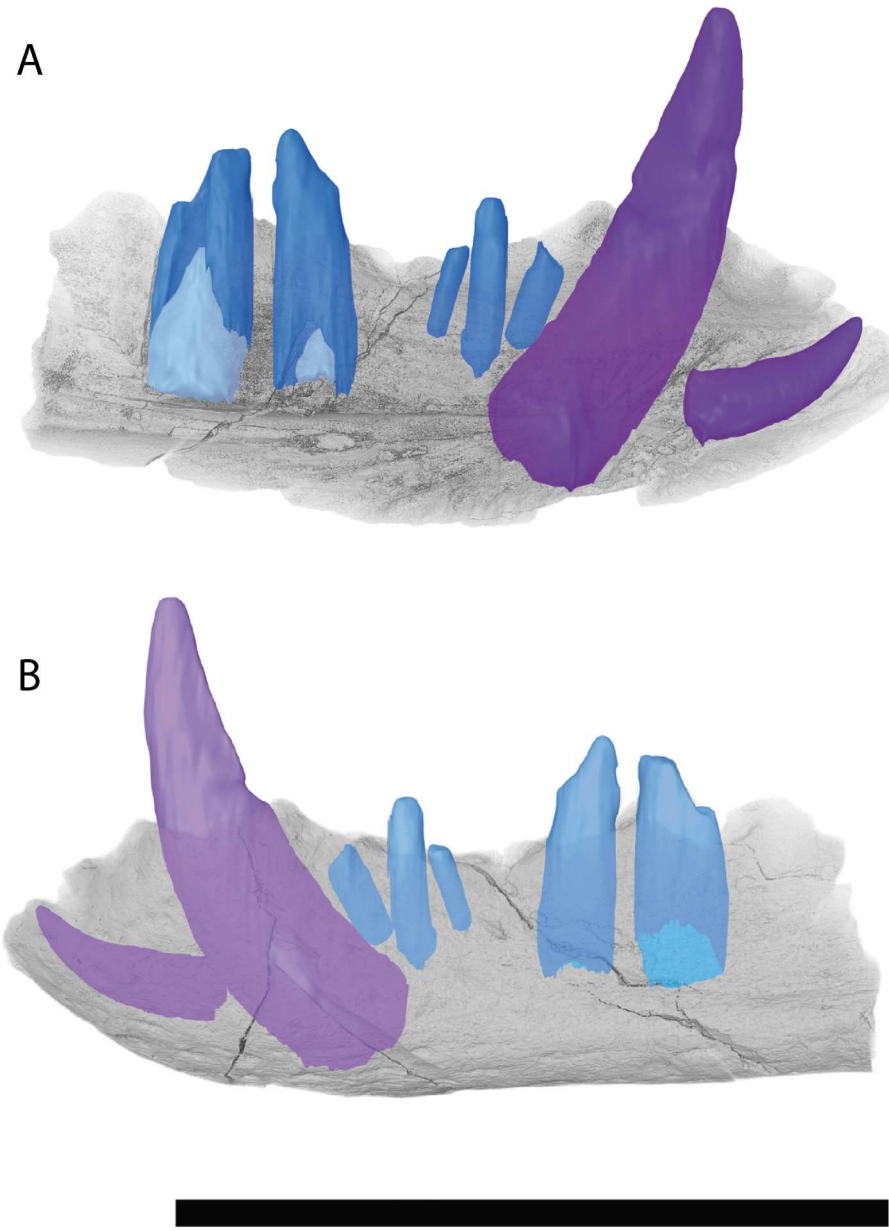


FIGURE 13. Computed tomography scans of the referred *Eremosuchus elkoensis* dentary (UOK 347) in: **A**, lateral view; and **B**, medial view. Scale bar equals 10 mm.

branches, outside of a bifurcation between Baurusuchia and Sphagesauria.

Analysis 2 – Extended Implied Weights Topology, $k = 3$

This analysis produced 42 MPTs of length 15,742.7 steps (Supplementary File 7) (Fig. S2) (Table 3). In the strict consensus tree, a monophyletic Sebecosuchia (Baurusuchia + Sebecoidea) is recovered, deeply nested within Ziphosuchia. Sebecoidea is formed of 10 species. Within this clade, *Dentaneosuchus* + *Bergisuchus* are one lineage of a basal bifurcation, the other of which is formed from *Barinasuchus* and *Iberosuchus* as successive sister taxa to a polytomy comprising (1) *Zulmasuchus*, (2) *Sebecus icaeorhinus*, (3) *Eremosuchus*, and (4) *Ogresuchus* as the sister taxon to *Ayllusuchus* + *Bretesuchus*. Amongst the 42 MPTs, *Eremosuchus* is relatively labile, though remains fairly nested within Sebecidae and is

commonly recovered either in a clade with *Sebecus icaeorhinus* and *Zulmasuchus* or as the sister taxon to all other taxa more derived than *Barinasuchus*.

Within Baurusuchia, *Stratiotosuchus maxhechti*, *Aphaurosuchus*, *Aplestosuchus*, *Campinasuchus dinizi* + *Pissarrachampsia*, and *Cynodontosuchus rothi* form successive sister taxa to a deeply nested, monophyletic Baurusuchia. These taxa comprise Baurusuchidae, as per the minimum-clade definition of Leardi et al. (2024). *Gondwanasuchus scabrosus* is recovered as a non-baurusuchid baurusuchian. *Doratodon* forms the sister taxon to Sebecosuchia. *Chimaerasuchus paradoxus* and *Razanadrongobe* are the earliest diverging taxa in the ‘sebecosuchian’ lineage.

At its base, Notosuchia bifurcates into Peirosauria and a clade comprising all other notosuchians. A monophyletic Uruguaysuchidae is not recovered, rather *A. tsangatsangana* and *Anatosuchus* form successive sister taxa to a group of South American

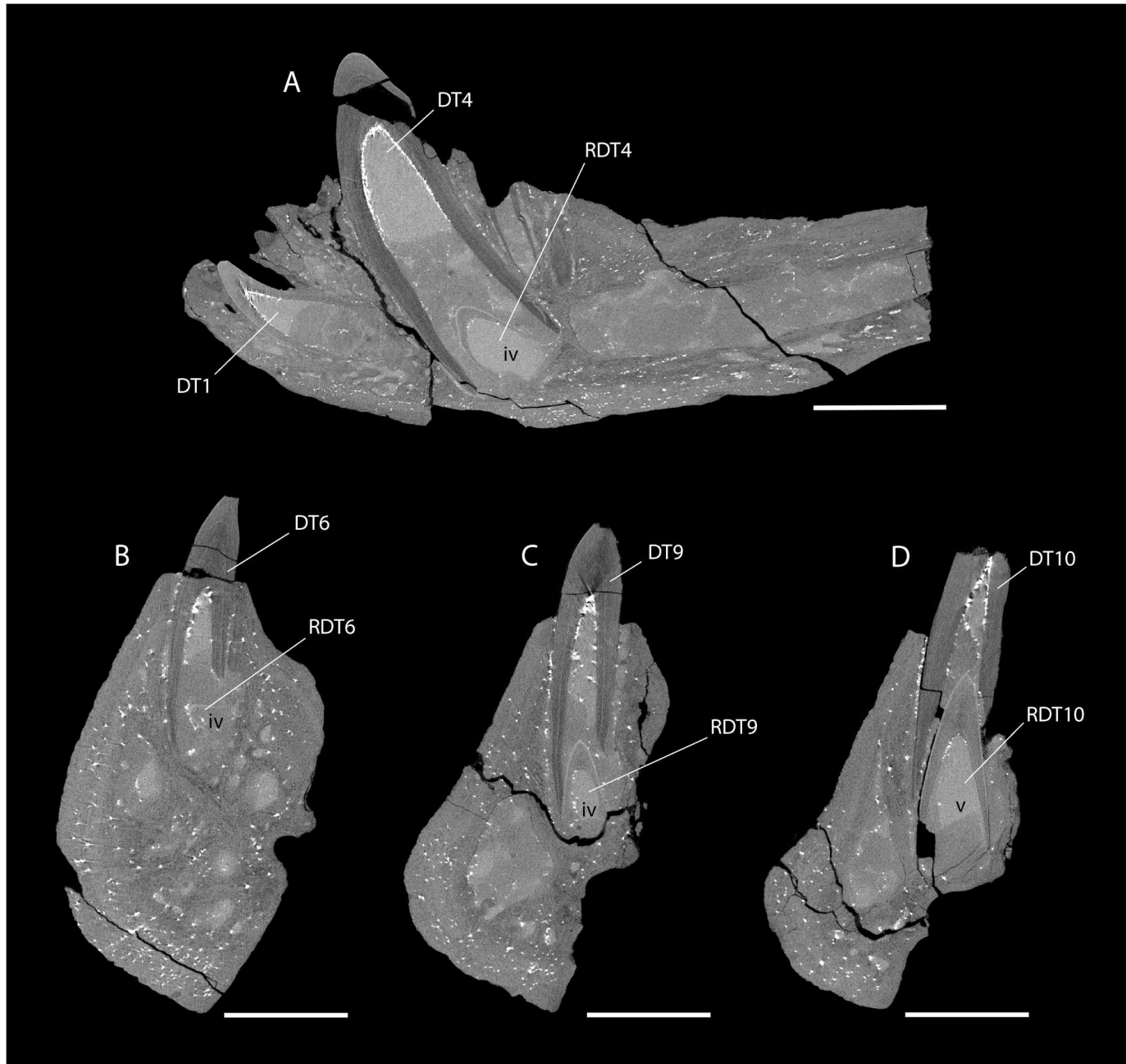


FIGURE 14. Computed tomography slices through the referred *Eremosuchus elkoensis* specimen UOK 347. **A**, longitudinal axis; **B**, transverse axis at the level of the 6th dentary tooth; **C**, transverse axis at the level of the 9th dentary tooth; **D**, transverse axis at the level of the 10th dentary tooth. **Abbreviations:** **DTX**, dentary tooth X; **RDTX**, replacement tooth X; **iv**: Stage IV of tooth growth; **v**: Stage V of tooth growth.

uruguaysuchids. *A. wegneri* forms the sister taxon to *Candidodon itapecuruense* + *Ziphosuchia*. *Sahitisuchus* and *Lorosuchus* are recovered as sister taxa outside of *Sebecosuchia*, and are placed within *Peirosauria* instead.

Analysis 3 – Extended Implied Weights Topology, $k = 8$

This analysis produced 15 MPTs of length 9371.1 steps (Supplementary File 8) (Figs. 19, S3) (Table 3). The strict consensus tree topology is broadly consistent with that recovered by Pol et al. (2014) and subsequent iterations of this matrix (e.g., Fiorelli et al., 2016; Leardi et al., 2015, 2018; Martin et al., 2023;

Martinelli et al., 2018; Martinez et al., 2018; Nicholl et al., 2021), in which Notosuchia splits into *Ziphosuchia*, and a clade comprising *Peirosauria* + *Uruguaysuchidae*. The overall topology of *Ziphosuchia* is broadly similar to Analysis 2, except for a few differences: (1) *Candidodon* is an early diverging *Ziphosuchian*, (2) *Pakasuchus* and *Malawisuchus* are not sphagesaurians, rather they form the sister taxon to *Candidodon*, and (3) *Ogresuchus*, *Ayllusuchus*, *Sebecus*, *Eremosuchus*, and *Bretesuchus* form a deeply nested polytomy within *Sebecidae*. *Sahitisuchus* and *Lorosuchus* are both recovered as *Peirosaurians* in a clade with *Zulmasuchus*. Amongst the MPTs, *Eremosuchus* is most commonly recovered in a highly nested

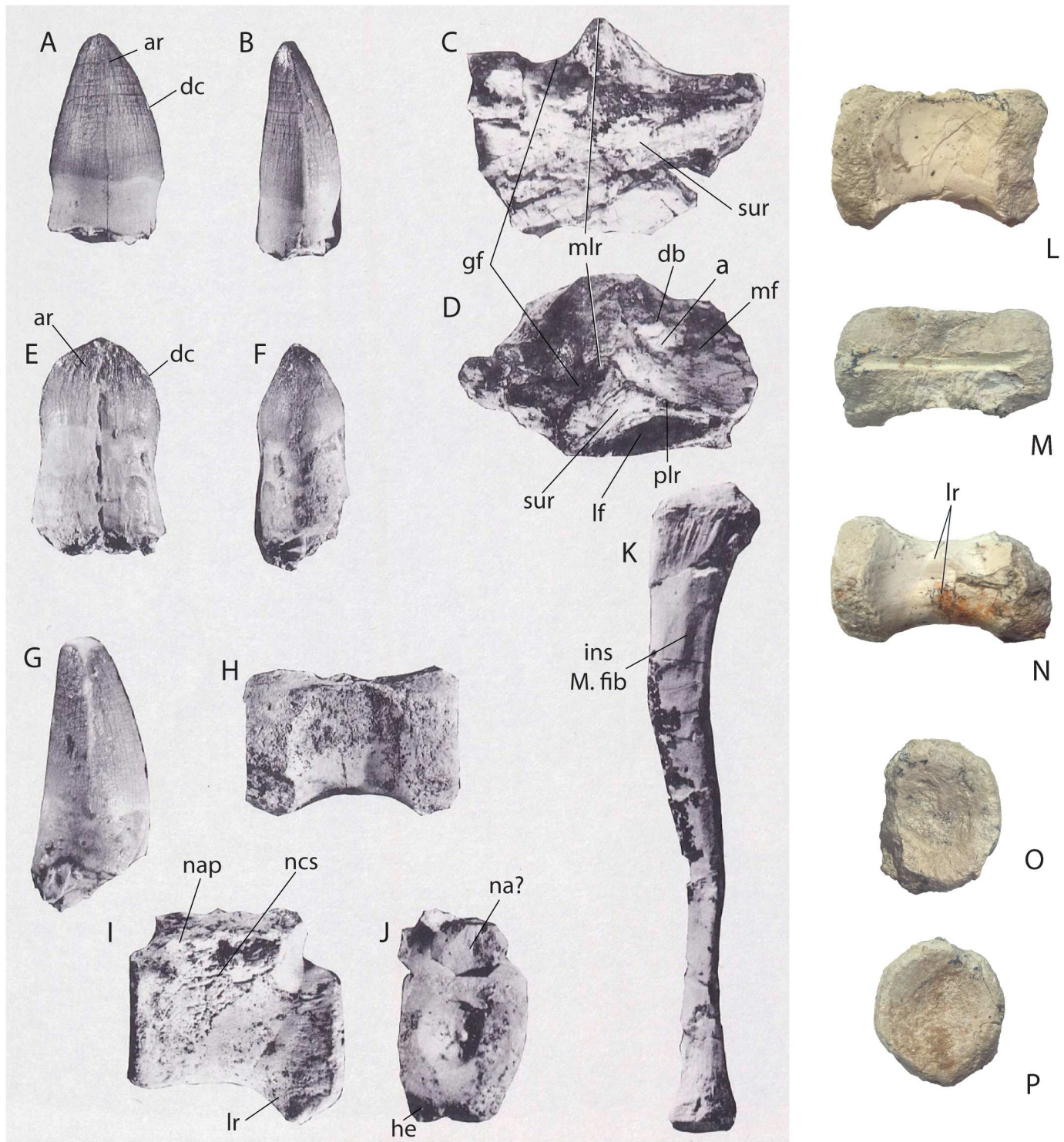


FIGURE 15. Tentatively referred remains of *Eremosuchus elkholicus*. Anterior tooth (UO-KA-117) in: **A**, medial view; and **B**, anterior view. Posterior mandibular fragment (UO-KA-401) in: **C**, lateral view; and **D**, dorsal view. Posterior tooth (UO-KA-402) in: **E**, medial view; and **F**, posterior view. Anterior tooth (UO-KA-118) in: **G**, posterior view. Caudal vertebra (UO-KA-408) in: **H**, right lateral view. Caudal vertebra (UO-KA-407) in: **I**, left lateral view; and **J**, posterior view. Right fibular (UO-KA-114) in: **K**, medial view. Caudal vertebra (UO-KA-408) in: **L**, left lateral; **M**, dorsal; **N**, ventral; **O**, anterior; and **P**, posterior views. **Abbreviations:** **ar**, anastomizing ridges; **db**, dorsal bulge; **dc**, denticulate carina; **gf**, glenoid facet; **he**, hemaphysis; **ins** **M. fib**, insertion for *M. iliofibularis*; **lf**, lateral facet of the retroarticular process; **lr**, longitudinal ridge; **mf**, medial facet of the retroarticular process; **mlr**, mediolateral ridge; **na**, neural arch; **nap**, neural arch pedicle; **ncs**, neurocentral suture; **plr**, posterolateral ridge; **sur**, surangular. **A–K** from Buffetaut (1989, plate 2). Permission to use the image from Buffetaut (1989) was granted by Schweizerbart Science Publishers (www.schweizerbart.de/journals/pala).

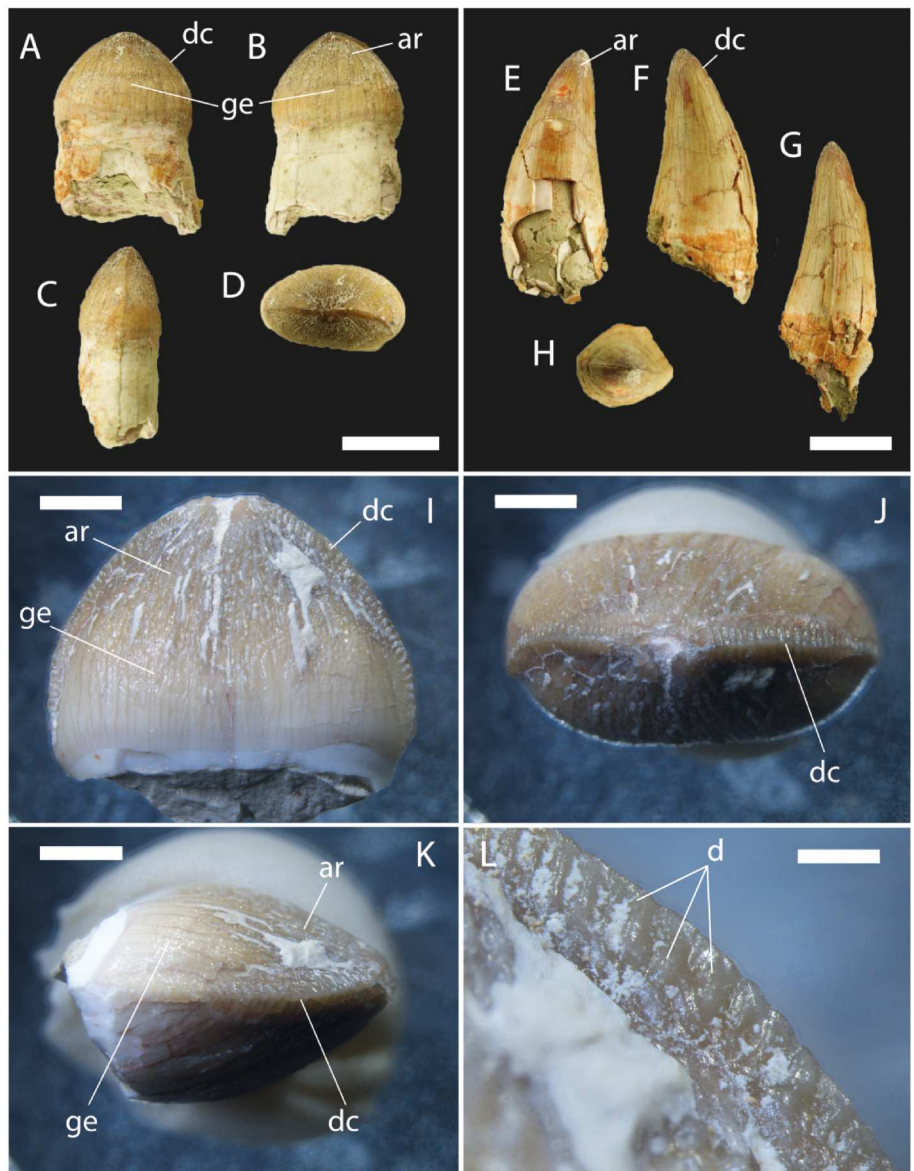


FIGURE 16. Tentatively referred remains of *Eremosuchus elkoensis*. Isolated posterior tooth UOK 344 in: **A**, labial view; **B**, lingual view; **C**, mesial view; and **D**, dorsal view. Isolated anterior tooth UOK 345 in: **E**, labial view; **F**, lingual view; **G**, mesial view; **H**, dorsal view. Isolated posterior tooth UOK 346 in: **I**, lingual view; **J**, dorsal view; **K**, mesial view; and **L**, close-up view of denticulated carina. Abbreviations: **ar**, anastomizing ridges; **d**, denticles; **dc**, denticulated carinae; **ge**, globular enamel. Scale bar equals 10 mm in **A-H**, 2 mm in **I-K** and 0.5 mm in **L**.

clade with either *Ayllusuchus* and *Bretesuchus* or with *Sebecus icaeorhinus* and *Ogresuchus*.

ANATOMICAL COMPARISONS WITH OTHER NOTOSUCHIANS

Given the consistent placement of *Eremosuchus* within Sebecidae in our phylogenetic analyses, as well as its position in earlier studies (Ortega et al., 1996; Turner & Calvo, 2005), anatomical comparisons are primarily made with other species recovered as sebecids herein. However, we also make comparisons with other notosuchians, particularly peirosaurids, baurusuchids, and taxa that have previously been regarded as sebecids. Unless otherwise specified, all measurements used to obtain ratios are taken from holotype specimens.

Dentary

The dentary of *Eremosuchus* is narrow and deep (Buffetaut, 1989), with a maximum mediolateral width to dorsoventral

height ratio at the level of the 4th dentary tooth of 0.55 and 0.66 in the holotype and referred specimen, respectively. In comparison, the only two European sebecids to fully preserve the relevant region, *Doratodon carcharidens* and *Dentaneosuchus*, have a ratio of 1.11 and 1.23, respectively (Martin et al., 2023; Rabi & Sebők, 2015). The latter two taxa are unusual in this aspect as, although incomplete, both *Bergisuchus* (Rossmann et al., 2000) and *Doratodon ibericus* (Company et al., 2005) appear to have a slenderer morphology, closer to that of *Eremosuchus* (Fig. 20C, F). The dentaries of other non-European sebecids are also slender, with values ranging from 0.45 (*Sebecus icaeorhinus* [Colbert et al., 1946]) to 0.85 (*Barinasuchus arveloi* [Paolillo & Linares 2007]). In general, this ratio is much higher amongst baurusuchians, with values often exceeding 0.80 as a result of a relatively mediolaterally broad dentary (e.g., *Baurusuchus salgadoensis*, *Baurusuchus pachecoi*, *Aplestosuchus*, *Campinasuchus*, *Pissarrachamps* [Carvalho et al., 2005, 2011; Godoy et al., 2014; Montefeltro et al., 2011; Price, 1945]). Peirosaurians typically also have much higher ratios as a result of narrowly dorsoventrally tapering dentaries and broad mandibular symphyses:

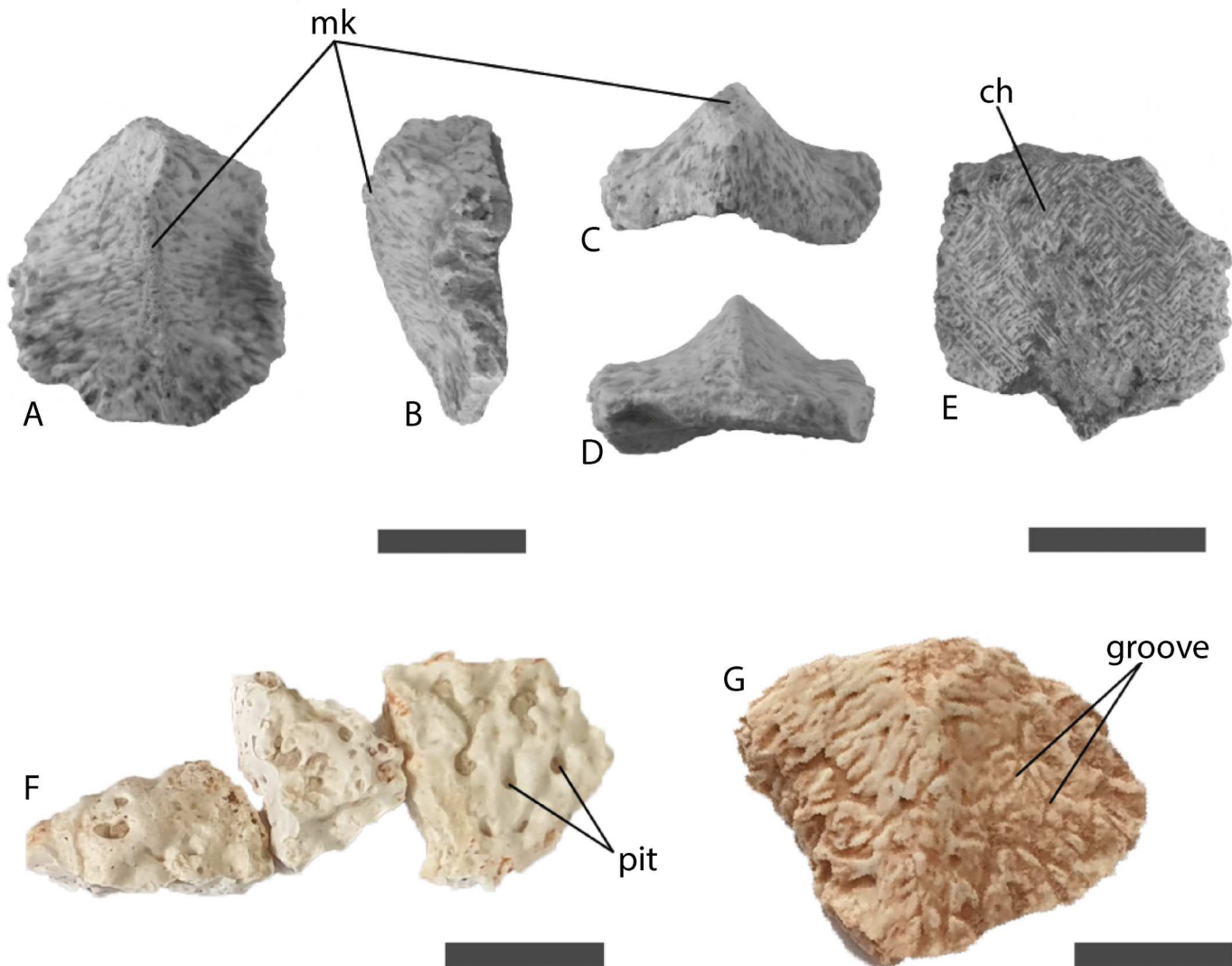


FIGURE 17. Tentatively referred isolated osteoderms of *Eremosuchus elkoholicus* from the KD locality. Singular osteoderm UT-KD-04 in: **A**, dorsal view; **B**, lateral view; **C**, anterior view; **D**, posterior view; and **E**, ventral view. Assorted osteoderms UT-KD-05 in: **F**, dorsal view, showing a pitted texture; and **G**, dorsal view showing a grooved texture. **Abbreviations:** **ch**, cross-hatching pattern; **mk**, median keel. Scale bars equal 10 mm.

Antaeusuchus taouzensis, *Hamadasuchus rebouli*, and *Montealtosuchus arrudacamposi* have width to height ratios of 1.77, 1.14, and 1.62, respectively (Barrios et al., 2016; Carvalho et al., 2007; Larsson & Sues, 2007; Nicholl et al., 2021).

Although the splenial of *Eremosuchus* is not preserved, it was most probably included in the mandibular symphysis, as is the case in all notosuchians (Pol et al., 2014) (Fig. 20). The mandibular symphysis was likely relatively anteroposteriorly elongate in *Eremosuchus*, most closely resembling the morphology of *Lorosuchus* (Pol & Powell, 2011), *Sebecus icaeorhinus* (Colbert et al., 1946), *Dentaneosuchus* (Martin et al., 2023), and *Barinasuchus arveloi* (Paolillo & Linares, 2007), as well as the peirosaurians *Bayomesasuchus hernandezi*, *Kinesuchus overoi*, *Patagosuchus anielensis*, *Hamadasuchus rebouli*, and *Antaeusuchus taouzensis* (Filippi et al., 2018; Larsson & Sues, 2007; Nicholl et al., 2021).

We interpret the dorsal mandibular symphyseal surface of *Eremosuchus* to have been strongly concave. This is a relatively widespread feature amongst sebecids, including *Doratodon ibericus* (Company et al., 2005), *Bergisuchus dietrichbergi* (Rossmann et al., 2000), *Sebecus icaeorhinus* (Colbert et al., 1946), and *Dentaneosuchus* (Martin et al., 2023), and also characterizes *Lorosuchus* (Pol & Powell, 2011) and *Pehuanchesuchus* (Turner

& Calvo, 2005). The mandibular symphysis in *Doratodon carcharidens* is also narrower and more deeply concave than in most other notosuchians (Rabi & Sebők, 2015), although it is not as well-developed as these aforementioned taxa. By contrast, the mandibular symphyseal dorsal surface is only slightly concave or essentially flat in notosuchian clades such as Uruguaysuchidae (e.g., *Araripesuchus*) and Peirosauridae (particularly *Montealtosuchus arrudacamposi*, *Barrosasuchus neuquenianus*, and *Bayomesasuchus hernandezi*, in which the dorsal surface of these taxa is mediolaterally expanded) (Barrios et al., 2016; Carvalho et al., 2007; Coria et al., 2019; Pol & Apesteguía, 2005). Although many sphagesaurians have highly concave mandibular symphyses, their morphology differs from that in sebecids in that the mandibular symphysis forms a tooth battery in members of the former clade (Andrade & Bertini, 2008; Pol et al., 2014).

In lateral view, the mandibular symphysis of *Eremosuchus* is deep and convex anteriorly, as is the case in most sebecids, as well as baurusuchians, in which this morphology is especially marked (Fig. 21) (Carvalho et al., 2005; Company et al., 2005; Godoy et al., 2014; Marinho et al., 2013; Montefeltro et al., 2011; Price, 1945; Riff & Kellner, 2011). Although the symphysis in *Lorosuchus* is also convex, it is dorsoventrally reduced in

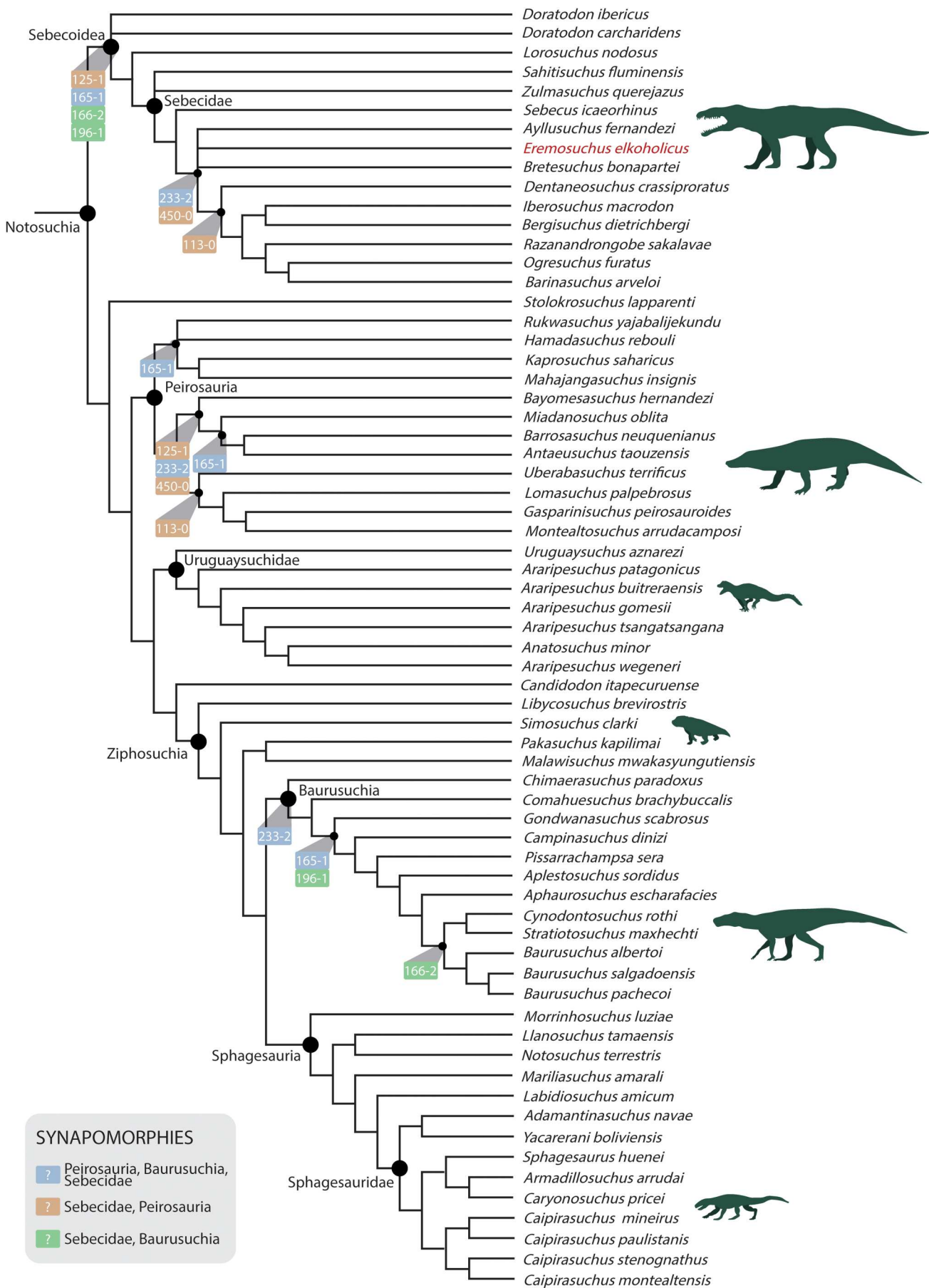


FIGURE 18. Reduced strict consensus topology recovered in Analysis 1 (equal weighting). Synapomorphies shown are those which support multiple clades amongst Sebecidae, Peirosauria, and Baurusuchia.

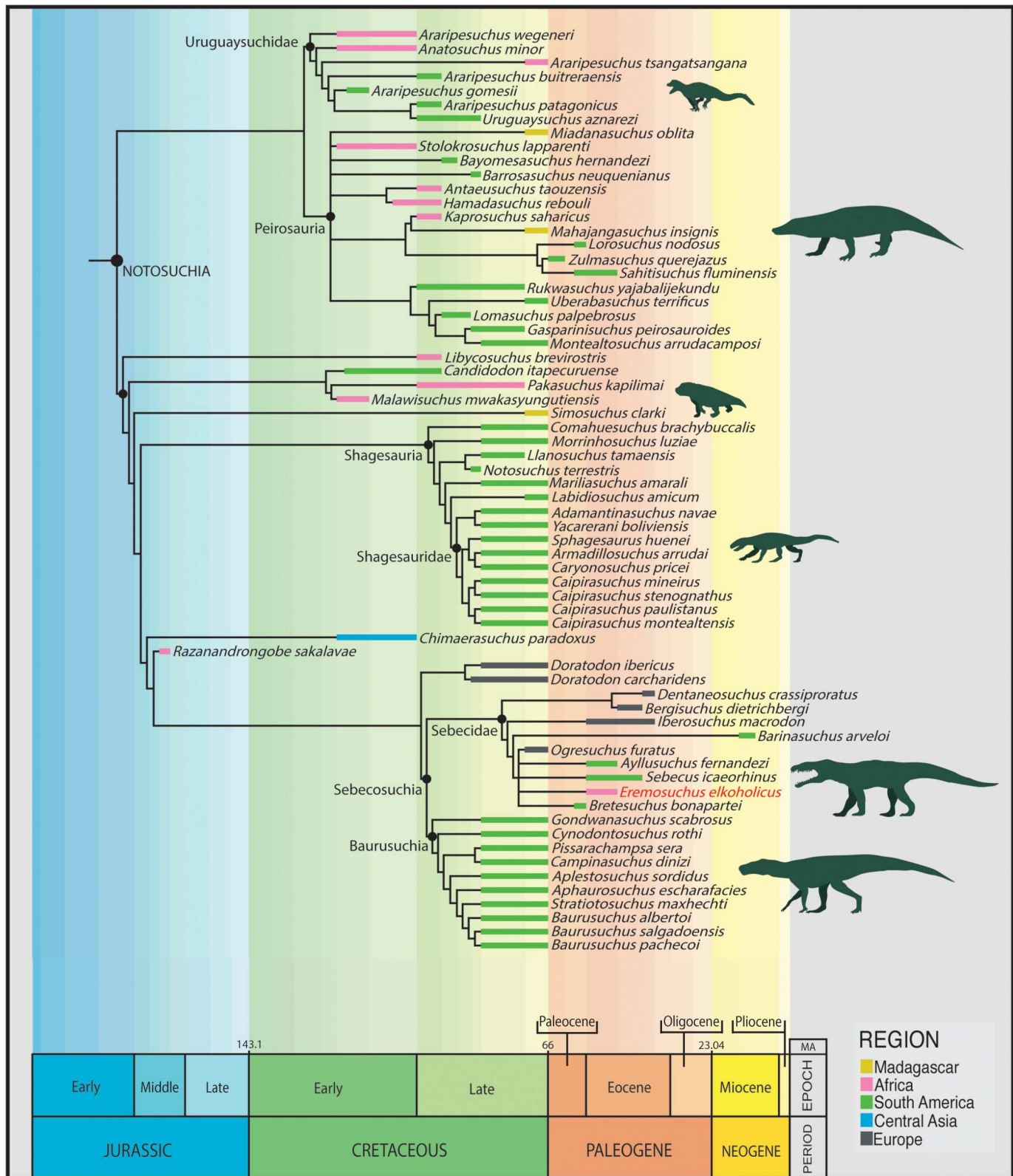


FIGURE 19. Time-calibrated phylogenetic topology of Notosuchia showing the reduced strict consensus tree in Analysis 3 (using extended implied weighting) plotted using the ranges of tips based on occurrence ages.

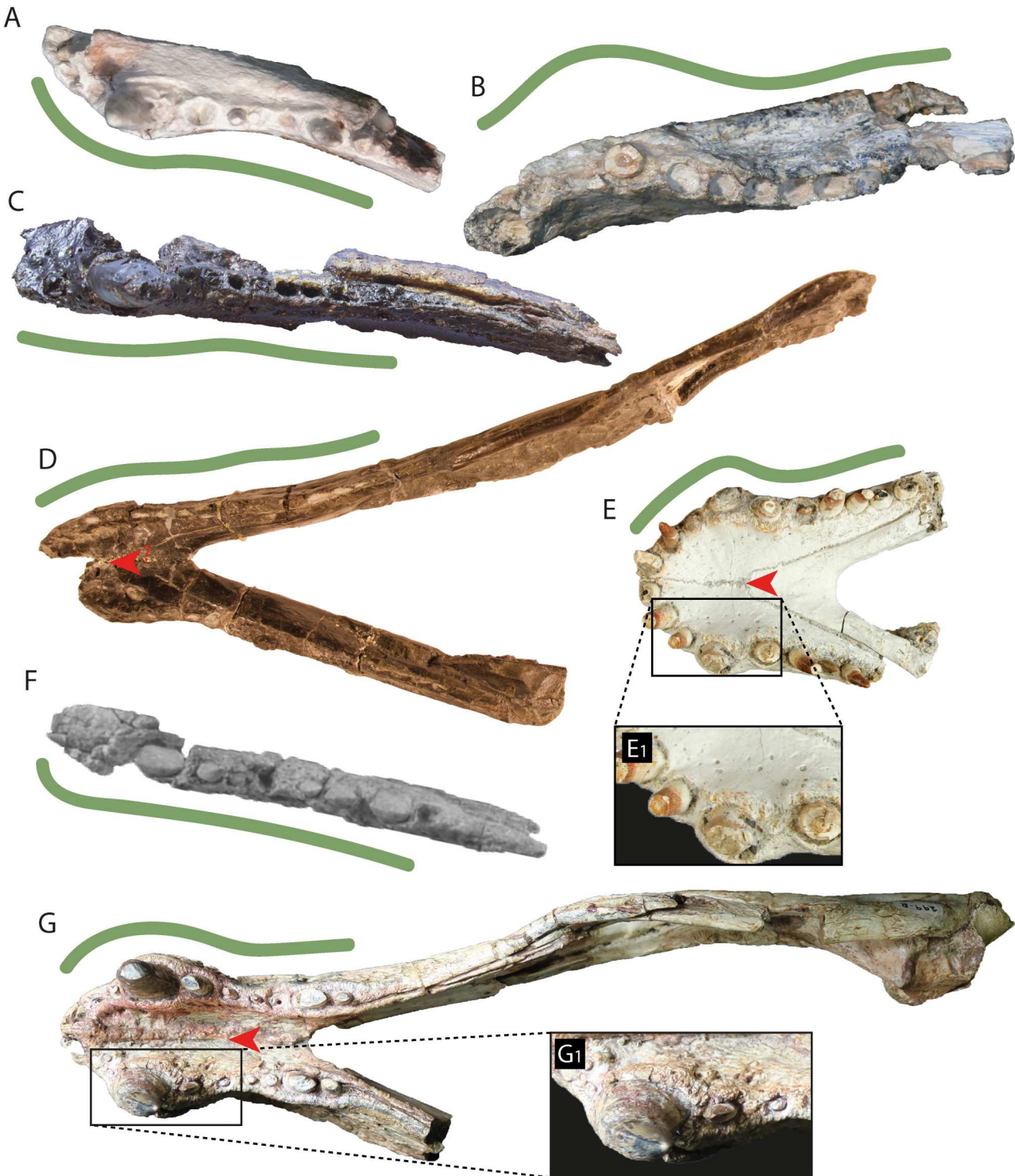


FIGURE 20. Notosuchian mandibular elements in dorsal view: **A**, *Eremosuchus elkoensis* (immature specimen); **B**, *Eremosuchus elkoensis* (KB-301); **C**, *Bergisuchus dietrichbergi* (GM XVIII-49); **D**, *Doratodon carcharidens* (IPUW 2349/5); **E**, *Dentaneosuchus crassiproratus* (MHNT.PAL.2011.20.1); **F**, *Doratodon ibericus* (MGUV 3201); **G**, *Baurusuchus pachecoi* (DGM 229-R). Line above each image denotes the shape of the dentary tooth row. Red arrow indicates the anteriormost point of the splenial on the dorsal surface of the mandibular symphysis. Pictures are not to scale. Images **E** and **F** are adapted from Martin et al. (2023), and Company et al. (2005), respectively.

comparison to these aforementioned taxa (Pol & Powell, 2011). Both species of *Doratodon* also have dorsoventrally reduced symphyses, although this is not to the same extent as that of *Lorosuchus* (Company et al., 2005; Rabi & Sebők, 2015). The

morphology of most peirosaurians contrasts with that of *Eremosuchus*, in that members of Peirosauria have dorsoventrally reduced anterior dentary regions that taper to an acute point (Nicholl et al., 2021).

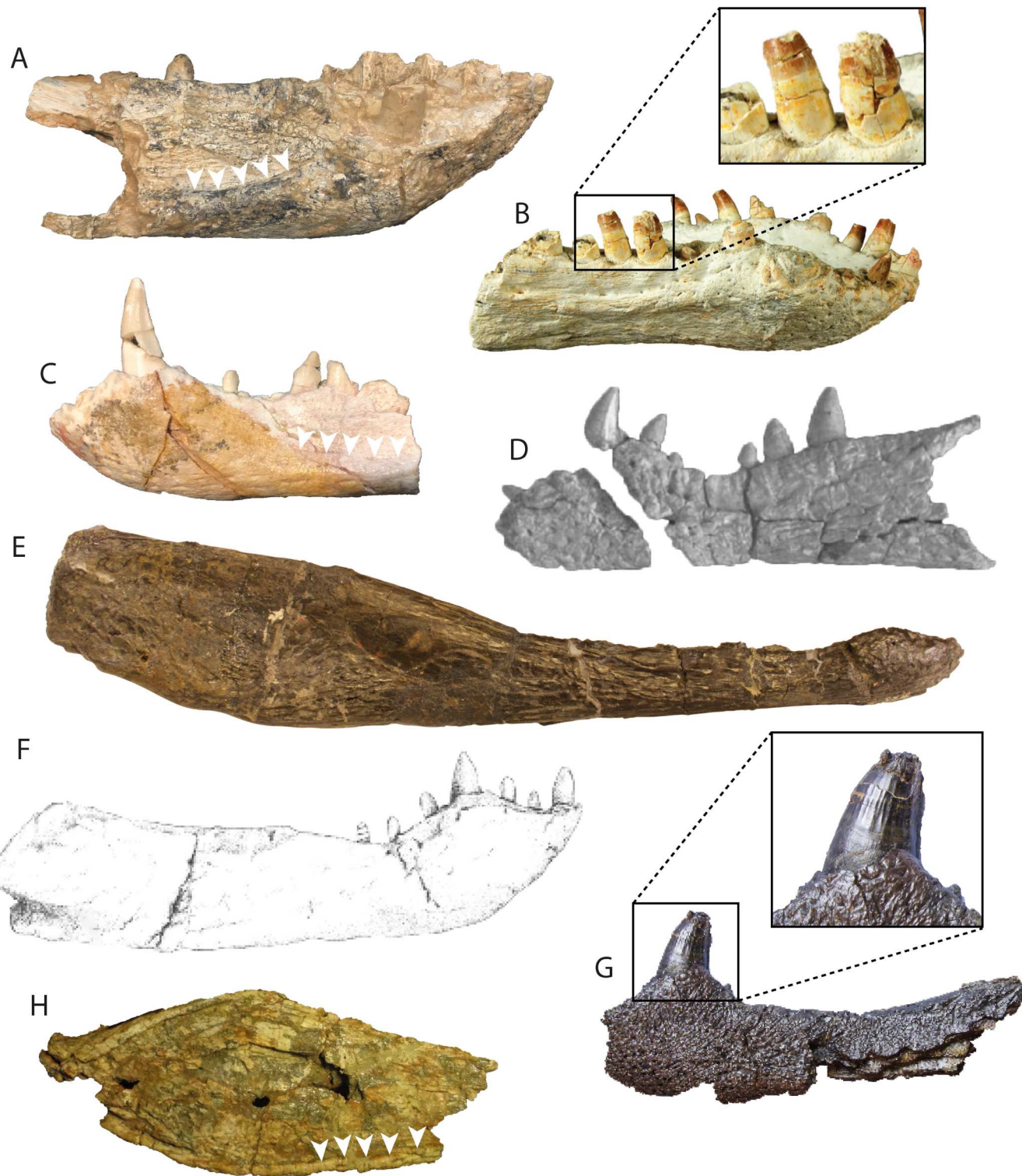


FIGURE 21. Notosuchian mandibular elements in lateral view: **A**, *Eremosuchus elkoensis* (KB-301); **B**, *Dentaneosuchus crassiproratus* (MHNT.PAL.2011.20.1); **C**, *Eremosuchus elkoensis* (immature specimen); **D**, *Doratodon ibericus* (MGUV 3201); **E**, *Doratodon carcharidens* (IPUW 2349/5); **F**, *Pehuenchesuchus enderi* (MAU-PV-CRS-440); **G**, *Bergisuchus dietrichbergi* (GM XVIII-49); **H**, Lumbra form (PVL 6385). White arrows denote the dorsal margin of the elongate dentary ridge. Pictures are not to scale. Images **B**, **D** and **G** are adapted from those provided in Martin et al. (2023), Company et al. (2005), Rabi and Sebok (2015), Ortega et al. (1996), and Turner and Calvo (2005), respectively.

It can be inferred that the splenial-dentary suture on the ventral surface of the mandibular symphysis was approximately 'V' shaped in both the holotype and referred specimen of

Eremosuchus. This morphology characterizes nearly all sebecids and baurusuchians (Bravo et al., 2021; Carvalho et al., 2005; Pol & Powell, 2011; Price, 1945; Riff & Kellner, 2011), with the

exception of *Campinasuchus*, in which the suture is more rounded anteriorly (Carvalho et al., 2011). The condition varies amongst peirosaurians, also being 'V' shaped in *Hamadasuchus*, *Bayomesasuchus*, *Kinesuchus*, *Patagosuchus*, and *Montealtosuchus* (Barrios et al., 2016; Carvalho et al., 2007; Filippi et al., 2018; Larsson & Sues, 2007; Lio et al., 2016). Ventrally, it can be estimated that the dentary-dentary suture of *Eremosuchus* extends posteriorly to a level between the 6th and 7th dentary alveoli in the holotype specimen and level with the 7th alveolus in the referred specimen. The condition in the holotype *Eremosuchus* specimen is most similar to the length reached in *Baurusuchus pachecoi* (6th–7th alveoli), *Pepesuchus deiseae* (6th alveolus), and potentially *Pissarrachamps* (estimated to be around the 6th alveolus) (Campos et al., 2011; Montefeltro et al., 2011; Price 1945), contrasting with taxa such as *Dentaneosuchus*, in which it reaches the level of the 5th alveolus (Martin et al., 2022), *Antaeusuchus taouzensis* (7th to 8th teeth) (Nicholl et al., 2021), and *Kinesuchus overoi* (8th to 9th alveoli) (Filippi et al., 2018).

In the holotype specimen of *Eremosuchus*, the dorsal exposure of the dentary symphysis extends posteriorly to approximately the level of the 5th alveolus, whereas in the referred specimen it reaches to a level between the 6th and 7th alveoli. A comparable posterior extension to the holotype also characterizes *Bergisuchus* (Rossmann et al., 2000), *Pehuanchesuchus* (Turner & Calvo, 2005), and *Doratodon carcharidens*, in which the dentary extends approximately to the region between the 4th and 5th alveoli (Rabi & Sebők, 2015) (Fig. 20). By contrast, and closer in morphology to the referred specimen, the dorsal exposure of the dentary symphysis extends further posteriorly in *Lorosuchus*, *Baurusuchus pachecoi*, and *Baurusuchus salgadoensis*, extending to either the 6th or 7th alveolus (Carvalho et al., 2005; Nicholl et al., 2021; Pol & Powell, 2011; Price, 1945). A greater posterior extent of this suture is more common in peirosaurians, extending to the 6th or 7th alveoli in *Gasparinisuchus*, *Colhuehuapisuchus*, and *Bayomesasuchus*, and the 8th alveolus in *Antaeusuchus* (Barrios et al., 2016; Lamanna et al., 2019; Martinelli et al., 2012; Nicholl et al., 2021).

Despite some damage to the region, the dorsal margin of the *Eremosuchus* dentary most closely resembles the condition present in the majority of sebecids and baurusuchians: the anterior region is mildly convex dorsally, with the greatest dorsoventral height coinciding with the position of the enlarged 4th dentary alveolus, whereas the posterior section is concave, curving smoothly and increasing in dorsoventral height posteriorly (Fig. 21) (Buckley & Brochu, 1999; Ortega et al., 1996). This contrasts with the morphology of peirosaurians, in which two distinct waves form the dorsal dentary margin (Pol et al., 2014; Nicholl et al., 2021). The anterior convexity in *Eremosuchus* is subtle, most closely resembling taxa such as *Baurusuchus* (Carvalho et al., 2005; Riff & Kellner, 2001), *Campinasuchus* (Carvalho et al., 2011), *Aphaurosuchus escharafacies* (Darlim et al., 2021), *Sahitisuchus* (Kellner et al., 2014), *Doratodon carcharidens* (Buffetaut, 1979; Company et al., 2005; Rabi & Sebők, 2015), and *Dentaneosuchus* (Martin et al., 2023). This morphology differs from that seen in peirosaurids (e.g., Carvalho et al., 2004; Larsson & Sues, 2007; Nicholl et al., 2021; Tavares et al., 2015), in which the dorsal margin of the dentary forms two distinct dorsal waves.

A concavity adjacent to the 7th dentary alveolus for the reception of a large maxillary tooth is present in *Eremosuchus*. Within Notosuchia, this morphology characterizes nearly all sebecids which preserve the relevant region, namely *Doratodon carcharidens*, *Doratodon ibericus*, the 'Fayum form,' *Bretesuchus*, *Dentaneosuchus*, *Sebecus huilensis*, and *Sebecus icaeorhinus*, although it is absent in *Bergisuchus* (Colbert et al., 1946; Langston, 1965; Martin et al., 2023; Price, 1945; Rabi & Sebők, 2015; Rossmann et al., 2000; Stefanic et al., 2019). It is also present in *Baurusuchus*

(Carvalho et al., 2005), as well as some peirosaurians and closely associated taxa, i.e., *Hamadasuchus rebouli*, *Antaeusuchus taouzensis*, *Barrosasuchus neuquenianus*, *Miadanasuchus oblita*, and *Mahajangasuchus insignis* (Coria et al., 2019; Larsson & Sues, 2007; Nicholl et al., 2021; Rasmussen Simons & Buckley, 2009; Turner & Buckley, 2008).

Eremosuchus has a distinct, prominent, ventrolaterally protruding ridge that runs anteroposteriorly along the dentary, extending posteriorly from the level of the 6th alveolus. A ridge in this location is otherwise restricted to *Bretesuchus* (Gasparini et al., 1993), *Lorosuchus* (Pol & Powell, 2011), the 'Lumbra form' (Pol & Powell, 2011), *Sahitisuchus* (Kellner et al., 2014), *Sebecus icaeorhinus* (Colbert et al., 1946), *Sebecus huilensis* (Langston, 1965), and the unpublished Lumbra Form; however, in all of these taxa it is a much more subtle feature, lacking the prominence that characterizes *Eremosuchus*. A similar ridge is present on the dentary of *Dentaneosuchus* (MHNT.PAL.2011.20.1), but in a more dorsal position. This region is gently convex in the sebecosuchians *Bergisuchus*, *Doratodon*, and the specimen from Fayum (Fig. 21) (Company et al., 2005; Ortega et al., 1996; Rabi & Sebők, 2015; Rossmann et al., 2000; Stefanic et al., 2019), but there is no distinct ridge in any of these taxa, nor in any baurusuchians or peirosaurians. This feature has not previously been recognized as a common feature of sebecids.

The ziphodont dentition of *Eremosuchus*, characterized by highly labiolingually compressed, serrated posterior teeth, has long been considered characteristic of sebecids (Pol et al., 2014), although serrated, compressed teeth are common across multiple archosaurian lineages (Andrade et al., 2010; Farlow et al., 1991; Hungerbühler, 2000; Langston, 1965). Despite many teeth being missing from both dentaries of *Eremosuchus*, the compression of the alveoli provides a proxy for tooth compression. The degree of labiolingual compression of the preserved teeth of *Eremosuchus* is similar to that of *Bergisuchus* (Rossmann et al., 2000) and probably the 'Fayum form' (Stefanic et al., 2019), but it is not as extreme as the condition in *Doratodon* (Company et al., 2005; Rabi & Sebők, 2015). The teeth of *Dentaneosuchus* (Martin et al., 2023; Ortega et al., 1996) are less labiolingually compressed, being closer in constriction to those of *Baurusuchus pachecoi*.

As with almost all sebecids, as well as most baurusuchians and peirosaurids (Turner & Calvo, 2005), the posterior teeth of *Eremosuchus* have denticulate carinae, formed by relatively homogeneous, symmetric denticles that have a sharp cutting edge. *Pehuanchesuchus* is the only member of one of these clades with preserved teeth that greatly differ from this morphology, with no denticles being present (Turner & Calvo, 2005). *Lorosuchus* also lacks denticles (Pol & Powell, 2011), but this could be the result of poor preservation. Although the teeth of *Doratodon ibericus* do possess denticles, they are not homogeneous, differing along the length of the carinae (Company et al., 2005). As is common amongst sebecids and baurusuchians (Buckley et al., 2000; Ortega et al., 1996), the teeth of *Eremosuchus* are constricted at the base of the crown.

In the *Eremosuchus* holotype, all of the dentary alveoli are separated by distinct, but relatively narrow, bony septa; this differs slightly in the referred specimen, in which the 6th and 7th alveoli are confluent (Fig. 20). Narrow septa between all of the dentary teeth characterize several other sebecids, including *Dentaneosuchus* (Martin et al., 2023), *Doratodon* (Company et al., 2005; Rabi & Sebők 2015). Although septa are also present in *Baurusuchus* and *Sebecus* (Carvalho et al., 2005; Colbert et al., 1946), the teeth are much more broadly separated in these taxa, with each septum almost equidimensional to a full tooth. Contrasting with most other peirosaurians in which the posterior dentary teeth occupy a single groove, the posterior teeth of *Kinesuchus* and *Patagosuchus* are also implanted in singular alveoli that are divided by septa (Filippi et al., 2018;

Lio et al., 2016). The presence of a diastema between the 7th and 8th dentary alveoli in the referred specimen of *Eremosuchus* is shared with *Doratodon ibericus* (Rabi & Sebők, 2015) and the ‘Fayum form’ (Fig. 20) (Stefanic et al., 2019). A diastema is absent in other sebecid taxa, including *Doratodon carcharidens*, *Bergisuchus*, and *Sebecus ayrampu*, as well as in the sebecosuchians *Pehuanchesuchus* and *Baurusuchus pachecoi* (Bravo et al., 2021; Carvalho et al., 2005; Rabi & Sebők, 2015; Rossmann et al., 2000; Turner & Calvo, 2005). A diastema in this position is absent from any peirosaurians.

The tooth row of *Eremosuchus* is sinusoidal, as is common amongst sebecids, baurusuchians, and peirosaurians, although this morphology varies between taxa. In *Eremosuchus*, the posterior-most concave curvature of the tooth row is fairly prominent, though this is not as curved as in several baurusuchid taxa, in which the maximum medial curvature is equivalent to at least the width of one adjacent alveolus (Carvalho et al., 2011; Company et al., 2005; Darlim et al., 2021; Godoy et al., 2014). The tooth row is much straighter in *Bergisuchus* (Rossmann et al., 2000) and *Dentaneosuchus*. In this regard, *Eremosuchus* most closely resembles the condition in *Doratodon* (Company et al., 2005; Rabi & Sebők, 2015).

The tooth row in *Eremosuchus* extends far posteriorly along the dentary. A similar morphology also characterizes the European notosuchians *Doratodon*, *Bergisuchus*, and *Dentaneosuchus* (Fig. 20) (Company et al., 2005; Martin et al., 2023; Ortega et al., 1996; Rossmann et al., 2000), as well as *Pehuanchesuchus*, *Sebecus icaeorhinus*, *Sahitisuchus*, the ‘Lumbra form,’ and most peirosaurians (e.g., *Montealtosuchus* and *Antaeusuchus*) (Carvalho et al., 2007; Colbert et al., 1946; Nicholl et al., 2021; Turner & Calvo, 2005). By contrast, in many baurusuchids (e.g., *Baurusuchus*, *Campinasuchus*, *Pissarrachamps*, *Gondwanasuchus*, *Aplestosuchus*, and *Aphaurosuchus escharafacies*), the tooth row is relatively short in comparison to the entire length of the dentary, the former often forming close to or less than half of the latter’s anteroposterior length (Carvalho et al., 2011; Company et al., 2005; Darlim et al., 2021; Godoy et al., 2014, 2016; Marinho et al., 2013; Montefeltro et al., 2011; Nascimento & Zaher, 2010; Price, 1945; Riff & Kellner, 2011).

Eremosuchus most likely has 12 dentary alveoli, which is probably the number in *Bergisuchus* too (Rossmann et al., 2000). *Doratodon ibericus* (Company et al., 2005) and *Doratodon carcharidens* (Rabi & Sebők, 2015) have 11 and 13 dentary alveoli, respectively. *Sebecus ayrampu* has a notably higher number (15) of dentary alveoli (Bravo et al., 2021). No other sebecids preserve a complete dentary or have a visible tooth row with which to assess the tooth count. With the exception of peirosaurians (e.g., *Montealtosuchus*, *Antaeusuchus*, *Gasparinisuchus*, *Kinesuchus*, and *Pepesuchus* [all with 18 alveoli]) (Carvalho et al., 2007; Filippi et al., 2018; Geroto & Bertini, 2019; Martinelli et al., 2012; Nicholl et al., 2021), *Stolokrosuchus* (at least 30 alveoli) (Larsson & Gado, 2000), and *Pehuanchesuchus*, which bears 16 dentary alveoli (Turner & Calvo, 2005), the number of dentary alveoli present in *Eremosuchus* is relatively high compared with many other notosuchians, with only nine alveoli likely to be present in *Losoruchus* (Pol & Powell, 2011), and 10 in *Campinasuchus* (Carvalho et al., 2011), *Baurusuchus salgadoensis*, and *Baurusuchus pachecoi* (Price 1945; Carvalho et al., 2005).

The dentary of *Eremosuchus elkoensis* maintains its dorsoventral height posterior to the 4th dentary alveolus, which differs from *Bergisuchus* (Rossmann et al., 2000), *Doratodon* (Company et al., 2005; Rabi & Sebők, 2015), *Sebecus icaeorhinus* (Colbert et al., 1946; Pol et al., 2012), and *Sahitisuchus* (Kellner et al., 2014), in which the same region is dorsoventrally constricted. The morphology of *Eremosuchus* more closely resembles that present in *Dentaneosuchus*, *Pehuanchesuchus* (Turner & Calvo, 2005), the baurusuchians *Gondwanasuchus*

(Marinho et al., 2013), *Campinasuchus* (Carvalho et al., 2011), *B. salgadoensis* (Carvalho et al., 2005), *B. pachecoi* (Price, 1945), *Aphaurosuchus* (Darlim et al., 2021), and most peirosaurians (e.g., *Antaeusuchus*, *Barrosasuchus*, and *Montealtosuchus* [Carvalho et al., 2007; Coria et al., 2019; Nicholl et al., 2021]).

Mandibular Fragment

The retroarticular process preserves a gently posterolaterally directed (approximately 15–20° from the sagittal plane) crest that separates its medial and lateral flanges. This is closest in morphology to *Sebecus icaeorhinus* and *Losoruchus*, as well as the peirosaurid *Montealtosuchus*, in which the crests are directed at approximately 20° and 25° from the sagittal axis, respectively (Carvalho et al., 2007; Colbert et al., 1946; Pol & Powell, 2011). Conversely, in baurusuchids, the crest is strongly deflected posterolaterally at an angle greater than 45° from the anteroposterior midline, e.g., *Baurusuchus pachecoi*, *Baurusuchus salgadoensis*, *Aphaurosuchus escharafacies*, and *Campinasuchus* (Carvalho et al., 2005, 2011; Darlim et al., 2021; Price, 1945). The glenoid facet of *Eremosuchus* is mediolaterally wider than it is anteroposteriorly long, which also characterizes *Sebecus icaeorhinus*, *Baurusuchus*, *Campinasuchus*, and *Losoruchus* (Carvalho et al., 2005, 2011; Colbert et al., 1946; Nascimento & Zaher, 2010; Pol & Powell, 2011; Price, 1945), as well as the peirosaurians *Uberabasuchus*, *Montealtosuchus*, and *Barrosasuchus* (Carvalho et al., 2004; 2007; Coria et al., 2019). In *Eremosuchus*, the lateral retroarticular flange is similar in anteroposterior length to the mediolateral width of the glenoid facet. This is comparable to the majority of sebecids and peirosaurians that preserve the relevant region, including *Sebecus icaeorhinus*, *Losoruchus*, *Sahitisuchus*, *Montealtosuchus*, *Lomasuchus*, *Uberabasuchus*, and *Barrosasuchus* (Carvalho et al., 2004, 2007; Coria et al., 2019; Gasparini et al., 1991; Kellner et al., 2014; Pol & Powell, 2011). This contrasts with the morphology in baurusuchians such as *Aphaurosuchus escharafacies*, *Baurusuchus salgadoensis*, and *Campinasuchus*, in which the length of the lateral flange is shorter than the mediolateral width of the glenoid facet (Carvalho et al., 2005, 2011; Darlim et al., 2021). In *Eremosuchus*, the medial flange is relatively limited in its medial expansion, lacking the large pendant flange present in baurusuchids (Darlim et al., 2021; Nascimento & Zaher, 2010; Price, 1945).

The substantial participation of the surangular in the glenoid facet is similar to the morphology of *Sebecus icaeorhinus*, the ‘Lumbra specimen,’ *Sahitisuchus*, and *Losoruchus* (Bravo et al., 2021; Kellner et al., 2014; CSCN based on obs. of photographs), as well as in peirosaurids (e.g., Carvalho et al., 2004; Coria et al., 2019; Larsson & Sues, 2007; Martinelli et al., 2012; Nicholl et al., 2021). This contrasts with baurusuchids (e.g., *Stratiotosuchus*, *Baurusuchus pachecoi*, *Baurusuchus salgadoensis*, *Aphaurosuchus escharafacies*, and *Campinasuchus*), in which the surangular is restricted to the lateral wall of the fossa (Carvalho et al., 2005, 2011; Darlim et al., 2021; Price, 1945; Riff & Kellner, 2011). As is the case in all notosuchians that preserve this element, and in contrast to the plesiomorphic crocodyliform condition (Pol et al., 2014), the medial flange of the retroarticular process is strongly inclined, such that its primary plane faces almost medially.

Vertebrae

All of the vertebrae assigned by Buffetaut (1989) to *Eremosuchus elkoensis* are posited to originate from either the thoracic region or an anterior position in the caudal vertebral series; thus, comparisons are made exclusively to vertebrae from these regions. The centra from both regions of the vertebral column are amphicoelous, which characterizes almost all notosuchians known to preserve these elements (Pol et al., 2012). Though

Georgi & Krause (2010) described a weakly opisthocoelous anteriormost caudal centrum of *Simosuchus clarki*, this condition is absent from other members of the clade. As in all members of Notosuchia (Pol, 2005), the vertebral centra are slightly mediolaterally compressed at their anteroposterior midpoint.

As no further descriptions of the dorsal vertebrae are available, and both elements are currently missing, comparisons herein are limited to the preserved and photographed caudal centra suggested to be from the anterior region of the series. As in *Sebecus huilensis* and several baurusuchids (e.g., *Baurusuchus albertoi*, *Baurusuchus salgadoensis*, *Aphaurosuchus escharafacies*, and *Campinasuchus*) (Cotts et al., 2017; Nascimento & Zaher, 2010), the neural arch pedicles of UO-KA-407 extend along approximately three quarters of the anteroposterior length of the centrum, with slight anterior bias. The vertebral centra are more anteroposteriorly expanded in *Eremosuchus* (dorsoventral height to anteroposterior length ratio of 0.6 in both UO-KA-407 and UO-KA-408) compared with vertebrae from the anterior caudal series of baurusuchids, including *Campinasuchus*, *Baurusuchus salgadoensis*, and *Baurusuchus albertoi*, which have a ratio of 0.8–0.9 (Cotts et al., 2017; Darlim et al., 2021; Nascimento & Zaher, 2010; Vasconcellos & Carvalho, 2010). The ridges leading to the hemapophyses in UO-KA-407 protrude ventrally to a similar level as those exposed in the anterior caudal vertebrae of some baurusuchids, *Baurusuchus salgadoensis* (Vasconcellos & Carvalho, 2010), *Baurusuchus albertoi* (Nascimento & Zaher 2010), and *Campinasuchus* (Cotts et al., 2017). This contrasts with other taxa, including *Notosuchus terrestris*, *Uruguaysuchus aznarezi*, *Araripesuchus gomesii*, *Caipirasuchus montealtensis*, and *Mahajangasuchus insignis* (Buckley & Brochu, 1999; Iori et al., 2016; Pol, 2005; Price, 1959), in which the hemapophyses and associated ridges are less protruded.

Fibula

The weak posterior projection of the proximal head of the fibula of *Eremosuchus* is in stark contrast to that of *Baurusuchus albertoi* (Nascimento & Zaher, 2010), *Stratiotosuchus* (Riff, 2007), and *Pissarrachampsia* (Godoy et al., 2016), in which a large, mediolaterally compressed wing projects strongly postero-medially. Although not as posteriorly well-developed, this projection in *Eremosuchus* has the condition characteristic of baurusuchids, in which the proximal head is slightly curved (Godoy et al., 2016). Of all other sebecids (*Iberosuchus*) and baurusuchids (*Baurusuchus albertoi*, *Baurusuchus salgadoensis*, *Campinasuchus*, *Stratiotosuchus*, *Pissarrachampsia*) that preserve fibulae, none have as substantial posterior bowing of the shaft distal to the attachment of *M. iliofibularis* as *Eremosuchus* (Cotts et al., 2017; Godoy et al., 2016; Nascimento & Zaher, 2010; Riff & Kellner, 2011; CSCN pers. obs.). The fibula crest for the insertion of the *M. iliofibularis* extends greater than 25% of the distance along the fibular shaft in *Eremosuchus*. By contrast, this crest is proximodistally shorter in all other sebecids and baurusuchids in which the fibula is preserved (Carvalho et al., 2005; Cotts et al., 2017; Godoy et al., 2016; Nascimento & Zaher, 2010; Riff & Kellner, 2011). Nonetheless, these taxa all share the general morphology of a fibula which gradually decreases in anteroposterior width along most of its total length, expanding again only towards the distal-most end.

Osteoderms

The presence of postcranial osteoderms is plesiomorphic for crocodyliforms (Godoy et al., 2016; Scheyer & Desojo, 2011), with this ancestral condition occurring in most internal nodes of this clade. Two sebecid lineages with well-preserved postcrania are found to lack osteoderms, the sebecid *Sebecus icaeorhinus*,

and the baurusuchid *Pissarrachampsia*. Though there are suggestions that this absence is more widespread amongst sebecids given a lack of associated dermal armor in all taxa bar *Dentaneosuchus*, it is important to consider that many sebecid remains are highly fragmentary, particularly with regards to postcranial material, and therefore a true absence of osteoderms, as opposed to a taphonomic signature, is often not possible to ascertain in these instances (though see Godoy et al., 2016). Because the osteoderms found at site KD are isolated, they cannot be accurately positioned within the dorsal armor, and therefore general comparisons are made with respect to the individual shape and ornamentation of each element.

In *Eremosuchus*, the most well preserved osteoderms are approximately quadrangular, albeit with highly rounded corners. This resembles the morphology present in *Dentaneosuchus* and *Iberosuchus*, the peirosaurids *Montealtosuchus*, *Uberabasuchus*, *Patagosuchus*, and *Barrosasuchus* (Coria et al., 2019; Lio et al., 2016; CSCN based on obs. of photographs), baurusuchids, e.g., *Baurusuchus albertoi*, *Baurusuchus pachecoi*, and *Aplestosuchus* (Darlim et al., 2021; Godoy et al., 2014; Martin et al., 2023; Nascimento & Zaher, 2010), and the indeterminate sebecosuchian described from the middle Eocene of France by Martin (2014), contrasting with the more angular morphology which characterizes uruguaysuchids, e.g., *Araripesuchus* and *Anatosuchus* (Price, 1959; Sereno & Larsson, 2009).

Of the almost complete osteoderms associated with *Eremosuchus*, the mediolateral width to anteroposterior length ratios form values between 0.88–1.27. The ratios are generally lower in other taxa; in *Dentaneosuchus* and *Iberosuchus*, the values for preserved osteoderms range between 0.64–0.88 and 0.33–0.92, respectively. Amongst baurusuchids, values are recovered between 0.39–0.99, i.e., in *Baurusuchus pachecoi*, *Aplestosuchus*, and *Campinasuchus*; however, in the peirosaurid *Patagosuchus*, the width to length ratio of the only preserved dorsal osteoderm is 1.77 (Lio et al., 2016). The sebecosuchian osteoderms from the middle Eocene of France described by Martin (2014) have values between 0.35–0.57. Of those taxa that preserve *in situ* osteoderms, the mediolaterally widest elements are positioned towards the anterior region of the tail; however, regardless of their positioning, the broadest osteoderm associated with *Eremosuchus* is significantly mediolaterally wider than those preserved in this region in sebecids and baurusuchids.

In both *Eremosuchus* and *Dentaneosuchus*, the lateral margins of the osteoderms are bevelled, indicating the possible articulation of dermal armor in these taxa. However, Godoy et al. (2014) and Montefeltro (2019) described how the parasagittal osteoderms are either slightly imbricating or are completely separated amongst baurusuchids (e.g. *Baurusuchus* and *Aplestosuchus*), potentially representing an intermediate condition towards their complete loss.

A prominent sagittal crest extends anteroposteriorly along the osteoderms associated with *Eremosuchus*, essentially reaching from the anterior to posterior margins of the shield. Amongst sebecids and closely allied taxa, a dorsal crest is present in both osteoderm morphotypes of *Dentaneosuchus* as well as in *Iberosuchus*. Both *Dentaneosuchus* and *Iberosuchus* display a similar morphology in one osteoderm morphotype; however, both taxa also possess osteoderms in which the sagittal crests are more anteroposteriorly restricted than in *Eremosuchus*, such that they resemble a spine at the approximate anteroposterior midpoint of the osteoderm.

In the osteoderms of *Eremosuchus*, the sagittal crest is relatively dorsally reduced, and its dorsoventral expansion remains approximately equal to the height of the main osteoderm body. This contrasts with the morphology of the preserved osteoderms assigned to *Iberosuchus macrodon* and *Dentaneosuchus crassiproratus*, which preserve an extreme dorsal projection of the medial crest (Antunes, 1975; Martin et al., 2022). The osteoderm

morphology of baurusuchians (*Baurusuchus pachecoi*, *Baurusuchus salgadoensis*, *Aplestosuchus*, *Aphaurosuchus escharafacies* and *Campinasuchus*) and peirosaurids (*Montealtosuchus*, *Uberabasuchus*, and *Barrosasuchus*) more closely resembles that of *Eremosuchus*, in which the crest remains low (Araújo-Júnior & Marinho, 2013; Cotts et al., 2017; Godoy et al., 2014; Nascimento & Zaher, 2010; Vasconcellos & Carvalho, 2005). In *Iberosuchus*, several osteoderms also preserve a pronounced, mediolaterally orientated ridge, crosscutting, and perpendicular to the sagittal ridge; however, a similar morphology is absent in *Eremosuchus* and other sebecids and baurusuchids. By contrast, the single preserved osteoderm of the peirosaurid *Patagosuchus* lacks any dorsal keel (Lio et al., 2016).

Martin et al. (2022) discussed how the ornamentation on the surface of the osteoderms of *Dentaneosuchus* most closely resembles that of the skull bones of this taxon, a pattern which can be seen across other notosuchian lineages, such as Baurusuchia (e.g., *Aplestosuchus* and *Baurusuchus*), Uruguaysuchidae (e.g., *Araripesuchus* and *Anatosuchus*), Peirosauridae (e.g. *Montealtosuchus* and *Uberabasuchus*), and Sphagesauria (e.g., *Mariliasuchus amarali*). Of those osteoderms from the El Kohol locality, two distinct patterns of ornamentation can be recognized (Fig. 17F, G). One morphotype comprises a series of narrow, undulating grooves radiating from the anteroposterior midline. This morphology most closely resembles that in baurusuchians preserving these elements, e.g., *Baurusuchus*, *Campinasuchus*, *Aplestosuchus*, *Aphaurosuchus escharafacies*, and *Pissarrachamps* (Araújo-Júnior & Marinho, 2013; Cotts et al., 2017; Godoy et al., 2014, 2016; Nascimento & Zaher, 2010; Vasconcellos & Carvalho, 2005). The second is characterized by a smoother ornamentation, marked with small, regularly spaced pits; amongst sebecids, this morphology is otherwise only present in *Dentaneosuchus* (Martin et al., 2022).

DISCUSSION

Do the El Kohol Dentaries Represent an Ontogenetic Series or Evidence for Sympatric Species?

Given their spatiotemporal proximity, as well as their high morphological similarity, it could be postulated that the holotype dentary of *Eremosuchus elkoeholicus* (UO-KB-310) and the smaller dentary represent individuals of an ontogenetic series of a single species. Nevertheless, several anatomical differences are present between the two specimens. Here, the competing hypotheses that they either represent a single ontogenetic series or two distinct sympatric species are discussed.

Assessing the ontogenetic stage of fossil crocodylomorphs, especially based on the mandible, is difficult. Ontogenetic studies of Crocodylomorpha are relatively uncommon, and are usually focused on extant taxa (e.g., Erickson et al., 2003; Gignac & O'Brien, 2016; Morris et al., 2022; Schwab et al., 2022; Vieira et al., 2018). Moreover, it is debatable as to whether taxa outside of Notosuchia are necessarily a good proxy for evaluating ontogenetic changes within the clade.

With regard to notosuchians, the majority of taxa are known only from a single individual, and most of these represent adults or at least sub-adults. In most instances in which the species is represented by a specimen that potentially displays juvenile features, there is no known adult specimen (Gerotto & Bertini, 2012; Godoy et al., 2016; Marinho et al., 2013; Martinelli et al., 2018; Martins dos Santos et al., 2024, 2021). Well-demonstrated ontogenetic series are therefore relatively rare amongst Notosuchia, with only a small number of species represented by well-preserved remains: *Mariliasuchus amarali*, *Notosuchus terrestris*, *Anatosuchus minor*, *Baurusuchus* spp., *Campinasuchus dinizi*, *Caipirasuchus catanduvensis*, and *Pissarrachamps sera* (Andrade & Bertini, 2008; Carvalho et al., 2011; Godoy et al.,

2016; Iori et al., 2024; Martins dos Santos et al., 2021; Sereno & Larsson, 2009; Vasconcellos & Carvalho, 2005, 2006; Zaher et al., 2006). Of these, only one of these species preserves an ontogenetic series for the mandible. Vasconcellos & Carvalho (2005) discussed differences occurring in the mandible through ontogeny in *Mariliasuchus amarali*. However, none of these features can be assessed in the El Kohol specimens, given that they relate to the position of the mandibular fenestra and the relative elongation of the mandibular symphysis, neither of which are suitably preserved in the holotype or immature specimen. Moreover, it is unclear whether either specimen had a mandibular fenestra.

Pochat-Cottilloux, Perrier et al. (2023) noted a number of ontogenetic changes in the mandible of extant crocodylians. Of these, several can be assessed in both the holotype of *Eremosuchus*, as well as the smaller specimen. Pochat-Cottilloux, Perrier et al. (2023) stated that the number of teeth involved in the dentary and mandibular symphyses of extant crocodylians rarely varies throughout ontogeny, despite occasional changes in the number of premaxillary teeth (Brown et al., 2015). At least the former of these conditions is true for the dentaries from El Kohol were they to represent an ontogenetic series, with the symphysis equivalent to the length of five alveoli in both specimens. Pochat-Cottilloux, Perrier et al. (2023) also commented that it is unusual for changes in lateral constriction of the dentary between the level of the 6th to 10th dentary alveoli to vary with ontogeny; in both El Kohol specimens, there is minimal variation in these morphologies. One difference between the El Kohol specimens pertains to the estimated degree of divergence of the mandibular rami, with an approximately 10° difference. Nevertheless, this degree of variation fits within the level of ontogenetic variation in extant crocodylians (Pochat-Cottilloux, Perrier et al., 2023).

A ventrolateral ridge runs anteroposteriorly along the dentary of both El Kohol specimens. This ridge is present in just a few notosuchian taxa (see comparisons), in which it is relatively weakly developed, as is also the case in the smaller El Kohol specimen, and not as prominent as in the *Eremosuchus* holotype. One interpretation is that a low ridge unites the smaller dentary with those other notosuchian taxa, distinguishing it from *Eremosuchus*. Alternatively, the increasing prominence of the anteroposterior ridge in the holotype compared with the smaller individual could instead be interpreted as evidence for the El Kohol specimens representing an ontogenetic series, with parts of the skull becoming progressively more ornamented in other crocodylomorphs through ontogeny (Martins dos Santos et al., 2024).

Based on measurements of the alveoli, the anteriormost tooth in the *Eremosuchus* holotype appears to be essentially the same size as the 4th tooth. Unfortunately, no tooth is preserved in the anterior alveolus, and so its exact size cannot be determined. This appears to differ from the smaller specimen, as the CT scans (Figs. 7, 13, 14) reveal that the 4th tooth of this specimen is substantially larger than the first. However, the anteroposterior diameter of the alveolus of the anterior tooth in the smaller specimen is only marginally smaller than that of the 4th tooth, raising concerns about the use of alveolus size as a suitable proxy for tooth size. Although the anteriormost alveolus of the *Eremosuchus* holotype is approximately equal in size to the 4th alveolus, it is not possible to ascertain that the tooth is equally as large, and therefore one of the largest in the tooth row. We therefore suggest that these differences alone do not form a reliable basis on which to consider the specimens as pertaining to different species.

A notable difference between the two El Kohol specimens is variation in alveolar size posterior to the enlarged 4th dentary tooth. In the holotype specimen of *Eremosuchus*, the alveoli are approximately the same anteroposterior length along the

remainder of the tooth row (Table 2). In the smaller specimen, there is some variation in alveolus size posterior to the 4th dentary alveolus. Given the propensity of dental morphologies to change considerably through ontogeny in multiple archosaur groups (Martins dos Santos et al., 2024), including fluctuations in the size of the teeth posterior to the 4th alveolus amongst crocodylomorphs (Pochat-Cottilloux, Perrier et al., 2023), these variations in alveolar dimensions between UOK 347 and UOK-301 are not sufficient to preclude referral of the smaller specimen to *Eremosuchus*. Nonetheless, ontogenetic series viewed in extant taxa (e.g., *Alligator sinensis*, *Crocodylus niloticus*) suggest that it would be unlikely for teeth varying in size in immature individuals to converge to be approximately equidimensional at maturity. The strength of this observation in determining whether the individuals represent two distinct species, or an ontogenetic series, also depends substantially on how accurate a proxy alveolar diameter is for tooth size. In this instance, the poor preservation in the larger specimen precludes the acceptance of alveolar diameter as a true representation of tooth size; for example, of the two preserved teeth, the anterior and posterior crowns have a basal mesiodistal tooth diameter to alveolar diameter ratio of 0.78 and 0.95, respectively, indicating that the substitution of alveolar diameter for tooth diameter is not highly accurate.

Edmund (1962) described how initially sharp-edged, blade-like teeth become more bulbous and molariform with increased maturity in *Alligator mississippiensis*. The posterior teeth preserved in the smaller El Kohol dentary have prominent and sharp carinae, with the almost complete ninth tooth converging at its apex into a sharp point. This contrasts with the preserved posterior tooth of the holotype *Eremosuchus* specimen, which is rounded at its apex, as well as the isolated tooth tentatively referred to *Eremosuchus*. Ontogenetic change in tooth morphology is directly associated with the change in feeding mechanisms in extant crocodylians (Erickson et al., 2003; Gignac & Erickson, 2016; Godoy et al., 2016), highlighting the propensity of the teeth to evolve with increased maturity in crocodyliforms. As such, it is possible to interpret the difference in tooth morphology in the two specimens via ontogenetic change.

Although the majority of alveoli in the El Kohol specimens are approximately evenly spaced, there is a clear diastema between the 7th and 8th alveoli in the small individual that is absent in the holotype. Alveolus spacing is considered in a large number of crocodylomorph phylogenetic matrices (e.g., Jouve, 2016; Pol et al., 2014; Rio & Mannion, 2021), but it is not unusual for this feature to show intraspecific variation, and spacing can even vary between either side of the same skull (Iordansky, 1973). The presence of a similar diastema between the 7th and 8th alveoli in the ‘Fayum form’ and *Doratodon ibericus* is noteworthy, and is potentially indicative of a feature with genuine phylogenetic relevance. Nevertheless, differences in alveolus spacing through ontogeny are difficult to assess given that changes in alveolus/tooth size with increasing maturity naturally leads to alterations in spacing. With this in mind, the difference in the morphology of the two El Kohol specimens is not necessarily enough to preclude the referral of the small specimen to *Eremosuchus*. Furthermore, the use of this feature in determining whether the two specimens belong to the same ontogenetic series is problematic given the lability of alveoli/teeth throughout the tooth row even within the same individual.

In summary, morphological differences between the holotypic and smaller dentaries pertain to the dentition, which is highly susceptible to ontogenetic changes, as well as being prone to intraspecific variation, and even variation within the same individual. As such, it is herein argued that these features are not enough to regard the smaller specimen as a distinct species. Considering the observations and the similarities in morphology, as well as the recovery of the specimens from the same stratigraphic

unit and general locality, the smaller specimen is assigned to *Eremosuchus elkoensis* as an immature individual of that species.

Can the Tentatively Referred Remains be Assigned to *Eremosuchus elkoensis*?

Dentition—Compared with the teeth preserved in the *Eremosuchus* dentaries, the enamel of the isolated teeth differs predominantly in its ornamentation. The fully preserved posterior tooth in the holotype specimen lacks any ornamentation on its enamel, whereas the newly described posterior teeth (UOK 345 and 346) possess fine-scale anastomizing apicobasal ridges that merge into a globular texture towards their bases. In the referred mandible of *Eremosuchus*, ornamentation of the anterior crown is also absent. However, in the isolated caniniform tooth (UOK 344), apicobasal ridges adorn the posterior-most region of the crown. As discussed by Prasad and Lapparent de Broin (2002), there can be substantial variation in tooth morphology within the same species or even individual. Given the absence of any other ziphodont lineages known from the El Kohol site, and the broad morphology of all isolated teeth being consistent with the morphotypes (e.g., bearing the true ziphodont condition) present in *Eremosuchus*, the teeth are tentatively referred to this genus.

Osteoderms—As discussed, fragments of osteoderms from the KD site preserving two distinct ornamentations have been recovered (Fig. 17F, G). Within those notosuchians preserving an almost complete series of dorsal armor, the type of osteoderm ornamentation (i.e., grooves, pitting) does not vary within a singular taxon. As such, three scenarios are plausible. The first of these posits that neither of the two ornamentations of osteoderm belongs to *Eremosuchus*. The true extent of osteoderms amongst sebecids is unknown; however, they appear to be genuinely absent in at least one member of this clade, *Sebecus icaeorhinus*, which preserves much of the postcrania. None of these El Kohol remains were found articulated with any of the holotype or referred material. The second possibility describes a condition unique to Notosuchia which characterizes *Eremosuchus*, in which two different ornamentations of osteoderms are present within one taxon. A final scenario suggests that only one of these morphologies is associated with *Eremosuchus*, and that the osteoderms represent at least two distinct lineages. Under both the first and last scenarios, the El Kohol locality would have a greater diversity of crocodyliforms than previously recognized.

Tooth Replacement in Notosuchia

In juvenile individuals of extant crocodylians, such as *Alligator* and *Crocodylus*, teeth are replaced in a posterior-to-anterior pattern, with replacement typically becoming less ordered throughout ontogenetic development (Brink & LeBlanc, 2023; Edmund, 1960, 1962). In the sphagesaurid *Caipirasuchus*, the replacement pattern in the premaxilla and maxilla seems to reflect a posterior-to-anterior pattern, whereas the mandible does not follow any distinct replacement pattern (Borsoni & Carvalho, 2024). A similar random arrangement characterizes *Eremosuchus*, in which the most posterior tooth preserved has the most advanced growth, whereas the most anterior tooth, shows no sign of replacement. The 4th and 9th teeth show similar stages of replacement teeth growth, whereas the 6th tooth is the least advanced.

Implications for the Phylogenetic Relationships of Sebecidae

Throughout our analyses, *Eremosuchus* is consistently placed within Sebecidae, a family established by Simpson (1937) to accommodate the highly distinct *Sebecus icaeorhinus* from all other crocodyliforms. Resolution within Sebecidae has often

been poor in previous studies (as well as some of those presented herein), and polytomies are not uncommon amongst strict consensus trees, particularly regarding *Sebecus* and closely related taxa (e.g., Kellner et al., 2014; Martin et al., 2022; Pol & Powell, 2011). The uncertainty in placement of these taxa is likely due to the high incompleteness of the remains precluding any real clarity on precise interrelationships; this is exemplified in the strict consensus tree of Analysis 1 (equal weighting), in which two polytomies (3-tomy and 4-tomy) are found within Sebecidae (Fig. 18). Of the 12 MPTs recovered from these analyses, *Eremosuchus* is found to be somewhat labile. In eight MPTs, *Eremosuchus* is closely allied to *Ayllusuchus fernandezii* and *Bretesuchus bonapartei*, either as the sister taxon to *Bretesuchus*, to *Ayllusuchus*, or to *Bretesuchus* + *Ayllusuchus*. In the former two configurations, this clade of three taxa is supported by two common synapomorphies, although the relevant anatomical regions are not preserved in *Eremosuchus*: (1) the absence of an incisive foramen; and (2) the presence of a sagittal torus on the maxillary palatal shelves. In two instances, a relatively early diverging *Eremosuchus* forms the sister taxon to a clade including *Ayllusuchus*, *Bretesuchus*, *Dentaneosuchus*, *Iberosuchus*, *Bergisuchus*, *Razanandrongobe*, *Ogresuchus*, and *Barinasuchus*, supported by one unambiguous synapomorphy: well separated 4th and 5th mandibular teeth. In a final two topologies, *Eremosuchus* is slightly more derived, forming the sister taxon to *Dentaneosuchus*, *Iberosuchus*, *Bergisuchus*, *Razanandrongobe*, *Ogresuchus*, and *Barinasuchus*. Within the MPTs, and despite the lability of *Eremosuchus*, a similar internal topology of Sebecidae is recovered to that of several other studies (e.g., Bravo et al., 2021, 2025; Kellner et al., 2014; Martin et al., 2022), in which (1) *Ayllusuchus* and *Bretesuchus* and (2) *Iberosuchus* and *Bergisuchus* are consistently allied. Following the a priori removal of *Sebecus huilensis* and the Lumbra form, the presence of a distinct “Sebecus” clade as recovered in these existing studies is not obtained.

Species-level resolution of Sebecidae is also relatively poor using extended implied weighting (Fig. 19). In Analysis 2, *Eremosuchus* is frequently recovered with close association to two South American forms: *Sebecus icaeorhinus* and *Zulmasuchus*, forming a clade with these two taxa in over half of the MPTs, either as the sister taxon to both species, in a deeply nested clade with *Sebecus icaeorhinus*, or allied to *Zulmasuchus* as the most derived sebecid clade. The majority of the remaining MPTs find an earlier diverging *Eremosuchus* which forms the sister taxon to a clade containing *Zulmasuchus*, *Sebecus*, *Ogresuchus*, *Ayllusuchus*, and *Bretesuchus*, which together are supported by a single common synapomorphy: an elongate ridge running along the ventrolateral surface of the dentary. In 3 MPTs, *Eremosuchus* forms the sister taxon to *Ogresuchus* and *Ayllusuchus* + *Bretesuchus* as the most derived clade in Sebecidae. This highly nested position of *Eremosuchus* amongst sebecids in the vast majority of the MPTs is in contrast to previous analyses such as Bravo et al. (2025), as despite the El Kohol taxon being found in close association to Sebecosuchia, it has yet to be consistently recovered within Sebecidae.

In Analysis 3, *Eremosuchus* is also found to be deeply nested in Sebecidae either: (1) in a clade with *Ayllusuchus* and *Bretesuchus*, supported by palatal parts of the premaxillae that meet posteriorly along contact with maxillae, the absence of an incisive foramen, and the presence of a sagittal torus on the palatal maxillary shelves; (2) in a group with *Ogresuchus* and *Sebecus icaeorhinus*, supported by a small ventrally opened notch on ventral edge of rostrum at premaxilla-maxilla contact and approximately parallel lateral margins of the posterior half of palatines between suborbital fenestrae; or (3) as the sister taxon to a clade containing all four of these taxa, supported by an elongate ridge running along the ventrolateral surface of the dentary. In all MPTs, these clades form the most derived group within Sebecidae, whereas

Barinasuchus occupies a position as their combined sister taxon. Several European species (*Bergisuchus*, *Dentaneosuchus*, and *Iberosuchus*) form successive sister taxa to these traditional sebecids, with *Dentaneosuchus* consistently finding close association to *Bergisuchus*, contrasting the latter’s common relationship with *Iberosuchus* in the majority of previous analyses (e.g., Bravo et al., 2021, 2025; Kellner et al., 2014; Martin et al., 2022).

As noted above, Sebecidae is found to occupy multiple positions within the notosuchian tree, evidenced here in the competing topologies recovered in Analysis 1 versus Analyses 2 and 3 (Figs. 18, 19). Under equal weighting, Sebecidae and closely related taxa (i.e., Sebecoidea) are recovered as the sister group to all other notosuchians, with members of the clade optimized as sharing several derived features common to all MPTs. These are: a deep and anteriorly convex mandibular symphysis in lateral view; seven maxillary teeth; a deep, well-defined longitudinal groove on the lateral surface of the anterior region of surangular and posterior region of dentary; a lateral concavity of the dentary adjacent to the 7th tooth; dorsal edge of the dentary with a single dorsal expansion and concave posterior region; strongly concave and narrow, trough shaped dorsal surface of the mandibular symphysis; and evaginated maxillary alveolar edges present as a continuous sheet. Sebecidae is supported by a single common synapomorphy: the external surface of the maxilla with a single plane facing laterally.

The position of Sebecidae and closely allied taxa near the ‘base’ of Notosuchia, as sister taxon to all other notosuchians, is a relatively unique tree topology (though see Martins dos Santos et al., 2024); most previous analyses have recovered sebecids in a sister relationship either with baurusuchians (=Sebecosuchia), or with peirosaurids and closely allied taxa (=Sebecia). In this context, the placement of Sebecidae outside of Sebecosuchia is also relatively unusual given that only in Pinheiro et al. (2018, 2021) has the monophyly of Sebecosuchia been broken up in an analysis based on an iteration of the Pol et al. (2012) data matrix.

Previous alternative placements of Sebecidae, either within Sebecia or Sebecosuchia, have perhaps been unsurprising given the high number of derived traits sebecids share with both baurusuchids and peirosaurids. In either tree topology, these characters are considered to be convergences of each lineage due to some of the similar characteristics exhibited by members of all three clades (Fig. 18). However, our equal weighted analysis fails to recover a sister relationship of Sebecidae with either baurusuchians or peirosaurians. Under this topology, several traits would have to have independently evolved in each lineage, including: dentary with a lateral concavity for an enlarged maxillary tooth adjacent to the 7th alveolus (Character 165); and a large concave surface of the periorbital fossa facing anteriorly, projecting anteroventrally from the external nares opening toward the alveolar margin (Character 233) (Fig. 18).

In both analyses using extended implied weighting (EIW), we recover a monophyletic Sebecosuchia that is well-nested within Notosuchia, consistent with the results of Pol et al. (2012) and subsequent iterations of this data matrix (e.g., Fiorelli et al., 2016; Leardi et al., 2015; Martin et al., 2022; Martinelli et al., 2018; Nicholl et al., 2021; Pol et al., 2014). This group has a very similar taxonomic content and almost identical topology when examined under alternative k -values (3 and 8), and in both analyses is supported by two unambiguous common synapomorphies: anterior dentary teeth opposite the premaxilla-maxilla contact that are more than twice the length of other dentary teeth; and a large and slot-like intermandibularis oralis, with an anteroposterior length approximately or more than 50% of the depth of the splenial.

As discussed, several authors have previously supported a sebecosuchian placement of *Eremosuchus* (Bravo et al., 2025; Montefeltro, 2013; Ortega et al., 1996; Turner & Calvo, 2005). Whereas Montefeltro et al. (2013) and Ortega et al. (1996)

found closer affinities of the dentary to baurusuchids, its placement is unclear in Turner and Calvo (2005), in which *Eremosuchus* forms part of a sebecosuchian polytomy, as well as in Bravo et al. (2025) in which it is highly labile. *Eremosuchus* is not recovered within Baurusuchidae, nor as a close relative (i.e., Baurusuchia), in any of our analyses. Although *Eremosuchus* does possess several morphological features common amongst sebecosuchians, there are no traits that it shares exclusively with baurusuchids (i.e., that are not also shared with several sebecids). In contrast, several features common to either all sebecids, or some sebecid lineages, are present in *Eremosuchus* that are completely absent in baurusuchians such as a ridge along the ventrolateral edge of the dentary and posterior teeth that are constricted at their base. If the posterior mandibular fragment tentatively assigned to *Eremosuchus* does belong to this taxon, these traits also include a surangular that forms approximately one-third of the mediolateral width of the glenoid fossa, and a lateral flange of the retroarticular process that is equal to or greater in anteroposterior length than the mediolateral width of the glenoid facet.

For a long time, ‘true’ sebecids were thought to be restricted to South America (Pol et al., 2012; Pol & Powell, 2011); however, recent discoveries have challenged this assumption (Martin et al., 2022; Sellés et al., 2020). The European Eocene taxa *Bergisuchus*, *Dentaneosuchus*, and *Iberosuchus*, are consistently recovered as successive sister taxa to the ‘classical’ sebecids in all of the MPTs of our EIW analyses. Their precise inclusion within, or just outside the clade, is unknown due to the migration of *Sahitisuchus* throughout the tree, and its inclusion as a clade specifier in the definition of Sebecidae by Leardi et al. (2024). Under the varying placement of Sebecidae in Analysis 1 (equal weighting), *Bergisuchus*, *Dentaneosuchus*, and *Iberosuchus* are found to be deeply nested amongst sebecids.

Using all weighting schemes, the European taxon *Ogresuchus* is also found in a relatively derived position and is commonly nested amongst South American taxa from the Cenozoic in those analyses using EIW. For example, in the analysis using a *k*-value of 8, *Ogresuchus* forms one branch of a polytomy with *Bretesuchus*, *Sebecus icaeorhinus*, *Ayllusuchus*, and *Eremosuchus*. Using a *k*-value of 3, the equivalent clade also contains *Zulmasuchus*. The placement of European taxa amongst highly derived South American taxa is not an uncommon result (e.g., Montefeltro, 2013; Pinheiro et al., 2018; Sellés et al., 2020). As discussed by Selles et al. (2020), either the suite of characters defining these clades was already present in early sebecids, remaining unchanged in both lineages, or these features are a result of convergent evolution.

Survival of a Second Notosuchian Lineage Across the K–Pg Mass Extinction?

Under the definition provided in Leardi et al. (2024), Sebecidae is defined as the least inclusive clade that contains *Sebecus icaeorhinus* Simpson 1937, *Bretesuchus bonapartei* Gasparini et al. 1993, *Barinasuchus arveloi* Paolillo and Linares 2007, and *Sahitisuchus* Kellner et al. 2014. However, both of our EIW analyses recover *Sahitisuchus* within Peirosauridae. In Analysis 2, *Sahitisuchus* forms the sister taxon to *Losoruchus*, a clade supported by six common synapomorphies: (1) a relatively anteroposteriorly elongate mandibular symphysis; (2) the presence of a ridge along the ventrolateral edge of the dentary; (3) an enlarged foramen intermandibularis; (4) mediolaterally elongated pterygoid flanges with an anteroposteriorly short lateral end; (5) evaginated maxillary alveolar edges present as a continuous sheet; and (6) a strongly convex, paddle-shaped medial flange of the retroarticular process. The shift in phylogenetic position of *Losoruchus* is not so surprising, with Pol and Powell (2011) reporting a highly autapomorphic cranial

anatomy strongly differing from that of sebecids (though note that the specimen seems heavily compressed dorsoventrally which may skew some character interpretation). This unique morphology has led to some uncertainty about the taxon’s precise position within the crocodyliform tree; most recently, under EIW schemes, Bravo et al. (2021) also recovered *Losoruchus* outside of Sebecidae, either as an early diverging notosuchian, a peirosaurid, or a ‘basal’ sebecosuchian. Pol and Powell (2011) had earlier demonstrated that the taxon can be positioned outside of Notosuchia with just two additional tree steps. *Sahitisuchus* has thus far only been positioned within Sebecidae (Kellner et al., 2014), though it should be noted that its phylogenetic affinities are not often tested. The position of *Losoruchus* and *Sahitisuchus*, as recovered in our EIW analyses (and *Zulmasuchus* at a *k*-value of 8), is particularly pertinent, as it suggests the potential survival of an additional crocodyliform lineage, and a second notosuchian lineage, across the K–Pg mass extinction event. It has long been suggested that less-specialized individuals are more likely to survive such catastrophic events (i.e., Cope’s ‘Law of the Unspecialized’, or Simpson’s ‘Rule of the survival of the relatively unspecialized’) (Cope, 1896; Raia et al., 2016; Raia & Fortelius, 2013; Simpson, 1944; Thompson, 1994), leaving generalized lineages from which post-extinction radiations occur (Hellert et al., 2023). Indeed, *Losoruchus* and *Sahitisuchus*, as well as *Zulmasuchus* are both known from late Paleocene to early Eocene deposits of South America, making them some of the most temporally adjacent notosuchians to the K–Pg boundary. It is also true that the former two of these lack many of the more derived features present in stratigraphically younger notosuchians (i.e., those distanced further from the K–Pg extinction event); for example, the high snouts of sebecids which developed in taxa from the Eocene through to the Miocene (Kellner et al., 2014), although it should be noted that the snout of *Sahitisuchus* is potentially dorsoventrally compressed.

McKinney (1997) cited a limited utilization of resources and habitats as one disadvantage of specialists in periods of drastic change. Many Late Cretaceous deposits preserve crocodyliform taxa with highly specialized morphologies, including those with teeth convergent with those of mammals and squamates (Melstrom & Irmis, 2019; Turner & Sertich, 2010). The termination of these lineages at the K–Pg mass extinction event (Castro et al., 2018) is particularly relevant in terms of the development of specialized feeding ecologies, which Colles et al. (2009) cited as being consistently negatively correlated with survivorship. Naturally, assertions that specializations are an ‘evolutionary dead-end’ have also been challenged, and the suggestion that the survival of this additional notosuchian lineage across the K–Pg boundary is due to an absence of highly derived features should be taken with caution (Colles et al., 2009; Day et al., 2016), particularly as quantifying the true degree of specialization in fossil organisms is in itself challenging.

Implications for Sebecid Biogeography

Sebecids are frequently suggested to have originated in South America (e.g., Buffetaut & Marshall, 1991; Gasparini, 1984; Gasparini et al., 1993; Langston, 1965; Paolillo & Linares, 2007; Pol & Powell, 2011; Simpson, 1937; Turner & Calvo, 2005), based on a large percentage of known species being from this continent, as well as the consistent placement of South American taxa as the earliest diverging members of the group (e.g., Bravo et al., 2021; Kellner et al., 2014; Pol & Powell, 2011). Indeed, sebecids had become highly diversified in South America by the Eocene, with a relatively widespread spatial distribution across the continent. Nevertheless, several taxa that are recovered as sebecids or close relatives are also known from Europe

(Antunes, 1975; Buffetaut, 1979; Bunzel, 1871; Company et al., 2005; Kuhn, 1968; Rossmann et al., 2000) and Africa (Buffetaut, 1989). Sebecids had also previously been considered an exclusively Cenozoic clade; however, the recovery of *Ogresuchus furatus* from the latest Cretaceous of Europe within the group (see also Martin et al., 2022; Sellés et al., 2020) increases the temporal range of the clade, suggesting an earlier origin of the group than previously considered.

The strong Gondwanan signal proposed in European taxa closely affiliated with sebecids (e.g., *Iberosuchus*, *Bergisuchus*, and *Doratodon*) has previously been explained by the ‘Euro-gondwanan model’ (Ezcurra & Agnolin, 2012), in which the separation of Europe from Africa at the end of the Hauterivian was followed by intermittent faunal links via land bridges from the Campanian until the Eocene. As noted by Martin et al. (2023), multiple terrestrial vertebrate lineages recovered from Eocene sediments of Europe support these trans-Tethyan faunal links (e.g., Augé & Santiago, 2020; Bolet & Evans, 2013; Gheerbrant & Rage, 2006; Laloy et al., 2013). If sebecids were to have dispersed from South America to Europe, their presence in Cretaceous sediments of both South America and Africa is necessitated, given the latter continent’s intermediate position between the other two landmasses. This is supported by the biogeographic analysis of Sellés et al. (2020), in which sebecids were estimated to have been established in South America and Africa before fragmentation of the two continents in the Albian. At present, no Cretaceous occurrences are known from either landmass, despite several highly sampled and productive regions in these spatiotemporal intervals that have yielded notosuchians. For example, the Late Cretaceous Bauru Basin of Brazil is well-studied, and is exceedingly productive with regards to other notosuchians (Martins dos Santos et al., 2024; Pol et al., 2014). The mid-Cretaceous Kem Kem Group of Morocco is also well studied, and has yielded several other notosuchian lineages (e.g., Larsson & Sues, 2007; Martin & Lapparent de Broin, 2016; Nicholl et al., 2021), although latest Cretaceous African deposits are generally less well-sampled (Mannion et al., 2019). Only one unequivocal sebecid occurrence from Africa is currently known: *Eremosuchus* from the early Eocene of Algeria, with the late Eocene ‘Fayum form’ potentially representing a second occurrence. However, their Eocene age and poor phylogenetic resolution within Sebecidae mean that it is not currently possible to determine whether they represent a long, independent African lineage of sebecids that has been obscured by pervasive under-sampling, or a Paleogene emigration of European taxa via the same trans-Tethyan pathways.

Given the absence of sebecid remains from the Cretaceous of Gondwana, we agree with Martin et al. (2023) that it is important to consider some opposing origins of Sebecidae, i.e., origination and dispersal from Europe into Gondwana, or from Africa into both Europe and South America. However, given such a poor fossil record during the Cretaceous, uncovering the group’s early evolutionary and biogeographic history remains problematic until further specimens are found.

CONCLUSION

The holotype specimen of *Eremosuchus elkoensis*, as well as referred remains from the same El Kohol locality in the early Eocene of Algeria, are redescribed and compared with numerous notosuchian taxa. *Eremosuchus* is considered to represent a valid taxon, for which we provide a new diagnosis. A smaller specimen from the same locality likely represents an immature individual of *Eremosuchus elkoensis*, providing an additional example of an ontogenetic series amongst Notosuchia. Under multiple phylogenetic weighting schemes, *Eremosuchus* is recovered as a sebecid. The position of Sebecidae varies depending on

the weighting scheme used. Under equal weighting, Sebecidae is placed as the sister taxon to all other notosuchians, an unusual positioning for this clade. Using extended implied weighting, a monophyletic Sebecosuchia is recovered. Several European taxa known from fragmentary remains (e.g., *Ogresuchus furatus*) are also recovered within Sebecidae, expanding the taxonomic and spatial content of the group, which until recently has been considered to be formed entirely of South American taxa. The temporal range of sebecids is also confirmed to extend into the Cretaceous; however, a dearth of fossil material inhibits a true understanding of the early evolutionary and biogeographic origin of the group.

ACKNOWLEDGMENTS

We are grateful to M. Kouvari for couriering the *Eremosuchus* specimens from Paris to London, as well as to E. Buffetaut for facilitating their loan. We also thank V. Fernandez for producing CT-scans of the specimens at the Natural History Museum, London. D. Pol and P. Godoy were kind enough to provide specimen photographs during preparation of the manuscript, and D. Hoffman generously offered discussion on tooth replacement. For technical and field assistance during the excavations at El Kohol (KD locus), RT and MM thank A. Charrault, L. Marivaux, L. Hautier, J. Crochet, and R. Lebrun (University of Montpellier), M. Adaci (University of Tlemcen), F. Mebrouk (University of Jijel), V. Lazzari (University of Poitiers), A. Ravel (Paris), and G. Abderramane (Brezina). Thanks also go to two anonymous reviewers, as well as Pedro Godoy, for their help in improving an earlier version of this manuscript. CSCN and EMM were funded by Royal Society grants (RGFR1180020, RGF\EA\180318) awarded to PDM. PDM’s contribution was supported by several Royal Society grants (RGFR1180020, RGF\EA\201037, UF160216, URF\221010), as well as funding from the Leverhulme Trust (RPG-2021-202) and NERC (NE/X014010/1). JEM was supported by a grant from Agence Nationale de la Recherche (SEBEK project no. ANR-19-CE31-0006-01). Field research was supported by the French ANR-ERC PALASIAFRICA Program (ANR-08-JCJC-0017).

AUTHOR CONTRIBUTIONS

CSCN and PDM conceived of the study and interpreted the results. CSCN, PDM, and JEM drafted the manuscript. Phylogenetic analyses were conducted by CSCN. Computed tomography scans were processed by PMJB. Figures were produced by CSCN, JEM, RT, and PMJB. All authors reviewed and edited the final version of the manuscript.

DATA AVAILABILITY

All data necessary to replicate the findings of the study are available in the paper or in the supplementary files. The X-ray computed tomography scans used in this study are available on Morphobank: <https://www.morphosource.org/concern/media/000790013?locale=en> and <https://www.morphosource.org/concern/media/000789599?locale=en>

DISCLOSURE STATEMENT

No potential conflict of interest was reported by the author(s).

LIST OF SUPPLEMENTARY FILES

Supplementary File 1.docx: supplementary Information including character list, taxon list, character score changes,

excluded characters, list of common synapomorphies for each analysis, and Figures S1–S3.

Supplementary File 2.nex: discrete character-taxon matrix (discrete data) in nexus format.

Supplementary File 3.tnt: combined character taxon matrix in tnt format.

Supplementary File 4.nex: continuous character-taxon matrix (continuous data) in nexus format.

Supplementary File 5.docx: README file containing instructions for running the analyses.

Supplementary File 6.tre: tree file for Analysis 1.

Supplementary File 7.tre: tree file for Analysis 2.

Supplementary File 8.tre: tree file for Analysis 3.

ORCID

Cecily S. C. Nicholl  <http://orcid.org/0000-0003-2860-2604>

Paul M. J. Burke  <http://orcid.org/0000-0003-0328-7003>

Philip D. Mannion  <http://orcid.org/0000-0002-9361-6941>

LITERATURE CITED

Andrade, M. D., & Bertini, R. J. (2008). A new *Sphagesaurus* (Mesoeucrocodylia: Notosuchia) from the Upper Cretaceous of Monte Alto city (Bauru Group, Brazil), and a revision of the Sphagesauridae. *Historical Biology*, 20(2), 101–136. doi:10.1080/08912960701642949

Andrade, M. B., Young, M. T., Desojo, J. B., & Brusatte, S. L. (2010). The evolution of extreme hypercarnivory in Metriorhynchidae (Mesoeucrocodylia: Thalattosuchia) based on evidence from microscopic denticle morphology. *Journal of Vertebrate Paleontology*, 30(5), 1451–1465. doi:10.1080/02724634.2010.501442

Antunes, T. (1975). *Iberosuchus*, crocodile Sebecosuchien nouveau, l'Éocène iberique au Nord de la Chaîne Centrale, et l'origine du canyon de Nazaré. *Comunicações dos Serviços Geológicos de Portugal*, 59, 285–330.

Araújo-Júnior, H. I., & da Silva Marinho, T. (2013). Taphonomy of a *Baurusuchus* (Crocodyliformes, Baurusuchidae) from the Adamantina Formation (Upper Cretaceous, Bauru Basin), Brazil: implications for preservational modes, time resolution and paleoecology. *Journal of South American Earth Sciences*, 47, 90–99. doi:10.1016/j.jsames.2013.07.006

Aubier, P., Jouve, S., Schnyder, J., & Cubo, J. (2023). Phylogenetic structure of the extinction and biotic factors explaining differential survival of terrestrial notosuchians at the Cretaceous–Palaeogene crisis. *Palaeontology*, 66(1), e12638. doi:10.1111/pala.12638

Augé, M. L., & Santiago, B. (2020). Transient presence of a teiid lizard in the European Eocene suggests transatlantic dispersal and rapid extinction. *Palaeobiodiversity and Palaeoenvironments*, 100(3), 793–817. doi:10.1007/s12549-019-00414-2

Barrios, F., Paulina-Carabajal, A., & Bona, P. (2016). A new peirosaurid (Crocodyliformes, Mesoeucrocodylia) from the Upper Cretaceous of Patagonia, Argentina. *Ameghiniana*, 53(1), 14–25. doi:10.5710/AMGH.03.09.2015.2903

Benoit, J., Crochet, J. Y., Mahboubi, M., Jaeger, J. J., Bensalah, M., Adaci, M., & Tabuce, R. (2016). New material of *Seggeurius amourensis* (Paenungulata, Hyracoidea), including a partial skull with intact basicranium. *Journal of Vertebrate Paleontology*, 36(1), e1034358. doi:10.1080/02724634.2015.1034358

Benton, M. J., & Clark, J. M. (1988). Archosaur phylogeny and the relationships of the Crocodylia. *The phylogeny and classification of the tetrapods*, 1, 295–338.

Berg D. E., & Crusafont M. (1970). Note sur quelques Crocodiliens de l'écène prépyrénaique. *Acta Geológica Hispanica*, 5:54–57.

Bolet, A., & Evans, S. E. (2013). Lizards and amphisbaenians (Reptilia, Squamata) from the late Eocene of Sossís (Catalonia, Spain). *Palaeontologia Electronica*, 6(1).1.8A, 1–23.

Borsoni, B. D. T., & Carvalho, I. D. S. (2024). Dental replacement in *Caipirasuchus* (Crocodyliformes) from the Brazilian Cretaceous. *Journal of South American Earth Sciences*, 105084. doi:10.1016/j.jsames.2024.105084

Bravo, G. G., Pol, D., & García-López, D. A. (2021). A new sebecid mesoeucrocodylian from the Paleocene of northwestern Argentina. *Journal of Vertebrate Paleontology*, 41(3), e1979020. doi:10.1080/02724634.2021.1979020

Bravo, G. G., Pol, D., Leardi, J. M., Krause, J. M., Nicholl, C. S., Rougier, G., & Mannion, P. D. (2025). A new notosuchian crocodyliform from the Early Paleocene of Patagonia and the survival of a large-bodied terrestrial lineage across the K–Pg mass extinction. *Proceedings B*, 292(2043), 20241980.

Brink, K. S., & LeBlanc, A. R. (2023). How the study of crocodylian teeth influences our understanding of dental development, replacement, and evolution in dinosaurs. *Ruling Reptiles: Crocodylian Biology and Archosaur Paleobiology*, 240–257. doi:10.2307/jj.6047951.14

Brown, C. M., VanBuren, C. S., Larson, D. W., Brink, K. S., Campione, N. E., Vavrek, M. J., & Evans, D. C. (2015). Tooth counts through growth in diapsid reptiles: Implications for interpreting individual and size-related variation in the fossil record. *Journal of Anatomy*, 226(4), 322–333. doi:10.1111/joa.12280

Buckley, G. A., & Brochu, C. A. (1999). An enigmatic new crocodile from the Upper Cretaceous of Madagascar. *Special papers in palaeontology (London)*, 60(60), 149–175.

Buckley, G. A., Brochu, C. A., Krause, D. W., & Pol, D. (2000). A pug-nosed crocodyliform from the Late Cretaceous of Madagascar. *Nature*, 405(6789), 941–944. doi:10.1038/35016061

Buffetaut, E. (1979). The evolution of the crocodilians. *Scientific American*, 241(4), 130–145. doi:10.1038/scientificamerican1079-130

Buffetaut, E. (1980). Histoire biogéographique des Sebecosuchia (Crocodylia, Mesosuchia): un essai d'interprétation. *Annales de Paléontologie (Vertébrés)*, v. 66, 1–18.

Buffetaut, E. (1982). A ziphodont mesosuchian crocodile from the Eocene of Algeria and its implications for vertebrate dispersal. *Nature*, 300(5888), 176–178. doi:10.1038/300176a0

Buffetaut, E. (1986). Un Mésosuchien ziphodont dans l'Éocène supérieur de La Livinière (Hérault, France). *Geobios*, 19(1), 101–113. doi:10.1016/S0016-6995(86)80038-9

Buffetaut, E. (1989). A new ziphodont mesosuchian crocodile from the Eocene of Algeria. *Palaeontographica. Abteilung A, Paläozoologie, Stratigraphie*, 208(1–3), 1–10.

Buffetaut, E., & Marshall, L. G. (1991). A new crocodilian, *Sebecus queretensis*, nov. sp. (Mesosuchia, Sebecidae) from the Santa Lucia formation (Early Paleocene) at Vila Vila, southcentral Bolivia. *Fósiles y Facies de Bolivia*, 1, 545–557.

Bunzel, E. (1871). *Die Reptilfauna der Gosau-Formation in der Neuen Welt bei Wiener-Neustadt*. Braumüller.

Busbey IIIA. B. (1986). New material of *Sebecus cf. huilensis* (Crocodylia: Sebecosuchidae) from the Miocene La Venta Formation of Colombia. *Journal of Vertebrate Paleontology*, 6(1), 20–27. doi:10.1080/02724634.1986.10011595

Campos, D. A., Oliveira, G. R., Figueiredo, R. G., Riff, D., Azevedo, S. A., Carvalho, L. B., & Kellner, A. W. (2011). On a new peirosaurid crocodyliform from the Upper Cretaceous, Bauru Group, southeastern Brazil. *Anais da Academia Brasileira de Ciências*, 83(1), 317–327. doi:10.1590/S0001-37652011000100020

Carvalho, I. d. S., Celso Arruda Campos, A. D., & Nobre, P. H. (2005). *Baurusuchus salgadoensis*, a new crocodylomorpha from the Bauru Basin (Cretaceous), Brazil. *Gondwana Research*, 8(1), 11–30. doi:10.1016/S1342-937X(05)70259-8

Carvalho, I. d. S., de Gasparini, Z. B., Salgado, L., de Vasconcellos, F. M., & da Silva Marinho, T. (2010). Climate's role in the distribution of the Cretaceous terrestrial Crocodyliformes throughout Gondwana. *Palaeogeography, Palaeoclimatology, Palaeoecology*, 297(2), 252–262. doi:10.1016/j.palaeo.2010.08.003

Carvalho, I. d. S., de Vasconcellos, F. M., & Tavares, S. A. S. (2007). *Montealtosuchus arrudacamposi*, a new peirosaurid crocodile (mesoeucrocodylia) from the Late Cretaceous Adamantina Formation of Brazil. *Zootaxa*, 1607, 35–46.

Carvalho, I. d. S., Ribeiro, L. C. B., & dos Santos Avilla, L. (2004). *Uberabasuchus terrificus* sp. nov., a new Crocodylomorpha from the Bauru Basin (Upper Cretaceous), Brazil. *Gondwana Research*, 7(4), 975–1002. doi:10.1016/S1342-937X(05)71079-0

Carvalho, I. d. S., Teixeira, V. D. P. A., Ferraz, M. L. D. F., Ribeiro, L. C. B., Martinelli, A. G., Neto, F. M., Sertich, J. J. W., Cunha, G. C., Cunha, I. C., & Ferraz, P. F. (2011). *Campinasuchus dinizi* gen. et sp. nov., a new Late Cretaceous baurusuchid (Crocodyliformes) from the Bauru Basin, Brazil. *Zootaxa*, 2871(1), 19–42.

Castro, M. C., Goin, F. J., Ortiz-Jaureguizar, E., Vieytes, E. C., Tsukui, K., Ramezani, J., Batezelli, A., Marsola, J. C. A., Langer, M. C. (2018). A Late Cretaceous mammal from Brazil and the first radioisotopic age for the Bauru Group. *Royal Society Open Science*, 5(5), 180482. doi:10.1098/rsos.180482

Colbert, E. H., Simpson, G. G., & Williams, C. S. (1946). *Sebecus*, representative of a peculiar suborder of fossil Crocodilia from Patagonia. *Bulletin of the AMNH*; v. 87, article 4.

Colles, A., Liow, L. H., & Prinzing, A. (2009). Are specialists at risk under environmental change? Neoecological, paleoecological and phylogenetic approaches. *Ecology letters*, 12(8), 849–863. doi:10.1111/j.1461-0248.2009.01336.x

Company, J., Suberbiola, X. P., Ruiz-Omeñaca, J. I., & Buscalioni, A. D. (2005). A new species of *Doratodon* (Crocodyliformes: Ziphosuchia) from the Late Cretaceous of Spain. *Journal of Vertebrate Paleontology*, 25(2), 343–353. doi:10.1671/0272-4634(2005)025[0343:ANSODC]2.0.CO;2

Cope, E. D. (1896). *The Primary Factors of Organic Evolution*. Open Court.

Coria, R. A., Ortega, F., Arcucci, A. B., & Currie, P. J. (2019). A new and complete peirosaurid (Crocodyliformes, Notosuchia) from Sierra Barrosa (Santonian, Upper Cretaceous) of the Neuquén Basin, Argentina. *Cretaceous Research*, 95, 89–105. doi:10.1016/j.cretres.2018.11.008

Coster, P., Benammi, M., Mahboubi, M., Tabuce, R., Adaci, M., Marivaux, L., Bensalah, M., Mahboubi, S., Mahboubi, A., Mebrout, F., Maameri, C., & Jaeger, J. J. (2012). Chronology of the Eocene continental deposits of Africa: Magnetostratigraphy and biostratigraphy of the El Kohol and Glib Zegdou Formations, Algeria. *Bulletin*, 124(9–10), 1590–1606.

Cott, L., Pinheiro, A. E. P., da Silva Marinho, T., de Souza Carvalho, I., & Di Dario, F. (2017). Postcranial skeleton of *Campinasuchus dinizi* (Crocodyliformes, Baurusuchidae) from the Upper Cretaceous of Brazil, with comments on the ontogeny and ecomorphology of the species. *Cretaceous Research*, 70, 163–188. doi:10.1016/j.cretres.2016.11.003

Court, N. (1994). Limb posture and gait in *Numidotherium koholense*, a primitive proboscidean from the Eocene of Algeria. *Zoological journal of the Linnean Society*, 111(4), 297–338. doi:10.1111/j.1096-3642.1994.tb01487.x

Dal Sasso, C., Pasini, G., Fleury, G., & Maganuco, S. (2017). *Razanandrongo sakalavae*, a gigantic mesoeucrocodylian from the Middle Jurassic of Madagascar, is the oldest known notosuchian. *PeerJ*, 5, e3481. doi:10.7717/peerj.3481

Darlim, G., Montefeltro, F. C., & Langer, M. C. (2021). 3D skull modelling and description of a new baurusuchid (Crocodyliformes, Mesoeucrocodylia) from the Late Cretaceous (Bauru Basin) of Brazil. *Journal of Anatomy*, 239(3), 622–662. doi:10.1111/joa.13442

Day, E. H., Hua, X., & Bromham, L. (2016). Is specialization an evolutionary dead end? Testing for differences in speciation, extinction and trait transition rates across diverse phylogenies of specialists and generalists. *Journal of evolutionary biology*, 29(6), 1257–1267. doi:10.1111/jeb.12867

Edmund, A. G. (1960). Tooth replacement phenomena in the lower vertebrates. *Life Sciences Division of the Royal Ontario Museum of Zoology, Paleontology Contribution*, 52, 1–190.

Edmund, A. G. (1962). Sequence and rate of tooth replacement in the Crocodilia. *Life Sciences Division of the Royal Ontario Museum of Zoology, Paleontology Contribution*, 56, 1–42.

Edmund, A. G. (1969). Dentition. In C. Gans, D. A. Bellairs, & T. S. Parson (Eds.), *Biology of the Reptilia* (pp. 117–200). London: Academic Press.

Erickson, G. M., Lappin, A. K., & Vliet, K. A. (2003). The ontogeny of bite-force performance in American alligator (*Alligator mississippiensis*). *Journal of Zoology*, 260(3), 317–327. doi:10.1017/S0952836903003819

Ezcurra, M. D., & Agnolín, F. L. (2012). A new global palaeobiogeographical model for the late Mesozoic and early Tertiary. *Systematic Biology*, 61(4), 553–566. doi:10.1093/sysbio/syr115

Farlow, J. O., Brinkman, D. L., Abler, W. L., & Currie, P. J. (1991). Size, shape, and serration density of theropod dinosaur lateral teeth. *Modern Geology*, 16(1–2), 161–198.

Filippi, L. S., Barrios, F., & Garrido, A. C. (2018). A new peirosaurid from the Bajo de la Carpa Formation (Upper Cretaceous, Santonian) of Cerro Overo, Neuquén, Argentina. *Cretaceous Research*, 83, 75–83. doi:10.1016/j.cretres.2017.10.021

Fiorelli, L. E., Leardi, J. M., Hechenleitner, E. M., Pol, D., Basilici, G., & Grellet-Tinner, G. (2016). A new Late Cretaceous crocodyliform from the western margin of Gondwana (La Rioja Province, Argentina). *Cretaceous Research*, 60, 194–209. doi:10.1016/j.cretres.2015.12.003

Gasparini, Z. B. (1971). Los Notosuchia del Cretácico de América del Sur como un nuevo infraorden de los Mesosuchia (Crocodilia). *Ameghiniana*, 8(2), 83–103.

Gasparini, Z. B. (1972). Los Sebecosuchia (Crocodylia) del territorio Argentino. Consideraciones sobre su status taxonómico. *Ameghiniana*, 9(1), 23–34.

Gasparini, Z. (1984). New Tertiary Sebecosuchia (Crocodylia: Mesosuchia) from Argentina. *Journal of Vertebrate Paleontology*, 4(1), 85–95. doi:10.1080/02724634.1984.10011988

Gasparini, Z., Chiappe, L. M., & Fernandez, M. (1991). A new Senonian peirosaurid (Crocodylomorpha) from Argentina and a synopsis of the South American Cretaceous crocodilians. *Journal of Vertebrate Paleontology*, 11(3), 316–333. doi:10.1080/02724634.1991.10011401

Gasparini, Z., Fernandez, M., & Powell, J. (1993). New tertiary sebecosuchians (Crocodylomorpha) from South America: phylogenetic implications. *Historical Biology*, 7(1), 1–19. doi:10.1080/10292389309380440

Gasparini, Z., Pol, D., & Spalletti, L. A. (2006). An unusual marine crocodyliform from the Jurassic-Cretaceous boundary of Patagonia. *Science*, 311(5757), 70–73. doi:10.1126/science.1120803

Georgi, J. A., & Krause, D. W. (2010). Postcranial axial skeleton of *Simosuchus clarki* (Crocodyliformes: Notosuchia) from the Late Cretaceous of Madagascar. *Journal of Vertebrate Paleontology*, 30(sup1), 99–121. doi:10.1080/02724634.2010.519172

Geroto, C. F. C., & Bertini, R. J. (2012). Descrição de um espécime juvenil de Baurusuchidae (Crocodyliformes: Mesoeucrocodylia) do Grupo Bauru (Neocretáceo): considerações preliminares sobre ontogenia. *Revista do Instituto Geológico*, 33(2), 13–29. doi:10.5935/0100-929X.20120007

Geroto, C. F. C., & Bertini, R. J. (2019). New material of *Pepesuchus* (Crocodyliformes; Mesoeucrocodylia) from the Bauru Group: implications about its phylogeny and the age of the Adamantina Formation. *Zoological Journal of the Linnean Society*, 185(2), 312–334. doi:10.1093/zoolinnean/zly037

Gheerbrant, E., & Rage, J. C. (2006). Paleobiogeography of Africa: how distinct from Gondwana and Laurasia? *Palaeogeography, Palaeoclimatology, Palaeoecology*, 241(2), 224–246. doi:10.1016/j.palaeo.2006.03.016

Gignac, P. M., & Erickson, G. M. (2016). Ontogenetic bite-force modeling of *Alligator mississippiensis*: implications for dietary transitions in a large-bodied vertebrate and the evolution of crocodylian feeding. *Journal of Zoology*, 299(4), 229–238. doi:10.1111/jzo.12349

Gignac, P., & O'Brien, H. (2016). Suchian feeding success at the interface of ontogeny and macroevolution. *Integrative and Comparative Biology*, 56(3), 449–458. doi:10.1093/icb/icw041

Godoy, P. L., Bronzati, M., Eltink, E., Marsola, J. C. D. A., Cidade, G. M., Langer, M. C., & Montefeltro, F. C. (2016). Postcranial anatomy of *Pissarrachamps sera* (Crocodyliformes, Baurusuchidae) from the Late Cretaceous of Brazil: insights on lifestyle and phylogenetic significance. *PeerJ*, 4, e2075. doi:10.7717/peerj.2075

Godoy, P. L., Montefeltro, F. C., Norell, M. A., & Langer, M. C. (2014). An additional baurusuchid from the Cretaceous of Brazil with evidence of interspecific predation among Crocodyliformes. *PLoS ONE*, 9(5), e97138. doi:10.1371/journal.pone.0097138

Goloboff, P. A., & Catalano, S. A. (2016). TNT version 1.5, including a full implementation of phylogenetic morphometrics. *Cladistics*, 32(3), 221–238. doi:10.1111/cla.12160

Goloboff, P. A., Farris, J. S., & Nixon, K. C. (2008). TNT, a free program for phylogenetic analysis. *Cladistics*, 24(5), 774–786. doi:10.1111/j.1096-0031.2008.00217.x

Groh, S. S., Upchurch, P., Barrett, P. M., & Day, J. J. (2020). The phylogenetic relationships of neosuchian crocodiles and their implications for the convergent evolution of the longirostrine condition. *Zoological Journal of the Linnean Society*, 188(2), 473–506.

Hanai, T., & Tsujihi, T. (2019). Description of tooth ontogeny and replacement patterns in a juvenile *Tarbosaurus bataar* (Dinosauria: Theropoda) using CT-scan data. *The Anatomical Record*, 302(7), 1210–1225. doi:10.1002/ar.24014

Hay, O. P. (1930). Second Bibliography and Catalogue of the Fossil Vertebrata of North America. *Washington: Carnegie Institution of Washington*, 390(II), 1–1074.

Hellert, S. M., Grossnickle, D. M., Lloyd, G. T., Kammerer, C. F., & Angielczyk, K. D. (2023). Derived faunivores are the forerunners of major synapsid radiations. *Nature Ecology & Evolution*, 7(11), 1903–1913. doi:10.1038/s41559-023-02200-y

Hungerbühler, A. (2000). Heterodonty in the European phytosaur *Nicosaurus kapffi* and its implications for the taxonomic utility and functional morphology of phytosaur dentitions. *Journal of Vertebrate Paleontology*, 20(1), 31–48. doi:10.1671/0272-4634(2000)020[0031:HITEPN]2.0.CO;2

Iordansky, N. N. (1973). The skull of the Crocodilia. In C. Gans, & T. S. Parsons (Eds.), *Biology of the Reptilia, Volume 4, Morphology D* (pp. 201–262). Academic Press.

Iori, F. V., de Souza Carvalho, I., & da Silva Marinho, T. (2016). Postcranial skeletons of *Caipirasuchus* (Crocodyliformes, Notosuchia, Sphagesauridae) from the Upper Cretaceous (Turonian–Santonian) of the Bauru Basin, Brazil. *Cretaceous Research*, 60, 109–120. doi:10.1016/j.cretres.2015.11.017

Iori, F. V., Ghilardi, A. M., Fernandes, M. A., & Dias, W. A. (2024). A new species of vocalizing crocodyliform (Notosuchia, Sphagesauridae) from the Late Cretaceous of Brazil. *Historical Biology*, 1–12.

Iori, F. V., Marinho, T. S., Carvalho, I. S., & Campos, A. C. D. A. (2013). Taxonomic reappraisal of the sphagesaurid crocodyliform *Sphagesaurus montealtensis* from the late Cretaceous Adamantina Formation of São Paulo State, Brazil. *Zootaxa*, 3686(2), 183–200.

Jouve, S. (2016). A new basal tomistomine (Crocodylia, Crocodyloidea) from Issel (Middle Eocene; France): palaeobiogeography of basal tomistomines and palaeogeographic consequences. *Zoological Journal of the Linnean Society*, 177(1), 165–182. doi:10.1111/zoj.12357

Kellner, A. W., Pinheiro, A. E., & Campos, D. A. (2014). A new sebecid from the Paleogene of Brazil and the crocodyliform radiation after the K-Pg boundary. *PLoS ONE*, 9(1), e81386. doi:10.1371/journal.pone.0081386

Klock, C., Leuzinger, L., Santucci, R. M., Martinelli, A. G., Marconato, A., Marinho, T. S., Luz, Z., & Vennemann, T. (2022). A bone to pick: stable isotope compositions as tracers of food sources and paleoecology for notosuchians in the Brazilian Upper Cretaceous Bauru Group. *Cretaceous Research*, 131, 105113. doi:10.1016/j.cretres.2021.105113

Kowalski, K. Rzebik-Kowalska. (1991). Mammals of Algeria. *Polish Academy of Sciences. Institute of Systematics and Evolution of Animals*.

Kuhn, O. 1968. *Die vorzeitlichen Krokodile*. Verlag Oeben, Munich, 124 pp.

Laloy, F., Rage, J. C., Evans, S. E., Boistel, R., Lenoir, N., & Laurin, M. (2013). A re-interpretation of the Eocene anuran *Thaumastosaurus* based on microCT examination of a ‘mummified’-specimen. *PLoS ONE*, 8(9), e74874. doi:10.1371/journal.pone.0074874

Lamanna, M. C., Casal, G. A., Ibáñez, L. M., & Martínez, R. D. (2019). A new peirosaurid crocodyliform from the Upper Cretaceous Lago Colhué Huapi Formation of Central Patagonia, Argentina. *Annals of Carnegie Museum*, 85(3), 193–211. doi:10.2992/007.085.0301

Langston, W. (1965). Fossil crocodilians from Colombia and the Cenozoic history of the Crocodilia in South America. *University California Publication Geological Sciences*, 52, 1–157.

Larsson, H. C., & Gado, B. (2000). A new Early Cretaceous crocodyliform from Niger; A new Early Cretaceous crocodyliform from Niger. *Neues Jahrbuch für Geologie und Paläontologie - Abhandlungen*, 217(1), 131–141. doi:10.1127/njgpa/217/2000/131

Larsson, H. C., & Sues, H. D. (2007). Cranial osteology and phylogenetic relationships of *Hamadasuchus rebouli* (Crocodyliformes: Mesoeucrocodylia) from the Cretaceous of Morocco. *Zoological Journal of the Linnean Society*, 149(4), 533–567. doi:10.1111/j.1096-3642.2007.00271.x

Leardi, J. M., Pol, D., & Gasparini, Z. (2018). New Patagonian baurusuchids (Crocodylomorpha; Notosuchia) from the Bajo de la Carpa Formation (Upper Cretaceous; Neuquén, Argentina): new evidences of the early sebecosuchian diversification in Gondwana. *Comptes Rendus Palevol*, 17(8), 504–521. doi:10.1016/j.crpv.2018.02.002

Leardi, J. M., Pol, D., Montefeltro, F., Marinho, T. S., Ruiz, J. V., Bravo, G. G., Pinheiro, A. E. P., Godoy, P. L., Nicholl, C. S. C., Lecuona, A., & Larsson, H. C. E. (2024). Phylogenetic nomenclature of Notosuchia (Crocodylomorpha; Crocodyliformes). *Bulletin of Phylogenetic Nomenclature*.

Leardi, J. M., Pol, D., Novas, F. E., & Suárez Riglos, M. (2015). The postcranial anatomy of *Yacarerani boliviensis* and the phylogenetic significance of the notosuchian postcranial skeleton. *Journal of Vertebrate Paleontology*, 35(6), e995187. doi:10.1080/02724634.2014.995187

Lio, G., Agnolín, F. L., Valieri, R. J., Filippi, L., & Rosales, D. (2016). A new peirosaurid (Crocodyliformes) from the Late Cretaceous (Turonian–comiacian) of Patagonia, Argentina. *Historical Biology*, 28(6), 835–841. doi:10.1080/08912963.2015.1043999

Maddison, W. P., & Maddison, D. R. (2023). Mesquite: a modular system for evolutionary analysis. Version 3.81 <http://www.mesquiteproject.org>.

Maganuco, S., & Dal Sasso, C. (2006). A new large predatory archosaur from the Middle Jurassic (Bathonian) of Madagascar. *Atti della Società italiana di scienze naturali e del Museo civico di storia naturale di Milano*, 147(1), 19.

Mahboubi, M., Ameur, R., Crochet, J. Y., & Jaeger, J. J. (1984a). Implications paléobiogéographiques de la découverte d'une nouvelle localité éocène à vertébrés continentaux en Afrique nord-occidentale: El Kohol (Sud-Oranais, Algérie). *Geobios*, 17(5), 625–629. doi:10.1016/S0016-6995(84)80033-9

Mahboubi, M., Ameur, R., Crochett, J. Y., & Jaeger, J. J. (1984b). Earliest known proboscidean from early Eocene of north-west Africa. *Nature*, 308(5959), 543–544. doi:10.1038/308543a0

Mahboubi, M., Ameur, R., Crochet, J. Y., & Jaeger, J. J. (1986). El Kohol (Saharan Atlas, Algeria): a new Eocene mammal locality in north-western Africa. Stratigraphical, phylogenetic and paleobiogeographical data. *Palaeontographica Abteilung A, Paläozoologie, Stratigraphie*, 192(1–3), 15–49.

Mannion, P. D., Chiarenza, A. A., Godoy, P. L., & Cheah, Y. N. (2019). Spatiotemporal sampling patterns in the 230 million year fossil record of terrestrial crocodylomorphs and their impact on diversity. *Palaeontology*, 62(4), 615–637. doi:10.1111/pala.12419

Marinho, T., Iori, F. V., de Souza Carvalho, I., & de Vasconcellos, F. M. (2013). *Gondwanasuchus scabrosus* gen. et sp. nov., a new terrestrial predatory crocodyliform (Mesoeucrocodylia: Bauruchidae) from the Late Cretaceous Bauru Basin of Brazil. *Cretaceous Research*, 44, 104–111. doi:10.1016/j.cretres.2013.03.010

Martin, J. E. (2014). A sebecosuchian in a middle Eocene karst with comments on the dorsal shield in Crocodylomorpha. *Acta Palaeontologica Polonica*, 60(3), 673–680.

Martin, J. E. (2016). April. New material of the ziphodont mesoeucrocodylian *Iberosuchus* from the Eocene of Languedoc, southern France. *Annales de Paléontologie*, 102(2), 135–144. Elsevier Masson. doi:10.1016/j.anpal.2016.05.002

Martin, J. E., & De Lapparent De Broin, F. (2016). A miniature notosuchian with multicuspid teeth from the Cretaceous of Morocco. *Journal of Vertebrate Paleontology*, 36(6), e1211534. doi:10.1080/02724634.2016.1211534

Martin, J. E., Pochat-Cottilloux, Y., Laurent, Y., Perrier, V., Robert, E., & Antoine, P. O. (2023). Anatomy and phylogeny of an exceptionally large sebecid (Crocodylomorpha) from the middle Eocene of southern France. *Journal of Vertebrate Paleontology*, 42(4), e2193828. doi:10.1080/02724634.2023.2193828

Martin de Jesús, S., Fuentes, E. J., Fincias, B., Del Prado, J. M., & Alonso, E. M. (1987). Los Crocodylia del Eoceno y Oligoceno de la Cuenca del Duero. Dientes y osteodermos. *Spanish journal of palaeontology*, 2(1), 95–108.

Martinelli, A. G., Marinho, T. S., Iori, F. V., & Ribeiro, L. C. B. (2018). The first *Caipirasuchus* (Mesoeucrocodylia, Notosuchia) from the Late Cretaceous of Minas Gerais, Brazil: new insights on sphagesaurid anatomy and taxonomy. *PeerJ*, 6, e5594. doi:10.7717/peerj.5594

Martinelli, A. G., Sertich, J. J., Garrido, A. C., & Praderio, Á. M. (2012). A new peirosaurid from the Upper Cretaceous of Argentina: Implications for specimens referred to *Peirosaurus tornimanni* Price (Crocodyliformes: Peirosauridae). *Cretaceous Research*, 37, 191–200. doi:10.1016/j.cretres.2012.03.017

Martínez, R. N., Alcober, O. A., & Pol, D. (2018). A new protosuchid crocodyliform (Pseudosuchia, Crocodylomorpha) from the Norian Los

Colorados Formation, northwestern Argentina. *Journal of Vertebrate Paleontology*, 38(4), 1–12. doi:10.1080/02724634.2018.1491047

Martins, K. C., Queiroz, M. V. L., Ruiz, J. V., Langer, M. C., & Montefeltro, F. C. (2024). A new Baurusuchidae (Notosuchia, Crocodyliformes) from the Adamantina Formation (Bauru group, upper cretaceous), with a revised phylogenetic analysis of Baurusuchia. *Cretaceous Research*, 153, 105680. doi:10.1016/j.cretres.2023.105680

Martins dos Santos, D., de Carvalho, J. C., de Oliveira, C. E. M., de Andrade, M. B., & Santucci, R. M. (2024). Cranial and postcranial anatomy of a juvenile baurusuchid (Notosuchia, Crocodylomorpha) and the taxonomical implications of ontogeny. *The Anatomical Record*, 1–46.

Martins dos Santos, D., Miloni Santucci, R., Maia de Oliveira, C. E., & Bandalise de Andrade, M. (2021). A baurusuchid yearling (Mesoeucrocodylia, Crocodyliformes), from the Adamantina Formation, Bauru Group, Upper Cretaceous of Brazil. *Historical Biology*, 34(11), 2137–2151. doi:10.1080/08912963.2021.2001807

McKinney, M. L. (1997). Extinction vulnerability and selectivity: combining ecological and paleontological views. *Annual review of ecology and systematics*, 28(1), 495–516. doi:10.1146/annurev.ecolsys.28.1.495

Melstrom, K. M., & Irmis, R. B. (2019). Repeated evolution of herbivorous crocodyliforms during the age of dinosaurs. *Current Biology*, 29(14), 2389–2395. doi:10.1016/j.cub.2019.05.076

Meunier, L. M., & Larsson, H. C. (2017). Revision and phylogenetic affinities of *Elosuchus* (Crocodyliformes). *Zoological Journal of the Linnean Society*, 179(1), 169–200.

Montefeltro, F. C. (2013). Revisão filogenética de Mesoeucrocodylia: irradiação basal e principais controvérsias (Doctoral dissertation, Universidade de São Paulo).

Montefeltro, F. C. (2019). The osteoderms of baurusuchid crocodyliforms (Mesoeucrocodylia, Notosuchia). *Journal of Vertebrate Paleontology*, 39(2), e1594242. doi:10.1080/02724634.2019.1594242

Montefeltro, F. C., Larsson, H. C., & Langer, M. C. (2011). A new baurusuchid (Crocodyliformes, Mesoeucrocodylia) from the Late Cretaceous of Brazil and the phylogeny of Baurusuchidae. *PLoS One*, 6(7), e21916. doi:10.1371/journal.pone.0021916

Morris, Z. S., Vliet, K. A., Abzhanov, A., & Pierce, S. E. (2022). Developmental origins of the crocodylian skull table and platyostrial face. *The Anatomical Record*, 305(10), 2838–2853. doi:10.1002/ar.24802

Nascimento, P. M., & Zaher, H. (2010). A new species of *Baurusuchus* (Crocodyliformes, Mesoeucrocodylia) from the Upper Cretaceous of Brazil, with the first complete postcranial skeleton described for the family Baurusuchidae. *Papéis avulsos de Zoologia*, 50, 323–361.

Nicholl, C. S., Hunt, E. S., Ouarhache, D., & Mannion, P. D. (2021). A second peirosaurid crocodyliform from the Mid-Cretaceous Kem Kem Group of Morocco and the diversity of Gondwanan notosuchians outside South America. *Royal Society open science*, 8(10), 211254. doi:10.1098/rsos.211254

Ortega, F., Buscalioni, A. D., & Jiménez-Fuentes, E. (1993). El cocodrilo de El Viso (Eoceno, Zamora): consideraciones acerca de los 'zifodontos' (Metasuchia, Sebecosuchia) del Eoceno de la Cuenca del Duero. *Anu Inst Estud Zamoranos 'Florían Ocampo'*. 1993:601–613.

Ortega, F., Buscalioni, A. D., & Gasparini, Z. (1996). Reinterpretation and new denomination of *Atacisaurus crassiproratus* (middle Eocene; Issel, France) as cf. *Iberosuchus* (Crocodylomorpha, Metasuchia). *Geobios*, 29(3), 353–364. doi:10.1016/S0016-6995(96)80037-4

Ortega, F., Gasparini, Z., Buscalioni, A. D., & Calvo, J. O. (2000). A new species of *Araripesuchus* (Crocodylomorpha, Mesoeucrocodylia) from the lower Cretaceous of Patagonia (Argentina). *Journal of Vertebrate Paleontology*, 20(1), 57–76. doi:10.1671/0272-4634(2000)020[0057:ANSOAC]2.0.CO;2

Paolillo, A., & Linares, O. J. (2007). Nuevos cocodrilos sebacosuchia del Cenozoico suramericano (Mesosuchia: Crocodylia). *Paleobiología Neotropical*, 3, 1–25.

Pinheiro, A. E. P., Luiz Gomes Costa Pereira, P. V., Mesquita Vasconcellos, F., Brum, A. S., Gomes De Souza, L., Costa, F. R., Castro, L. O. R., Da Silva, K. S., & Bandeira, K. L. N. (2023). New Itasuchidae (Sebecia, Ziphosuchia) remains and the radiation of an elusive Mesoeucrocodylia clade. *Historical Biology*, 35(12), 2280–2305. doi:10.1080/08912963.2022.2139179

Pinheiro, A. E. P., Pereira, P. V. L. G. D. C., de Souza, R. G., Brum, A. S., Lopes, R. T., Machado, A. S., Bergqvist, L. P., & Simbras, F. M. (2018). Reassessment of the enigmatic crocodyliform "Goniopholis" paulistanus Roxo, 1936: Historical approach, systematic, and description by new materials. *PLoS ONE*, 13(8), e0199984.

Pinheiro, A. E. P., Souza, L. G. D., Bandeira, K. L., Brum, A. S., Pereira, P. V. L. G., Castro, L. O. R., Ramos, R. R. C., & Simbras, F. M. (2021). The first notosuchian crocodyliform from the Araçatuba Formation (Bauru Group, Paraná Basin), and diversification of sphagesaurians. *Anais da Academia Brasileira de Ciências*, 93(suppl.2), e20201591. doi:10.1590/0001-3765202120201591

Pochat-Cottilloux, Y., Martin, J. E., Faure-Brac, M. G., Jouve, S., de Muizon, C., Cubo, J., Lécuyer, C., Fourel, F., & Amiot, R. (2023). A multi-isotopic study reveals the palaeoecology of a sebecid from the Paleocene of Bolivia. *Palaeogeography, Palaeoclimatology, Palaeoecology*, 625, 111667. doi:10.1016/j.palaeo.2023.111667

Pochat-Cottilloux, Y., Perrier, V., Amiot, R., & Martin, J. E. (2023). A peirosaurid mandible from the Albian–Cenomanian (Lower Cretaceous) of Algeria and the taxonomic content of *Hamadasuchus* (Crocodylomorpha, Peirosauridae). *Papers in Palaeontology*, 9(2), e1485. doi:10.1002/spp2.1485

Pol, D. (2003). New remains of *Sphagesaurus huenei* (Crocodylomorpha: Mesoeucrocodylia) from the late Cretaceous of Brazil. *Journal of Vertebrate Paleontology*, 23(4), 817–831. doi:10.1671/A1015-7

Pol, D. (2005). Restos postcraneanos de *Notosuchus terrestris* Woodward (Archosauria: Crocodyliformes) del Cretácico Superior de Patagonia, Argentina. *Ameghiniana*, 42(1), 21–38.

Pol, D., & Apesteguia, S. (2005). New *Araripesuchus* remains from the early late cretaceous (Cenomanian–Turonian) of Patagonia. *American Museum Novitates*, 2005(3490), 1–38. doi:10.1206/0003-0082(2005)490[0001:NARFTE]2.0.CO;2

Pol, D., Ji, S. A., Clark, J. M., & Chiappe, L. M. (2004). Basal crocodyliforms from the Lower Cretaceous Tugulu Group (Xinjiang, China), and the phylogenetic position of *Edentosuchus*. *Cretaceous Research*, 25(4), 603–622. doi:10.1016/j.cretres.2004.05.002

Pol, D., & Leardi, J. M. (2015). Diversity patterns of Notosuchia (Crocodyliformes, mesoeucrocodylia) during the cretaceous of Gondwana. *Publicación Electrónica de la Asociación Paleontológica Argentina*, 15, 172–186.

Pol, D., Leardi, J. M., Lecuona, A., & Krause, M. (2012). Postcranial anatomy of *Sebecus icaeorhinus* (Crocodyliformes, Sebecidae) from the Eocene of Patagonia. *Journal of Vertebrate Paleontology*, 32(2), 328–354. doi:10.1080/02724634.2012.646833

Pol, D., Nascimento, P. M., Carvalho, A. B., Riccomini, C., Pires-Domingues, R. A., & Zaher, H. (2014). A new notosuchian from the Late Cretaceous of Brazil and the phylogeny of advanced notosuchians. *PLoS ONE*, 9(4), e93105. doi:10.1371/journal.pone.0093105

Pol, D., & Powell, J. E. (2011). A new sebecid mesoeucrocodylian from the Rio Loro Formation (Palaeocene) of north-western Argentina. *Zoological Journal of the Linnean Society*, 163(suppl_1), S7–S36. doi:10.1111/j.1096-3642.2011.00714.x

Pol, D., Turner, A. H., & Norell, M. A. (2009). Morphology of the Late Cretaceous crocodylomorph *Shamosuchus djadochaensis* and a discussion of neosuchian phylogeny as related to the origin of Eusuchia. *Bulletin of the American Museum of Natural History*, 2009(324), 1–103.

Poole, D. F. G. (1961). Notes on tooth replacement in the Nile crocodile *Crocodylus niloticus*. *Proceedings of the Zoological Society of London*, 136(1), 131–140. doi:10.1111/j.1469-7998.1961.tb06083.x

Prasad, G. V., & de Broin, F. D. L. (2002, January). Late Cretaceous crocodile remains from Naskal (India): comparisons and biogeographic affinities. *Annales de Paléontologie*, 88(1), 19–71. Elsevier Masson. doi:10.1016/S0753-3969(02)01036-4

Price, L. I. (1945). A new reptile from the Cretaceous of Brazil. *Notas Preliminares e Estudos, Serviço Geologia Mineralogia do Brasil*, 25, 1–8.

Price, L. I. (1959). *Sobre um crocodilideo notossuquio do Cretáceo Brasileiro*. Serviço Gráfico do Instituto Brasileiro de Geografia e Estatística.

Rabi, M., & Sebők, N. (2015). A revised Eurogondwana model: Late Cretaceous notosuchian crocodyliforms and other vertebrate taxa suggest the retention of episodic faunal links between Europe and Gondwana during most of the Cretaceous. *Gondwana Research*, 28(3), 1197–1211. doi:10.1016/j.gr.2014.09.015

Raia, P., Carotenuto, F., Mondanaro, A., Castiglione, S., Passaro, F., Saggesi, F., Melchionna, M., Serio, C., Alessio, L., Silvestro, D., & Fortelius, M. (2016). Progress to extinction: increased specialisation causes the demise of animal clades. *Scientific Reports*, 6(1), 30965. doi:10.1038/srep30965

Raia, P., & Fortelius, M. (2013). Cope's law of the unspecialized, Cope's rule, and weak directionality in evolution. *Evolutionary Ecology Research*, 15(7), 747–756.

Rasmussen Simons, E. L., & Buckley, G. A. (2009). New material of “*Trematochampsia*” *oblita* (Crocodyliformes, Trematochampsidae) from the Late Cretaceous of Madagascar. *Journal of Vertebrate Paleontology*, 29(2), 599–604. doi:10.1671/039.029.0224

Ravel, A., Marivaux, L., Tabuce, R., Adaci, M., Mahboubi, M., Mebrrouk, F., & Bensalah, M. (2011). The oldest African bat from the early Eocene of El Kohol (Algeria). *Naturwissenschaften*, 98(5), 397–405. doi:10.1007/s00114-011-0785-0

Riff, D. (2007). Anatomia apendicular de *Stratiotosuchus maxhechti* (Baurusuchidae, Cretáceo Superior do Brasil) e análise filogenética dos Mesoeucrocodylia. *Unpublished DPhil thesis, Universidade Federal do Rio de Janeiro*.

Riff, D., & Kellner, A. W. A. (2011). Baurusuchid crocodyliforms as theropod mimics: clues from the skull and appendicular morphology of *Stratiotosuchus maxhechti* (Upper Cretaceous of Brazil). *Zoological Journal of the Linnean Society*, 163(suppl_1), S37–S56. doi:10.1111/j.1096-3642.2011.00713.x

Rio, J. P., & Mannion, P. D. (2021). Phylogenetic analysis of a new morphological dataset elucidates the evolutionary history of Crocodylia and resolves the long-standing gharial problem. *PeerJ*, 9, e12094. doi:10.7717/peerj.12094

Ristevski, J., Price, G. J., Weisbecker, V., & Salisbury, S. W. (2021). First record of a tomistomine crocodylian from Australia. *Scientific Reports*, 11(1), 12158. doi:10.1038/s41598-021-91717-y

Rossmann, T., Rauhe, M., & Ortega, F. (2000). Studies on Cenozoic crocodiles: 8. *Bergisuchus dietrichbergi* Kuhn (Sebecosuchia: Bergisuchidae n. fam.) from the Middle Eocene of Germany, some new systematic and biological conclusions. *PalZ*, 74(3), 379–392. doi:10.1007/BF02988108

Ruiz, J. V., Branzati, M., Ferreira, G. S., Martins, K. C., Queiroz, M. V., Langer, M. C., & Montefeltro, F. C. (2021). A new species of *Caipirasuchus* (Notosuchia, Sphagesauridae) from the Late Cretaceous of Brazil and the evolutionary history of Sphagesauria. *Journal of Systematic Palaeontology*, 19(4), 265–287. doi:10.1080/14772019.2021.1888815

Scheyer, T. M., & Desojo, J. B. (2011). Palaeohistology and external microanatomy of rauisuchian osteoderms (Archosauria: Pseudosuchia). *Palaeontology*, 54(6), 1289–1302. doi:10.1111/j.1475-4983.2011.01098.x

Schneider, C. A., Rasband, W. S., & Eliceiri, K. W. (2012). NIH Image to ImageJ: 25 years of image analysis. *Nature methods*, 9(7), 671–675. doi:10.1038/nmeth.2089

Schwab, J. A., Young, M. T., Walsh, S. A., Witmer, L. M., Herrera, Y., Brochu, C. A., Butler, I. B., & Brusatte, S. L. (2022). Ontogenetic variation in the crocodylian vestibular system. *Journal of Anatomy*, 240(5), 821–832. doi:10.1111/joa.13601

Sellés, A. G., Blanco, A., Vila, B., Marmi, J., López-Soriano, F. J., Llácer, S., Frigola, J., Canals, M., & Galobart, A. (2020). A small Cretaceous crocodyliform in a dinosaur nesting ground and the origin of sebecids. *Scientific reports*, 10(1), 15293. doi:10.1038/s41598-020-71975-y

Sereno, P., & Larsson, H. (2009). Cretaceous crocodyliforms from the Sahara. *ZooKeys*, 28, 1–143. doi:10.3897/zookeys.28.325

Sereno, P. C., Larsson, H. C., Sidor, C. A., & Gado, B. (2001). The giant crocodyliform *Sarcosuchus* from the Cretaceous of Africa. *Science*, 294(5546), 1516–1519. doi:10.1126/science.1066521

Sereno, P. C., Sidor, C. A., Larsson, H. C. E., & Gado, B. (2003). A new notosuchian from the Early Cretaceous of Niger. *Journal of Vertebrate Paleontology*, 23(2), 477–482. doi:10.1671/0272-4634(2003)023[0477:ANNFTE]2.0.CO;2

Simpson, G. G. (1937). New reptiles from the Eocene of South America. *American Museum novitates*; no. 927.

Simpson, G. G. (1944). *Tempo and mode in evolution*. Columbia University Press.

Stefanic, C. M., Nestler, J. H., Seiffert, E. R., & Turner, A. H. (2019). New crocodylomorph material from the Fayum depression, Egypt, including the first occurrence of a sebecosuchian in African late Eocene deposits. *Journal of Vertebrate Paleontology*, 39(6), e1729781. doi:10.1080/02724634.2019.1729781

Tavares, S. A. S., Ricardi-Branco, F., & de Souza Carvalho, I. (2015). Osteoderms of *Montealtosuchus arrudacamposi* (Crocodyliformes, Peirosauridae) from the Turonian-Santonian (Upper Cretaceous) of Bauru Basin, Brazil. *Cretaceous Research*, 56, 651–661. doi:10.1016/j.cretres.2015.07.002

Thompson, J. N. (1994). *The coevolutionary process*. University of Chicago press.

Turner, A. H., & Buckley, G. A. (2008). *Mahajangasuchus insignis* (Crocodyliformes: Mesoeucrocodylia) cranial anatomy and new data on the origin of the eusuchian-style palate. *Journal of Vertebrate Paleontology*, 28(2), 382–408. doi:10.1671/0272-4634(2008)28[382:MICMCA]2.0.CO;2

Turner, A. H., & Calvo, J. O. (2005). A new sebecosuchian crocodyliform from the Late Cretaceous of Patagonia. *Journal of Vertebrate Paleontology*, 25(1), 87–98. doi:10.1671/0272-4634(2005)025[0087:ANSCFT]2.0.CO;2

Turner, A. H., & Sertich, J. J. (2010). Phylogenetic history of *Simosuchus clarki* (Crocodyliformes: Notosuchia) from the late cretaceous of Madagascar. *Journal of Vertebrate Paleontology*, 30(sup1), 177–236. doi:10.1080/02724634.2010.532348

Vasconcellos, F. M., & de Souza Carvalho, I. (2005). Estágios de desenvolvimento de *Mariliasuchus amarali*, Crocodyliformes Mesoeucrocodylia da Formação Adamantina, Cretáceo Superior da Bacia Bauru, Brasil. *Anuário do Instituto de Geociências*, 28(1), 49–69. doi:10.11137/2005_1_49-69

Vasconcellos, F. M., & de Souza Carvalho, I. (2010). Paleoichnological assemblage associated with *Baurusuchus salgadoensis* remains, a Baurusuchidae Mesoeucrocodylia from the Bauru Basin, Brazil (Late Cretaceous). *Bulletin of the New Mexico Museum of Natural History and Science*, 51, 227–237.

Vasconcellos, F. M., & de Souza Carvalho, I. (2006). Condicionante etológico na tafonomia de *Uberabasuchus terrificus* (Crocodyliformes, Peirosauridae) da Bacia Bauru (Cretáceo Superior). *Geosciences- Geociências*, 25(2), 225–230.

Vieira, L. G., Lima, F. C., Mendonça, S. H. S. T., Menezes, L. T., Hirano, L. Q. L., & Santos, A. L. Q. (2018). Ontogeny of the postcranial axial skeleton of *Melanosuchus niger* (Crocodylia, Alligatoridae). *The Anatomical Record*, 301(4), 607–623. doi:10.1002/ar.23722

Walker, A. D. (1970). A revision of the Jurassic reptile *Hallopus victor* (Marsh), with remarks on the classification of crocodiles. *Philosophical Transactions of the Royal Society of London. B, Biological Sciences*, 257(816), 323–372. doi:10.1098/rstb.1970.0028

Westergaard, B., & Ferguson, M. W. (1990). Development of the dentition in *Alligator mississippiensis*: upper jaw dental and craniofacial development in embryos, hatchlings, and young juveniles, with a comparison to lower jaw development. *American Journal of Anatomy*, 187(4), 393–421. doi:10.1002/aja.1001870407

Whetstone, K. N., & Whybrow, P. J. (1983). A “Cursorial” crocodilian from the Triassic of Lesotho (Basutoland), Southern Africa. *Occasional Papers of the Museum of Natural History* No. 106, University of Kansas, Lawrence, 1–37.

Wilson, J. A., Malkani, M. S., & Gingerich, P. D. (2001). New crocodyliform (Reptilia, Mesoeucrocodylia) from the Upper Cretaceous Pab Formation of Vitakri, Balochistan (Pakistan). *Contributions from the Museum of Paleontology, the University of Michigan*, 30, 321–336.

Wu, X. C., & Sues, H. D. (1996). Anatomy and phylogenetic relationships of *Chimaerasuchus paradoxus*, an unusual crocodyliform reptile from the Lower Cretaceous of Hubei, China. *Journal of Vertebrate Paleontology*, 16(4), 688–702. doi:10.1080/02724634.1996.10011358

Zaher, H., Pol, D., Carvalho, A. B., Riccomini, C., Campos, D., & Nava, W. (2006). Redescription of the cranial morphology of *Mariliasuchus amarali*, and its phylogenetic affinities (Crocodyliformes, Notosuchia). *American Museum Novitates*, 2006(3512), 1–40. doi:10.1206/0003-0082(2006)3512[1:ROTCMO]2.0.CO;2

Handling Editor: Pedro Godoy.

Phylogenetics Editor: Pedro Godoy